PLATFORMS FOR EXPLORING HOST-PATHOGEN INTERACTIONS IN HEPATITIS C VIRUS INFECTION

By

KARTIK TREHAN

M.S.E. Biomedical Engineering
The Johns Hopkins University, 2008

M.S.E. Applied Mathematics and Statistics
The Johns Hopkins University, 2008

B.S. Biomedical Engineering/Applied Mathematics and Statistics
The Johns Hopkins University, 2007

SUBMITTED TO THE HARVARD-MIT DIVISION OF HEALTH SCIENCES AND TECHNOLOGY
IN PARTIAL FULLFILLMENT OF THE REQUIREMENTS FOR THE DEGREE OF

DOCTOR OF PHILOSOPHY IN BIOMEDICAL ENGINEERING

AT THE

MASSACHUSETTS INSTITUTE OF TECHNOLOGY

JUNE 2012

Signature of Author: _____
Harvard-MIT Division of Health Sciences and Technology
May 10, 2012

Certified by: _____
Sangeeta N. Bhatia, MD, PhD
Howard Hughes Medical Investigator
Professor of Health Sciences and Technology &
Professor of Electrical Engineering and Computer Science
Thesis Supervisor

Accepted by: _____
Ram Sasisekharan, PhD
Director, Harvard-MIT Division of Health Sciences and Technology
Edward Hood Taplin Professor of Health Sciences and Technology/Biological Engineering

PLATFORMS FOR EXPLORING HOST-PATHOGEN INTERACTIONS IN HEPATITIS C VIRUS INFECTION

By

KARTIK TREHAN

Submitted to the Harvard-MIT Division of Health Sciences and Technology on May 10, 2012 in Partial Fulfillment of the Requirements for the Degree of Doctor of Philosophy in Biomedical Engineering

Abstract

Afflicting almost 200 million worldwide, hepatitis C virus (HCV) mounts a chronic infection of liver hepatocytes that causes substantial morbidity and mortality. An understanding of host-virus interactions will drive the development of therapeutics, but research is restrained by available experimental tools. Due to the cost and unreliability of existing humanized mouse and primate *in vivo* models, HCV research is almost exclusively performed using *in vitro* platforms which suffer from three major limitations. First, challenges in primary hepatocyte culture and the general non-permissiveness of liver cell lines have necessitated the use of a uniquely permissive hepatoma line derived from a single donor, questioning the generalizability of findings to the broader population. Second, this cell line deviates appreciably from native liver in functions central to HCV infection, including innate immune signaling, polarization, and proliferation. Third, infection is typically studied using bulk assays with suboptimal specificity, sensitivity, and content. Here, we describe three technologies for overcoming these limitations in the study of host-virus interactions. We demonstrate their utility in exploring innate immune signaling, a clinically significant component of HCV pathogenesis.

Section I describes an *in vitro* platform for investigating inter-host variations in the natural history of infection and treatment response. We show that directed differentiation of induced pluripotent stem cells (iPSCs) yields patient-specific liver tissue that is permissive to HCV and responds to infection with a robust innate immune response, opening the door to "personalizing" the study and treatment of infection.

In Section II, we demonstrate that tissue-engineered, micropatterned co-cultures (MPCCs) of primary hepatocytes and supportive stroma are permissive to HCV, enabling investigations in a more natural host. We then show that innate immune signaling curtails infection in this model, and that its inhibition enhances infection 2-3 orders of magnitude. Lastly, we use MPCCs to uncover a novel liver immunoregulatory mechanism whereby innate immune surveillance is depressed, permitting efficient replication of hepatotropic pathogens.

Finally, Section III details a high-content imaging assay that enables visualization and enumeration of single viral genomes in individual cells. We demonstrate that single-cell, multiplexed quantification of viral genomes and host gene transcripts can be used to dissect host-virus interactions, yielding an unexpected positive correlation between stage of infection and response to an innate immune cytokine.

The solutions described here will enable the pursuit of previously intractable research questions for HCV and other viruses, accelerating progress towards the development of antivirals and vaccines. Further, the insights gained regarding the interplay between HCV and innate immunity have important clinical ramifications, including a novel therapeutic strategy.

Thesis Supervisor: Sangeeta N. Bhatia, MD, PhD
Title: Professor, Health Sciences and Technology/Electrical Engineering and Computer Science

Acknowledgements

I have so many people to thank for my progress over the past few years.

First and foremost, to Sangeeta Bhatia, for being the best possible mentor and role model I could have had to guide me through graduate school. She gave me opportunities to work in extremely exciting areas, on highly integrative projects that would likely be impossible elsewhere. Moreover, she has helped me improve in so many ways over the years, to the point where I could literally see how much I had changed for the better on a weekly basis – as a thinker, as a communicator, as a team player, as a manager, and as a more effective person overall. Finally, she has been incredibly caring and understanding, and I am grateful to her for much beyond work as well. Thank you so much, Sangeeta.

To my thesis committee members – Lee Gehrke, Ray Chung, and Ram Sasisekharan – for their time and guidance. Their demands for excellence, alongside their supportiveness and encouragement, enabled me to do my best.

To the Laboratory for Multiscale Regenerative Technologies for being such a great place to perform graduate studies. Intellectually, the group is so diverse, and everyone works and thinks at the cutting edge of their fields; working alongside of them, I have learned much about so many different fields. Socially, the lab has been an ideal environment – the lab members want to give work their very best yet maintain so much care for and interest in their peers. To Kevin Lin and Nate Reticker-Flynn, for being some of my closest buddies at MIT; Yin Ren and David Braga Malta for being great friends; Justin Lo, Gabe Kwong, and Rob Schwartz for sharing the "urban" side of the lab with me, and for having tons of great conversations; Dave Wood for his amazing southern accent and Big Lebowski recollections, can't wait to see the great things his lab produces; Cheri Li for spiffing things up with her artsy ways; Alex Bagley aka EnderBags for keeping it "lazy ambitious;" Jing Shan for sharing her experiences at the movies; the malaria duo Sandra March and Shengyong Ng for awesome collaborations, chats, and tales of Ibiza; Ani Galstian aka AniG and Kathleen Christine aka Kathy for keeping my ego in check by rejecting my coffee invitations; Kelly Stevens for occasional inappropriate jokes; Tal Danino for similar interests and "vibrance alive" ginger smoothies; Sabine Hauert for sharing my habit of pacing for no reason sometimes; previous graduate students Geoff von Maltzahn and Alice Chen for being incredibly helpful and inspiringly successful, and thereby making it much harder to graduate; previous post-doc Salman Khetani, I started grad school on the shoulders of a giant; Neetu Singh for her infectious curiosity in and appreciation of the most mundane things; Greg Underhill for occasional pearls of great wisdom; lab personnel Heather Fleming, Sue Kangiser, Steve Katz, and Lia Ingaharro for making a zoo out of a jungle, adding some cheer, and putting up with Rob; Hamsika Chandrasekar aka Hams for being an amazing UROP with the best handwriting humanly possible; Salil Desai for participating in the gentle revolution that is shape screen and for having the pickiest eating preferences I've ever seen; Gaya Murugappan for well-timed and well-meant profanity; Vyas Ramanan for blossoming under my tutelage; Warren for putting up with people calling him Andrew; and all the other UROPs I got to know in my time that made things so much more fun.

To fantastic collaborators – the labs of Charlie Rice at The Rockefeller University, Alexander van Oudenaarden at MIT, Bob Langer/Dan Anderson at MIT, and various others from all over the US. I have to single out the Rice Lab in particular (especially Tim Sheahan, Alex Ploss, Linda Andrus, Joe Luna, Maria Teresa Catanese, and Meg Scull) for their significant contributions both to my own improvement and to all the work in this thesis. As an engineer

beginning work on infectious disease, I lacked a solid background in much of the pre-requisite basic science. The Rice Lab members are world experts in virology, and interacting with them in bimonthly conference calls, lab retreats, and joint experiments has brought me up to speed and indeed made all this work possible. I view Charlie as a key mentor in my scientific development, and his group has been better colleagues than I could've asked for.

To so many great non-lab friends from MIT, Harvard, and Boston – my HST classmates, other departments, Sidney Pacific, the Koch Institute, World Tour, BadFriends, and more. They have greatly enriched my time as a graduate student. I should call out perhaps the two closest friends among these, Raj Manrai aka Raju and Adeeti Ullal aka Deets, for being some of the most amazing people on the planet. They have been so supportive (e.g. checking in periodically to make sure I was still alive) and have helped me achieve my best. In the last few months at MIT, I've got to spend a lot of time with Harry Jenq aka Big Harry J from the Jacks Lab down the hall from us – awesome discussions about philosophy and goals, and just tons of good times.

To the awesome undergraduates of Simmons Hall where I lived for 3 years as a Graduate Resident Tutor. I got to know 30-40 students each year, and though I was supposed to be a mentor for them, the exchange has been more bi-directional than they may think. Their intelligence and enthusiasm have been inspiring, and their warmth has been so welcoming. I've loved every moment of my stay there, and my activities with these students have been among my most satisfying experiences as a grad student. The other House Masters and other members of the Simmons House Team have also been wonderful colleagues to have in my home community.

To Blizzard Entertainment, Riot Games, Valve, PokerStars, and YouTube for adding an extra year to my stay at MIT. To Voltage Coffee in Kendall for making me amazing drinks daily. To my body for not imploding after an entire year of neglect.

To the Koch Institute for having the most beautiful building on campus and for being a community of exceptional scholars. Having such diverse research programs under one roof leads to an exciting cross-fertilization of ideas, and I am all the more enriched for having been exposed to it. I've made wonderful friends among these people, who made it that much easier to stay in lab until 3am. To HST, for being the best department at MIT – eminent faculty, supportive (and patient!) staff, and impressive students. I have gotten so many amazing opportunities through HST, and don't think another department would've suited me better. To MIT, I hope to honor your name for all that you've given me; through you, I've received first class resources and been exposed to some of the world's greatest minds, and thus feel that I have an obligation going forward to give my best back to society. To Harvard, partly for introducing me to so many great people and for the experiences in med school classes and clinical rotations, but largely for encouraging the establishment of many excellent restaurants at an easily accessible location on the Red Line – MIT has a lot to learn from you in this respect, and I look forward to seeing Kendall Square evolve in the years to come.

To two of my brothers Lil Wayne and Drake, representing the Young Money Cash Money Billionaires (YMCMB), and to 50 cent. I think people misunderstand the message they stand for since they cover it up with profanity, womanizing, and materialism ☺ – for me, they've represented the pride that comes from hard work, and the ability to improve your situation in life through perseverance. They also have excellent advice for living life; e.g., Lil Wayne once said, "Real G's move in silence like lasagna." (Props to Leilani Chirino of the Jacks Lab for pointing this gem out – she thought it was inane, for the record).

Finally, to my Family, thank you for making me who I am today. Your support is the only reason all of this has been possible.

Biographical Information

ACADEMIC QUALIFICATIONS

- Massachusetts Institute of Technology and Harvard University, Cambridge, MA — 2008 – 2012
  Harvard-MIT Division of Health Science and Technology
  - Ph.D. in Biomedical Engineering (advisor: Prof. S. Bhatia)
    - Thesis: "Platforms for exploring host-pathogen interactions in hepatitis C virus infection"
  - National Science Foundation Graduate Research Fellow
  - Grade point average (GPA): **5.0 / 5.0**

- The Johns Hopkins University, Baltimore, MD — 2007 – 2008
  - M.S.E. in Biomedical Engineering (advisor: Prof. HQ. Mao.)
    - Thesis: "Multilayered hydrogel microfibers for cell and tissue engineering"
  - M.S.E. in Applied Mathematics and Statistics (advisors: Profs. S. Kuo & C. Priebe)
    - Thesis: "Characterization of nanostructure in actin-based motility"
  - Grade point average (GPA): **4.0 / 4.0**

- The Johns Hopkins University, Baltimore, MD — 2003 – 2007
  - B.S. in Biomedical Engineering/Applied Mathematics and Statistics (Minor in Mathematics)
  - Richard J. Johns Academic Achievement Award/AMS Achievement Award
  - Grade point average (GPA): **3.97 / 4.0** (Rank **1** in both departments)
  - SAT I: Reasoning Test: **1600/1600**

TECHNOLOGY DESIGN AND RESEARCH

My research and technology design experience at Massachusetts Institute of Technology, Harvard University, and The Johns Hopkins University has spanned a broad range of disciplines and applications, culminating in papers, conference presentations, patents, technology grants, academic awards, and business efforts. Keywords: *infectious disease, virology, quantitative high-content imaging, single-cell heterogeneity, personalized medicine, induced pluripotent stem cells, immunomodulation, immunotherapy, microfabrication, micropatterning, microenvironment, liver, disease model development, biomaterials, tissue engineering, vascular and neural engineering, orthopedics, osteoporosis, biomechanics, bioinstrumentation, obstetrics, cell mechanics, biomedical optics, biochemistry, mathematical modeling*

- Technologies for the study of viral infection — 2009 – 2012
  Laboratory for Multiscale Regenerative Technologies, MIT (advisor: Prof. S. Bhatia)
  - Developing culture and imaging technologies for studying HCV infection
  - Mentored 2 undergraduates and collaborated with >15 people across 7 research labs

- Multilayered hydrogel microfibers for tissue engineering — 2005 – 2008
  Polymeric Biomaterials and Tissue Engineering Lab, JHU (advisor: Prof. HQ. Mao)
  - Managed team of 5 to develop novel fibrous scaffolds for vascular/neural engineering
  - Mentored 3 undergraduates
    - 1st Place Poster Award at ASME Biomedical Devices Conference
    - Maryland TEDCO University Technology Fund ($50,000)
    - National Collegiate Inventors and Innovators Alliance Grant ($20,400)

- Pull-out resistant pedicle screw for osteoporotic patients — 2005 – 2007
  The Johns Hopkins University Medical School, JHU (advisor: Dr. A. Khanna)
  - Worked in a group of 6 to develop a rehabilitative spinal screw for osteoporotic patients
    - Technology licensed to Port City Group (Muskegon, MI)
    - National Collegiate Inventors and Innovators Alliance Grant ($19,000)
    - 1st Place in the JHU CLE Business Plan Competition ($5,000)
    - Winner of the NCIIA March Madness of the Mind Competition

- Bioimpedance probe for the detection of preterm labor in pregnant women 2003 – 2004
  The Johns Hopkins University Medical School, JHU (advisors: Dr. E. Gurewitsch & Prof. R. Allen)
  - Worked in a group of 10 to develop bioinstrumentation for early preterm labor prediction
    - Technology licensed to serial entrepreneur
    - 2nd Place in the National NCIIA BME IDEA Competition ($2,500)
    - Finalist in the National Collegiate Inventors Competition (CIC) ($1,000)
    - Finalist in IEEE EMBS Student Paper Contest
    - 2nd Place in the MoshPit Greater Baltimore Business Plan Contest
    - 1st Place in the JHU W.P. Carey Business Plan Competition ($5,000)
    - National Collegiate Inventors and Innovators Alliance Grant ($8,750)

- Statistical Characterization of Nanostructure in Actin-Based Cell Motility 2003 – 2008
  Cell Mechanics and Biomedical Optics Lab, JHU (advisors: Profs. S. Kuo & C. Priebe)
  - Research involved determining mechanisms of actin filament production
    - MAA Joint Mathematics Meetings Poster Session Award

PEER-REVIEWED JOURNAL PUBLICATIONS

- **Trehan K** et al., "Tolerization of interferon signaling in adult hepatocytes enhances liver infection," *in preparation*
- **Trehan K** et al., "Quantifying single-cell heterogeneity in RNA virus infection using single-genome imaging," *submitted*
- Schwartz RE*/**Trehan K***, Andrus L, Sheahan TP, Ploss A, Duncan SA, Rice CM, Bhatia SN, "Modeling hepatitis C virus infection using human induced pluripotent stem cells," *Proceedings of the National Academy of Sciences*, 2012
- Andrus L, Marukian S, Jones CT, Catanese MT, Sheahan TP, Schoggins JW, Barry WT, Dustin LB, **Trehan K**, Ploss A, Bhatia SN, Rice CM, "Expression of paramyxovirus V proteins promotes replication and spread of hepatitis C virus in cultures of primary human fetal liver cells," *Hepatology*, 2011
- Ploss A*/Khetani SR*, Jones CT, Syder AJ, **Trehan K**, Gaysinskaya VA, Ritola K, Rice CM, Bhatia SN, "Persistent hepatitis C virus infection in microscale primary human hepatocyte culture," *Proceedings of the National Academy of Sciences*, 2010

** denotes equal contribution by authors.*

PATENTS

- (provisional application) "Single viral genome imaging," May 2012
- (in preparation) "Composite nanofiber and microfiber nerve guides," December 2007
- (provisional application) "Multilayered hydrogel microfibers for cell and drug encapsulation," April 2007
- (full patent pending) "Pedicle screw," March 2007

INVITED TALKS

- **Trehan K**, "'Hepatitis C virus – exposed!' and more: advancing the study of viral infection," Koch Cancer Institute Seminar Series, Cambridge, MA, March 2012
- **Trehan K**, "Engineered models for studying hepatitis C virus," Infectious Disease & Human Health Research Center Planning Committee, SkTech MIT Initiative/Skolkovo Institute, Cambridge, MA, February 2012
- **Trehan K**, "Studying hepatitis C virus in engineered hepatic tissues," Center for the Study of Hepatitis C Seminar Series, The Rockefeller University, New York, NY, April 2011

CONFERENCE TALKS

- **Trehan K**, Ploss A*/Khetani SR*, Jones, CT, Syder AJ, Gaysinskaya VA, Ritola K, Rice CM, Bhatia SN, "Persistent hepatitis C virus infection in microscale primary human hepatocyte culture," 2010 Biomedical Engineering Society Annual Meeting, Austin Convention Center, Austin, TX, October 2010

- Ploss A*/Khetani SR*, Jones, CT, Syder AJ, **Trehan K**, Gaysinskaya VA, Ritola K, Rice CM, Bhatia SN, "Persistent hepatitis C virus infection in microscale primary human hepatocyte culture," 16th International Symposium on Hepatitis C virus and Related Viruses, Nice, France, October 2009
- **Trehan K**, Hong K, Pao H, "Simulated annealing as a flexible tool for refined districting," Mathematical Association of America (MAA) Spring 2007 MD-DC-VA Regional Meeting, Roanoke College, Salem, VA, April 2007
- Hoe YS et al., "Probe for measuring bioimpedance of the human uterine cervix," BME Design Day, Johns Hopkins University, May 2006
- Ponnusamy K, Iyer S*/Gupta G*/Hui A*/**Trehan K***/Yu C*, Khanna A, "Pull-out resistant pedicle screw for osteoporosis," BME Design Day, Johns Hopkins University, May 2006
- **Trehan K**, Chivukula R, Choi J, "Physical and digital optimization of a constrained irrigation system," Mathematical Association of America (MAA) Spring 2006 MD-DC-VA Regional Meeting, Loyola College, Baltimore, MD, April 2006
- Hoe YS et al., "Bioimpedance probe to detect preterm labor," Medical Design Excellence Awards (MDEA) Ceremony, Medical Design and Manufacturing (MDM) East Conference, New York City, NY, June 2005
- Hoe YS et al., "Measuring bioimpedance of the human uterine cervix: towards early detection of preterm labor," 26th Annual International Conference of the IEEE EMBS, San Francisco, CA, September, 2004

CONFERENCE POSTERS

- Love KT, **Trehan K**, Langer R, Bhatia SN, Anderson DG, "Non-viral delivery of the hepatitis C genome," 11th US-Japan Symposium on Drug Delivery Systems, Lahaina, HI, December 2011
- Ploss A*/Khetani SR*, **Trehan K**, Chen A, Jones CT, Syder AJ, Ong L, Gaysinskaya VA, Mu K, Ritola K, Rice CM, Bhatia SN, "Development of microscale primary human hepatocyte cultures for studying hepatitis C virus infection," Gordon Research Conference: Signal Transduction by Engineered Extracellular Matrices, University of New England, Biddeford, ME, June 2010
- **Trehan K***/Yu C*, Bakhru S, Tsao J, Gokhale T, Mao HQ, "Coculture applications of multilayered hydrogel microfibers for tissue engineering," Institute for NanoBioTechnology Symposium, Johns Hopkins University School of Medicine, Baltimore, MD, May 2008
- **Trehan K***/Yu C*, Bakhru S, Tsao J, Gokhale T, Mao HQ, "Coculture applications of multilayered hydrogel microfibers for tissue engineering," Materials Research Society (MRS) 2008 Spring Meeting, Moscone West and San Francisco Marriot, San Francisco, CA, March 2008
- **Trehan K***/Yu C*, Bakhru S, Tsao J, Gokhale T, Mao HQ, "Multilayered hydrogel microfibers for cell and tissue engineering," NCIIA March Madness of the Mind Exhibition, Museum of Science and Industry, Dallas, TX, March 2008
- **Trehan K**, Priebe C, Torcaso F, Kuo S, "Towards the characterization of nanostructure in actin-based motility using a Brownian stepping model," Mathematical Association of America (MAA) Joint Mathematics Meeting (JMM), San Diego Convention Center, San Diego, CA, January 2008
- **Trehan K***/Yu C*, Bakhru S, Tsao J, Mao HQ, "Multilayered hydrogel microfibers for cell and tissue engineering," Biomedical Engineering Society (BMES) 2007 Annual Meeting, Los Angeles, CA, September 2007
- Ponnusamy K, Iyer S*/Gupta G*/Hui A*/**Trehan K***/Yu C*, Khanna A, "A pull-out resistant pedicle screw for the osteoporotic spine," American Society of Mechanical Engineers (ASME) Frontiers in Biomedical Devices Conference, Irvine, CA, June 2007
- **Trehan K***/Yu C*, Bakhru S, Mao HQ, "Novel hydrogel microfibers for tissue engineering," American Society of Mechanical Engineers (ASME) Frontiers in Biomedical Devices Conference, Irvine, CA, June 2007
- Ponnusamy K, Iyer S*/Gupta G*/Hui A*/**Trehan K***/Yu C*, Khanna A, "Pull-out resistant pedicle screw for osteoporotic patients," NCIIA March Madness of the Mind Exhibition, Museum of Science and Industry (MOSI), Tampa, FL, March 2007

ABSTRACTS

- **Trehan K***/Yu C*, Bakhru S, Mao HQ, "Novel hydrogel microfibers for tissue engineering," Proceedings of the Frontiers in Biomedical Devices Conference, American Society of Mechanical Engineers (ASME), 2007

- Ponnusamy K, Iyer S*/Gupta G*/Hui A*/**Trehan K***/Yu C*, Khanna A, "A pull-out resistant pedicle screw for the osteoporotic spine," Proceedings of the Frontiers in Biomedical Devices Conference, American Society of Mechanical Engineers (ASME), 2007

BOOK CHAPTERS

- Shan J, Stevens K, **Trehan K**, Chen AA, Underhill G, Bhatia SN, "Hepatic tissue engineering," Molecular Pathology of Liver Diseases, Springer, 2011
- Lim SH, Christopherson GC, **Trehan K**, Mao HQ. "Nanotechnology", Regenerative Medicine, First Edition, Jones and Bartlett Publishers, *in press*

SELECTED STUDENT ORGANIZATION LEADERSHIP

- President of the JHU Mathematics Club 2004 – 2006
- Vice-President of the JHU Tau Beta Pi (TBII) Student Chapter 2006 – 2007
- Vice-President of the JHU Alpha Eta Mu Beta (AEMB) Student Chapter 2006 – 2007
- Vice-President of the JHU Biomedical Engineering Society (BMES) Student Chapter 2005 – 2007

SERVICE IN MENTORSHIP, TEACHING, EDUCATION, AND ACADEMICS

- Mentored >5 undergraduates in research laboratories at JHU and MIT 2005 – 2012
  - Outstanding Mentor Award by the MIT Biology Undergrad Research Symposium 2012
- Graduate Resident Tutor (GRT) for MIT Undergraduates (Simmons Hall) 2009 – 2012
  - Social/academic mentoring, conflict resolution, personal development for >100 undergraduates
- Abstract reviewer for Annual Biomedical Research Conference for Minority Students (ABRCMS) 2011
- Volunteer organizer for IEEE Engineering in Medicine and Biology (EMBS) Conference 2011
- Co-Founder & Director of TripleIntegral (high school math education group, Baltimore, MD) 2004 – 2008
  - Involved >30 student volunteers
  - Raised $21,000 for annual math contest and competition training
  - Involved 1000+ high school students and 30+ high school math teachers
- Co-Director of the Johns Hopkins Mathematics Tournament (JHMT) 2003 – 2007
- Teacher's Assistant (TA) for JHU undergraduate courses 2006 – 2007
  - 020.306 Cell Biology, *Spring 2006*
  - 550.111 Statistical Analysis I, *Spring 2006*
  - 600.107 Introductory Programming in Java, *Summer 2006*
  - 580.424 Physiological Foundations Lab II, *Spring 2007*
- Volunteer organizer for Translational Health Science and Technology Institute (THSTI) India recruiting 2010
- Student representative for Harvard-MIT HST to the MIT Corporation Visiting Committee 2010
- Volunteer organizer for Keys to Empowering Youth (KEYS) young women's education 2010
- Volunteer services planning committee for Biomedical Engineering Society (BMES) Conference 2005
- Writer for the Johns Hopkins Academic Course Evaluation (ACE) Guide 2006
- Student representative for the JHU Whiting School of Engineering Curriculum Committee 2004 – 2006
- Undergraduate tutor at JHU (Calculus I/II, Physics I/II) 2004 – 2005

OTHER WORK EXPERIENCE

- Introduction to Clinical Medicine (Harvard Medical School, Boston, MA) 2011 – 2012
  - 3 months of clinical rotations
  - Study clinical medicine, learn patient interaction, and understand medical challenges
- Business Intern for startup Cogito Health (Cambridge, MA) 2008
  - Team project to assess value proposition of voice-based depression diagnostics
  - Reported directly to CEO and VP Operations

OTHER ACHIEVEMENTS AND HONORS

- National Science Foundation (NSF) Graduate Research Fellowship (GRFP) 2007 – 2010
- Interservice/Industry Training, Simulation & Education Conference (IITSEC) Fellowship 2007

- USA Today All-USA College Academic Team 2007
- Two-Time Winner of the JHU Applied Mathematics and Statistics Modeling Competition Prize 2006 – 2007
- Two-Time Winner of the JHU Applied Mathematics Club Modeling Contest 2006 – 2007
- Tau Beta Pi Scholarship 2006
- *Meritorious* Winner of the COMAP Mathematical Contest in Modeling (MCM) 2006
- 2nd Place in the TopCoder JHU College Tour Programming Contest 2006
- Scored 29 on Putnam Mathematics Competition (Top 300 of 3545) 2006
- College Scholarships: William Baxter Brown, Upakar, GreenPoint, William Wallace 2003 – 2007

SOCIETAL AFFILIATIONS

- Biomedical Engineering Society (BMES)
- Alpha Eta Mu Beta (AEMB) BME Honors Society
- Tau Beta Pi (TBΠ) Engineering Honors Society
- Society for Industrial and Applied Math (SIAM)
- Mathematical Association of America (MAA)
- Society for Biomaterials (SFB)
- Materials Research Society (MRS)
- American Society for Cell Biology (ASCB)

HOBBIES

Sports and games: Badminton (founded the MIT "BadFriends" Club of >20 people), bodybuilding, Texas hold 'em
Arts: gullible Hollywood film watcher, dancing, tolerable pianist/drummer, YouTube music surfer
Foreign languages: Hindi (fluent conversation), Spanish (basic conversation)
Other: Ethnic cuisine (founded the Boston World Tour Cuisine Club of > 15 people)

Table of Contents

Table of Figures

acquire all such spots in target cells. Using custom software, spots can be identified in three dimensions and quantified over a wide dynamic range, ranging two orders of magnitude from zero to several hundred spots per cell; alternatively, for cells with too many spots to identify individually, an estimate can be obtained by integrating the fluorescence intensity in the cell. Comparison with real-time polymerase chain reaction (RT-PCR) corroborates transcript enumeration by smFISH spot counting, showing that smFISH is quantitative. **(B)** Co-localization of diffraction-limited spots in infected Huh-7.5 hepatoma cultures (16 hours post infection) was determined by simultaneously introducing two spectrally distinct probe sets (coupled to Cy5 and Alexa594 respectively) targeting different portions of the same genomic vRNA strand. Typical images of positive (***Left***, Z-stack projection, scale bar ≈ 5.0 μm; ***Inset***, ~2x zoom) and negative (***Center***, Z-stack projection, scale bar ≈ 4.0 μm; ***Inset***, ~2x zoom) strands shown. Percentage of Cy5 and Alexa594 spots that co-localize with the other channel shown for both strands (***Right***). **(C)** Histogram representation of integrated intensity distribution for spots 24 hours post infection (hpi) for both strands. **(D)** Number of positive strands in individual cells at 12 and 24 hpi (means in red). Difference was statistically significant: $****p < 0.0001$ (two-tailed t test). **(E)** Number of positive strands in individual cells in DMSO or the HCV NS5B polymerase inhibitor 2'CMA at 24 hpi (means in red). Difference was statistically significant: $****p < 0.0001$ (two-tailed t test). **(F)** NS3/4A activity reporter [57] deems cells infected based on nuclear fluorescence and uninfected based on cytosolic fluorescence. The Huh-7.5 Clone 8 line which carries this reporter stably was used to compare NS3/4A imaging with smFISH. Sample images from the same field of view for both NS3/4A reporter (***Left***, scale bar ≈ 18.5 μm) and smFISH (***Center***, ≈ 18.5 μm) are shown. Number of positive strands in NS3/4A- or NS3/4A+ cells 24 hpi are provided (***Right***). Stat. significant diff: $****p < 0.0001$ (two-tailed t test). 82

Figure 4-2. Specific and sensitive imaging of viral RNA in hepatoma and primary hepatocyte culture models. (A) Uninfected Huh-7.5 hepatoma cells imaged with probe sets for both the positive and negative strand (Z-stack projection, scale bar ≈ 4.9 μm). **(B)** Infected Huh7.5 cells imaged 24 hours post infection (hpi) on DAPI, Cy5, and Alexa594 channels but without FISH probe sets (Z-stack projection, scale bar ≈ 6.2 μm). **(C)** Structured illumination microscopy (SIM) of HCV (Cy5) and ER (Alexa594) (scale bar ≈ 3.0 μm) in infected Huh-7.5 cells 24 hpi. **(D)** SIM of HCV (Cy5) and HCV NS5A (Alexa594) (scale bar ≈ 3.7 μm) in infected Huh-7.5 cells 48 hpi. **(E)** Primary induced pluripotent stem-cell (iPSC)-derived hepatocyte-like cells imaged 1 week post infection [181] using confocal microscopy (scale bar ≈ 4.7 μm). Alexa594 (green) imaging performed without probe sets as a control to aid in the identification of frequent lipid-like autofluorescent foci (green arrows) distinct from diffraction-limited spots specific to the delivered probe set. **(F)** Primary human fetal liver cells (HFLCs) imaged 48 hpi by the J6/JFH Clone 2 strain of HCV (Z-stack projection, scale bar ≈ 4.2 μm).

ISG mRNA transcripts in individual cells pre-IFN (gray) or at various times post-IFN-β treatment (10 U/mL) (red) for *EIF2AK2* (*Left*) and *ISG15* (*Right*). Means are shown as dashed or solid lines for pre- and post-IFN treatment, respectively. Difference between pre-IFN and 6 hours post-IFN are statistically significant for both *EIF2AK2* (****$p < 0.0001$) and *ISG15* (****$p < 0.0001$). All differences between post-treatment IFN time-points are non-significant (n.s.) for both *EIF2AK2* and *ISG15* ($p > 0.05$) as determined by one-way ANOVA with Tukey's post-test. **(C)** Number of HCV positive strands in individual cells pre-IFN-β and post-IFN-β (10 U/mL) for 12 h (means in black). Difference was n.s. by two-tailed *t* test ($p > 0.05$). **(D)** Single-cell distribution of number of positive strands visualized as frequency histogram reveals bimodality with (i) poorly infected and (ii) highly infected modes. **(E)** Number of ISG transcripts in individual cells for both *EIF2AK2* (*Left*) and *ISG15* (*Right*) (means in black). On each plot, the number of transcripts in uninfected cells is shown (HCV-), and on the right (HCV+), the number of transcripts is presented for each cell after splitting cells into a poorly and highly infected bin based on the number of positive strands (using 200 strands as a threshold). The difference in ISG expression between uninfected cells and poorly infected cells is n.s. for both *EIF2AK2* and *ISG15* ($p > 0.05$) as determined by two-tailed *t* test. The difference in ISG expression between poorly and highly infected cells is highly significant for both *EIF2AK2* (****$p < 0.0001$) and *ISG15* (****$p < 0.0001$) by two-tailed *t* test. 99

Chapter 1. Introduction

1.1. Motivation: advancing the study of viral infection

Viruses are obligate intracellular parasites that infect most known forms of life, and human viruses such as the hepatitis viruses, influenza virus, and human immunodeficiency virus mount a significant disease burden worldwide. The development of antivirals and vaccines hinges on our understanding of viruses. Since the onset of modern virology in the 19th century, researchers have made strides in understanding the origin and evolution of viruses, the viral life cycle, viral pathogenesis, and host-virus interactions. As in scientific research broadly, many of these discoveries have been the direct result of advances in tools to assist with experimental investigation. The use of Chamberland filters in the late 1800s revealed that viral infectious disease was comprised of material smaller than bacteria. Advances in cell culture and epidemiology in the early 1900s revealed that variants of the same virus isolated from different geographic locations had phenotypic differences that could change, suggesting that viruses had mutable genetic material like other forms of life. Developments in x-ray crystallography enabled the first visualization of virions in the mid-1900s. And the relatively recent emergence of recombinant DNA technology in the 1900s opened the door to reverse genetics for dissecting viral gene function. In this thesis, we consider the study of a clinically relevant liver virus, hepatitis C virus (HCV). Despite research progress, much about HCV host-virus interactions remains experimentally intractable due to the limitations of existing research tools. The overall goal of this thesis was to leverage advances in cell sourcing, tissue engineering, and high-content imaging to develop technology platforms for overcoming these limitations.

1.2. A clinically relevant pathogen: hepatitis C virus

1.2.1. Hepatitis C virus as a major clinical problem

Hepatitis C virus (HCV) is transmitted parenterally [1-3]; after the molecular identification of HCV and development of diagnostics [4, 5], unsafe therapeutic injections was largely supplanted by intravenous drug use as the primary mode of transmission in developing nations [1, 2]. With a notable tendency towards establishing a chronic liver infection in as many as 80% of infected patients [1, 3, 6, 7], HCV has reached epidemic proportions, chronically infecting 170-200 million individuals worldwide [1, 3, 8]. HCV is five times as prevalent as human immunodeficiency virus 1 (HIV-1), and indeed the most common chronic blood-borne infection in the United States [1, 9]. Acute infection is typically asymptomatic and thus not diagnosed [1, 3, 10], but persistent infection and consequent liver inflammation leads to hepatic fibrosis over decades post infection [1, 3, 6, 7] ; as such, HCV is the major cause of chronic liver hepatitis, cirrhosis, and hepatocellular carcinoma (HCC) worldwide [10, 11], the major cause of death from liver disease [3], and the leading indication for liver transplantation [1, 3, 10, 12, 13]. Despite ongoing effort, there is no HCV vaccine available [14], and the standard-of-care therapeutic cocktail of pegylated interferon (IFN)-α and ribavirin is ineffective in 50% of patients [15]. As such, HCV places a significant burden on the global healthcare system [16]. Drug development research [17] has recently culminated in the development of the exciting new protease inhibitors telaprevir and boceprevir that can enhance the cure rate of interferon therapy to 75-90% of patients [18, 19]; despite this impressive advance, however, research towards the development of prophylactics and therapeutics must continue unabated [20] given that we still cannot treat 10-25% of patients, the side effects and costs of these therapies, and the looming fear of resistance emergence.

1.2.2. Molecular nature and life cycle

Viruses consists of populations of viral particles or virions [21]. These virions contain the viral genetic nucleic acids that describe how to build new virions and perform viral processes. As obligate parasites, they depend on hosts to execute their life cycle, which consists of virion entry into cells, replication of the genetic material within cells, assembly of new virions, and dissemination from the infected cells for transmission (**Figure 1-1**). Despite debate regarding the classification of viruses as living organisms, viruses are subject to the same Darwinian forces of evolution which tend to maximize ability of viruses to replicate and successfully transmit themselves. As such, viruses have evolved very different structures and functional strategies in order to enhance their transmission, and information about viruses should always be interpreted in this context.

A member of *Flaviviridae hepacivirus* genus [22], HCV is classified in the same family as yellow fever virus and dengue virus. HCV is an enveloped, single-stranded RNA virus – HCV virions consist of a single strand of RNA packaged within a protein capsid that is in turn enclosed within a glycoprotein-studded lipid bilayer envelope. The single strand of RNA, which is the HCV genome, is approximately 10 kilobases (kb) long, and has 5' and 3' untranslated regions (UTRs) [11, 23]. The 5' UTR includes an internal ribosomal entry site (IRES) that is able to recruit ribosomes in infected hepatocytes without a 5' cap [24]; because the 5' and 3' UTRs flank a single open reading frame, ribosomal recruitment leads to the production of one large polyprotein on the endoplasmic reticulum membrane. This polyprotein is subsequently cleaved by host and viral proteases to generate the 10 viral proteins that enact the HCV viral life cycle.

The proteins are divided into two categories – the structural proteins (core, E1, and E2) and the non-structural proteins (p7, NS2, NS3, NS4A, NS4B, NS5A, and NS5B). While the structural proteins comprise the virion capsid and membrane glycoproteins, the non-structural proteins have various functions such as replication, antagonism of immunity, and assembly of new virions for infecting other hepatocytes as well as maintaining an infectious blood reservoir for transmission to other humans.

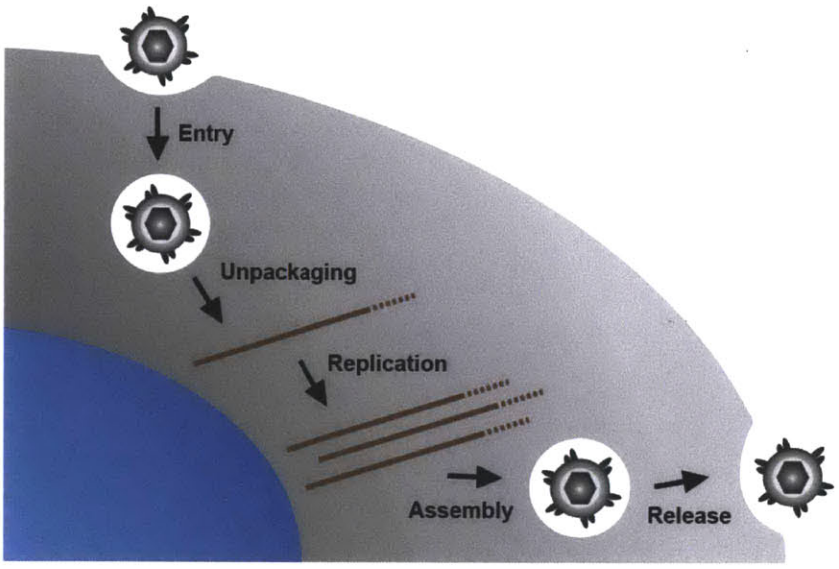

Figure 1-1. Essential steps of the viral life cycle for hepatitis C virus (HCV). HCV virions enter target hepatocytes, and from within the endosomal compartments, undergo a complex series of un-packaging reactions that culminates in release of the viral nucleic acid into the cytosol. This nucleic acid is known as positive-sense, because it is able to directly recruit a ribosome using an internal ribosomal entry site (IRES) and direct the production of viral proteins. These proteins are localized on the endoplasmic reticulum, from where they help replicate the viral genome (through a negative-sense replicative intermediate that cannot direct protein synthesis); perform essential viral functions such as disruption of host immune responses; assemble new virions; and ultimately disseminate them from the cell. This same framework – a life cycle "flow" from entry to release – holds for viruses broadly.

1.3. How we study hepatitis C virus: model systems and assays

Model systems and assays are two central tools in the study of biology and the focus of this thesis. In this section, we discuss these tools and their use for investigating hepatitis C virus.

1.3.1. Model selection and development

In vitro (cell culture) and *in vivo* (animal) model systems are central to the advancement of basic biology and therapy development. No model is perfect, but at the cost of sacrificing completeness, models enable researchers to experimentally manipulate and interrogate biology. Model systems can be evaluated in terms of numerous parameters, including the extent of normal physiology or pathophysiology they are presumed to capture; their amenability to certain types of experimentation; their accessibility to investigators; and their technical complexity and associated costs. Models have pros and cons in terms of such parameters, and it is important to choose a model appropriate for the research goal, which could vary from answering a specific biological question to high-throughput screening of compounds for therapeutic efficacy. Model selection is nontrivial; the discontinuity and nonlinearity of biology makes it difficult to predict whether a given model will faithfully recapitulate physiology in the domain of inquiry, even given evidence of "good behavior" in related domains. Of course, pragmatism mandates that we make such educated guesses in model selection, but it is thus important to understand that any model alone has unclear relevance to "true" physiology (put in quotations as we are gradually appreciating significant inter-person variation in physiology, rendering "true" physiology an elusive notion). Findings made in one model will ideally be coupled with findings made in other models, as consensus between various model systems is presumably more reliable.

These concepts of model selection guide model development, the goal of which is to create models that improve one of the above-mentioned evaluation parameters of models; e.g. producing a model that captures more of a particular domain of physiology, or a miniaturized model that is amenable to high-throughput screening. In this thesis, we describe two model development projects with the former goal – helping virologists study infection phenomena that were previously intractable with existing models. We focus particularly on the development of *in vitro* models; this work runs in parallel to exciting work being performed both in our lab and in others for the development of animal models for HCV. *In vivo* models have important pros and cons relative to *in vitro* models. They permit an appreciation of complex features for which *in vitro* models may be too simplistic, such as systems-scale phenomena across numerous organ systems, pharmacodynamics and bio-distribution, and off-target effects of interventions; further, they are central to the current Food & Drug Administration (FDA) paradigm for drug translation. However, *in vivo* models are costly, not as easily accessible, not as amenable to experimentation, and morally questionable. On the other hand, *in vitro* model systems are relatively cheap and amenable to high-throughput screening, far more accessible, have greater experimental flexibility, and generally do not raise ethical questions; as such, they are the staple of most research programs. The author believes that there is another often under-appreciated advantage of *in vitro* models. The thought leader Richard Feynman once said, "What I cannot create, I do not understand;" to this end, *in vitro* model systems permit us to more fully understand bio-systems from a "bottom-up" methodology that will ideally intersect with "top-down" studies performed *in vivo*. Conversely, the author also believes that there is an over-cited limitation of *in vitro* models. The prevailing view and practice of science and translation almost force us to believe that *in vitro* model systems sacrifice a large portion of normal physiology that *in vivo*

models "obviously" represent more accurately. However, it is unlikely that this is strictly true for all or even most bio-systems given that animals may be a poor reflection of human physiology; that *in vitro* models at least permit the study of human cells; and that *in vitro* models enable manipulation of cells to address very specific questions of interest, easing the interpretation of findings in these models. The author feels that a more balanced view of the relative roles of *in vitro* and *in vivo* models will be in order; this will be particularly important given that both governmental and commercial entities are placing increasing fiscal constraints on biomedical research that may deter significant *in vivo* experimentation. Progress to this end could benefit from research aiming to more methodically understand how model systems recapitulate certain components of physiology but not others, improving our ability to predict the regimes within which they converge to or diverge from a reasonable approximation of "true" physiology. The use of tissue engineering and microtechnology tools in developing "human-on-a-chip" models of physiology is a promising step forward.

1.3.2. Models of hepatitis C virus infection

Because of the narrow species tropism of HCV, the only robust *in vivo* model system is the chimpanzee [25], which is very costly, general unavailable, and morally questionable. Recently, several groups have demonstrated progress in developing humanized mouse models of HCV infection [26, 27], though these still suffer from general inaccessibility and unreliability. As such, investigation of HCV *in vivo* continues to be challenging, forcing many investigations to remain *in vitro*.

This thesis focuses on HCV *in vitro* model development. In a simple sense, an *in vitro* model system for studying viral infection requires two parts – some component of the host, and some component of the virus. If uniting these two components enables some part of the viral life cycle to occur, the combination constitutes an *in vitro* model of HCV infection. Parallel to the difficulties of studying HCV *in vivo*, HCV research has undergone a long and tortuous trajectory of *in vitro* model development, involving numerous host cell models, viral RNAs, and sources of virions [23, 28-32]. One major challenge in HCV research has been the notorious challenge associated with culturing primary hepatocytes [33-36], which has forced researchers to rely on hepatoma cell lines that dubiously replicate hepatic phenotype, displaying abnormal cell proliferation, dysregulated gene expression, dysfunctional mitochondria, aberrant signaling, and abnormal endocytic functions [37-45]. Cultivation of HCV in these cell lines proved difficult, requiring investigators to utilize transfection of sub-genomic and genomic viral RNAs to observe any replication. Twenty years after the discovery of HCV [4, 5], research revealed that the problem was due to the lack of both an appropriate strain of HCV that could replicate in culture as well as an appropriate cell line – it was only after the coupling of the Huh-7 hepatoma cell line [46] with the Japanese fulminant hepatitis (JFH)-1 strain of HCV [47] that a successful model of the full HCV life cycle was developed [48-50]. The current state-of-the-art model for robust HCV infection involves the infection by JFH-1 and its derivatives of the particularly permissive Huh-7.5 sub-line [51], whose unique permissiveness is likely due to defective innate immune signaling [52]. Unfortunately, despite significant research efforts, it remains unclear why only JFH-1 and its derivatives are infectious *in vitro*, and why the Huh-7 hepatoma cell line is uniquely permissive.

Though the JFH-1/Huh-7.5 model has proven invaluable to HCV research, it has at least three major limitations. First, hepatoma cells diverge significantly from primary adult hepatocytes as described, often rendering it challenging to interpret findings. Further, primary adult hepatocytes may also be superior for certain therapeutic development applications, as they have more physiologic absorption, distribution, metabolism, and excretion/toxicity (ADME/tox) properties [53]. Studying infection in primary adult hepatocytes would only be possible with platforms that enable primary hepatocytes to maintain their liver phenotype long-term. A second limitation of the JFH-1/Huh-7.5 model is that because Huh-7.5s are derived from one original donor, they fail to capture genetic variations between individual people; this forces researchers to contextualize findings within the background of a single individual. Genome-wide association studies (GWAS) have demonstrated genetically driven inter-host differences in HCV infection natural history and treatment response [54-56], but cell culture models that enable the investigation of infection in different genetic contexts do not exist. As such, it would be ideal to "personalize" the study of HCV infection. Finally, a third limitation of the JFH-1/Huh-7.5 model is that it cannot be generalized to the study of non-JFH-1-based strains of HCV. It is recognized that different strains of HCV can have significant variations in terms of pathogenesis and treatment response [23], and an ideal model of HCV infection would enable studies of HCV infection broadly.

1.3.3. Assays for hepatitis C virus infection

Infection is a complex process involving the interplay between host and virus, starting at the subcellular level; host properties shape viral behavior, and viruses in turn modulate the host. Ideal assays would provide a window into the systems biology of this process. Unfortunately, existing assays – such as polymerase chain reaction (PCR) for host/viral nucleic acids and

immunostaining for viral proteins – blindfold researchers in several ways. First, most assays are suboptimally sensitive and specific, requiring the accumulation of sufficient viral material for detection, and having poor discrimination between viral positive and negative strands; sensitivity for HCV assays are especially poor in primary culture systems which have high autofluorescent background and low infection. Further, they are generally bulk, involving lysis of populations of cells for quantifying host/viral RNAs or viral proteins and thus sacrificing single-cell phenomena. Additionally, most assays involve terminal processing and thus do not enable long-term monitoring of infection behavior [57]. Another limitation is that assays typically do not yield much information, at best returning quantification of a single parameter. Access to tools that overcome these limitations will prove invaluable in better elucidating host-virus interactions, and quantitative, multi-parametric data in general will help advance our understanding of infection through mathematical modeling.

1.4. Advances in cell sourcing, tissue engineering, and high-content imaging

1.4.1. Advances in hepatocyte sourcing

Hepatocytes can proliferate *in vivo* [58-61], but despite extensive research, human hepatocytes have not been made to proliferate *in vitro*. Because human hepatocytes are necessary for the investigation of human hepatotropic pathogens such as HCV which have a narrow species tropism, and because it is not practically feasible to obtain sufficiently large quantities of adult hepatocytes from a single human host, alternative strategies are being pursued to source *in vitro* liver modeling. Advances in stem cell research are one promising avenue for hepatocyte sourcing. Functional hepatocyte-like cells have been obtained from embryonic stem cells [62-68], fetal and adult progenitor cells [69-75], and extra-hepatic stem cells and progenitors [76]. A

major recent advance is the discovery that expression of certain transcription factors in "terminally" differentiated cells induces reprogramming into pluripotent cells, known as induced pluripotent stem cells (iPSCs) [77-81]; these iPSCs can in turn be directed towards hepatocytes [82-84]. This raises the exciting possibility of obtaining virtually limitless hepatocytes in the same way as ES cells, with the exciting added advantage of being able to produce person-specific hepatocytes from arbitrary individuals of diverse genetic backgrounds. This feature will be employed in the efforts to "personalize" the study of HCV infection described in this thesis.

1.4.2. Advances in *in vitro* liver model development

Since its inception as a field [85], tissue engineering has broadened in scope to be appreciated as the use of the tools, methods, and analyses of classic engineering to engineer cellular constructs for both regenerative medicine as well as models of physiology and pathophysiology. Classic model development by basic biologists has typically involved random, two-dimensional cultivation of cell types. While this has proven fruitful for a vast body of research, the application of tissue engineering to developing more complex models has broadened the range of biological phenomena we can recapitulate *in vitro* [86-88].

Particularly relevant to this thesis is the *in vitro* modeling of liver. Given the challenge associated with cultivating primary hepatocytes *in vitro* [33-36], researchers have employed numerous alternative liver platforms including perfused whole organs, wedge biopsies, and precision-cut liver slices [36, 89, 90]; purified liver fractions and single enzyme systems [91, 92]; and cell lines from hepatoblastomas or immortalization of primary hepatocytes [93-96]. However, since primary hepatocytes are the ideal platform, many efforts have been made to stabilize their

phenotype *in vitro*, initially by manipulating three basic parameters: culture medium, extracellular matrix, and heterotypic interactions with non-parenchymal cells. Researchers have used serum-free culture medium preparations [97]; culture medium supplemented with serum, physiological factors such as hormones and amino acids [33, 98, 99]; non-physiologic factors such as phenobarbital and dimethylsulfoxide [100, 101]; and medium with elevated oxygen tension [102]. Extracellular matrix and alternate surface chemistries, both in monolayer or gel configurations, have been utilized to control attachment and maintain hepatocyte phenotype by presenting specific biological and mechanical stimuli [33, 103-110]. Finally, co-culture with nonparenchymal cells has successfully been used to provide hepatocytes with heterotypic interactions that preserve their liver phenotype [45, 111]. Aside from such two-dimensional culture schemes, it is possible to manipulate primary hepatocytes such that they aggregate into three-dimensional spheroids on various surfaces upon which they can be cultured with improved longevity [33, 104, 112-126]; alternatively, spheroids can be encapsulated to control cell-cell interactions [127-130]. Numerous bioreactor cultures of hepatocytes and hepatocyte aggregates have also been developed, with advanced features such as fluid flow, precise control over culture parameters, and recapitulation of liver nutrient and oxygen gradients [34, 36, 131-140].

A major advance in the development of *in vitro* model systems is the manipulation of cell-cell and cell-matrix interactions using microtechnology tools adopted from the semiconductor industry [141-145]; these tools also enable miniaturization of assays [146], studies with dynamic control of stimuli [145, 147], and assembly of complex cellular structures [148, 149]. Our lab has used micropatterning methods to control the balance between homotypic and heterotypic interactions in primary hepatocyte co-cultures with nonparenchymal stromal cells [45, 150]; the

resulting micropatterned co-cultures (MPCCs) provide long-term expression of liver-specific functions, and is the basis of the primary hepatocyte HCV model development efforts described in this thesis.

1.4.3. Advances in high-content imaging

The increasing sophistication of imaging and downstream image analysis are giving rise to assays that simultaneously reveal many kinds of information about bio-systems of interest; these high-content or multi-parametric imaging modalities are powerful tools for accelerating biology and enabling high-throughput screening [151-157]. One class of such technologies is imaging methods for quantitatively assessing the molecular composition of single cells, in turn illuminating inter-cell biochemical and phenotypic heterogeneity [158-162]. As RNA viral genomes are central to the infect by RNA viruses such as HCV, and because host gene expression can be viewed at the messenger RNA level, we are particularly interested in imaging assays that could overcome limitations of existing assays in the detection of RNA. A relatively recent breakthrough in RNA imaging is quantitative single-molecule RNA imaging [163-172]. Through experimentally facile methods and standard epifluorescence microscopy, it is possible to visualize single molecules of RNA, allowing single-cell quantification and RNA localization; it is also possible to multiplex numerous RNA species simultaneously, synergistically enhancing the information obtained [173]. In this thesis, we will use single-molecule RNA imaging in our efforts to develop an infection assay that better reveals the host-side of infection.

1.5. Thesis overview

The overall goal of our research is to enable investigators to better understand the host-virus interactions in HCV infection. The state-of-the-art model systems and assays for studying HCV *in vitro* suffer from several limitations as described. In this thesis, we employ advances in cell sourcing, tissue engineering, and high-content imaging to provide technological solutions to these problems. Further, we demonstrate the value of these platforms by exploring innate immune signaling, an aspect of host-virus interactions for which existing tools have been particularly limiting. The technologies developed here address questions that can be conceptualized at three progressively smaller size scales (**Figure 1-2**). First, we describe a "personalized" *in vitro* model of HCV infection that can be used to elucidate inter-host variations in infection. We then develop a primary hepatocyte model for HCV infection that we use to understand how innate immune signaling in the liver controls viral infection. Finally, we detail a quantitative imaging assay for studying the intercellular heterogeneity of viral infection. We conclude with perspectives and future directions for these projects.

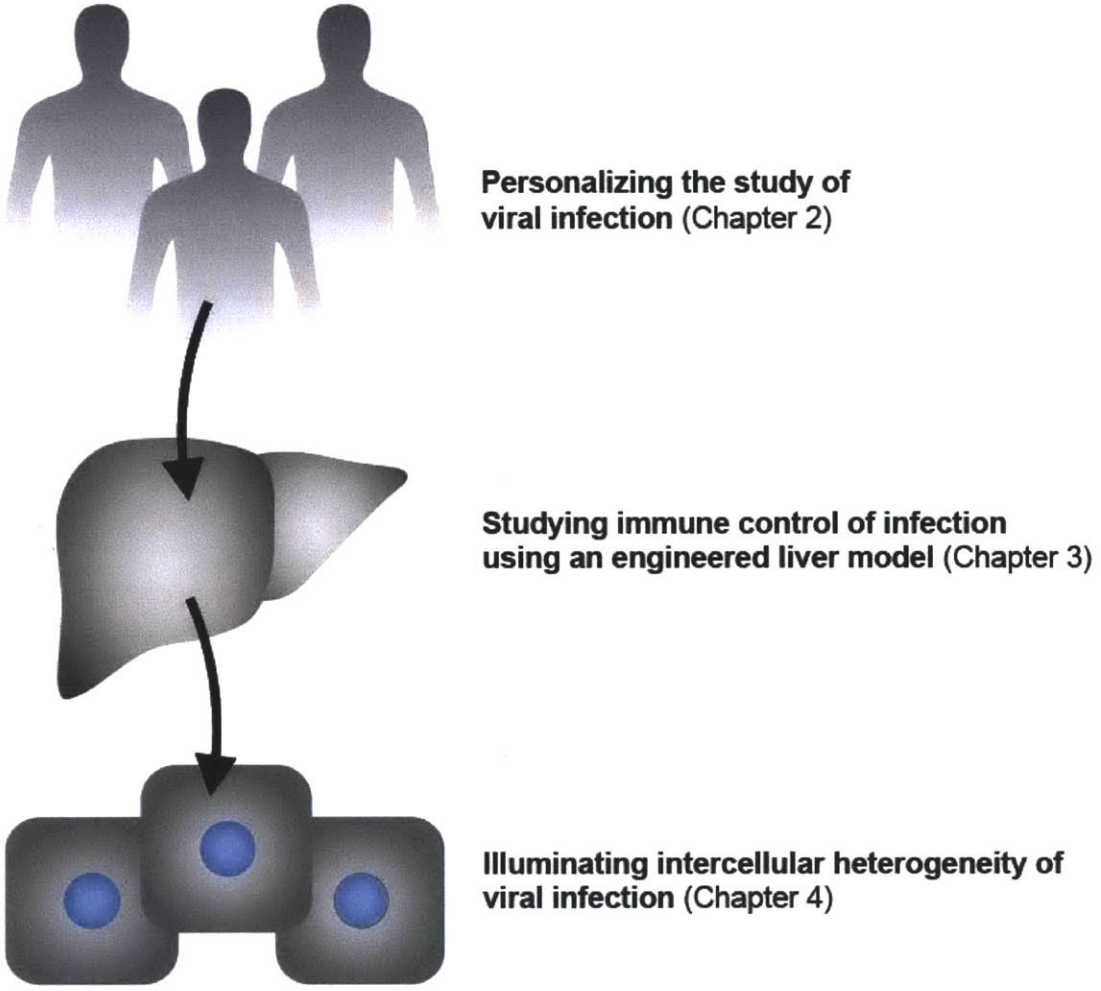

Figure 1-2. Thesis overview: addressing questions of host-virus interactions at three size scales. At the person size scale, we develop a technological solution to understanding differences in infection between individual people. We then create a model to understand the organ-scale question of how liver immunity controls hepatotropic infection. Finally, we describe an imaging assay for capturing the cellular compartmentalization of virus among individual host cells and the host gene expression interplay with the virus.

Chapter 2. Personalizing the study of viral infection

2.1. Introduction

Human pathogens impact patient well-being through complex host-pathogen interactions. Despite the importance of host genetics in this interplay, *in vitro* model systems for studying the role of host genetic variation in infection are often unavailable due to tissue scarcity and challenges in primary culture. The discovery of cellular reprogramming and the ability to generate host- and tissue-specific cells from induced pluripotent stem cells (iPSCs) have the potential to transform the study of development, infectious disease, and degenerative disorders [174, 175]. For example, iPSCs have been used for the mechanistic study of a variety of cells types implicated in a wide diversity of disease (e.g. Friedreich's ataxia, long QT syndrome, LEOPARD syndrome, Rett syndrome, and alpha-1 antitrypsin deficiency) [176-180]. However, no iPSC models of any infectious disease have been reported to date. In this study [181], we describe the use of iPSC-derived hepatocytes as a model system for studying host-pathogen interactions for the hepatitis C virus.

Afflicting over 170 million worldwide, hepatitis C virus (HCV) is a prototypic pathogen for which host genetic factors have been implicated in modulating disease natural history and treatment response but whose functions remain poorly understood due to the lack of robust experimental systems. For example, genome-wide association studies have identified host polymorphisms in the interleukin-28B (IL-28B) locus that correlate with spontaneous HCV clearance and viral response to interferon-based therapy [54]. Additionally, individuals with mutations in genes that are critical for HCV entry (e.g. LDLR, CD81, SRBI, CLDN1), assembly (ApoE, ApoB), or immune response (STAT1) have been described [54, 182-186]. Despite our

awareness that host genetics impacts viral pathogenesis in such individuals, the mechanistic basis for these correlations remain unclear due largely to the lack of a robust experimental system incorporating host cells with these genetic backgrounds. The development of an iPSC-derived HCV model has the potential to further elucidate the role of these host factors on disease pathogenesis.

2.2. Results and discussion

2.2.1. Induced pluripotent stem cell-derived hepatocyte-like cells (iHLCs) express HCV host factors

To test the hypothesis that iPSC-derived differentiated cells are permissive to infection, we sought to model hepatitis C virus infection (**Figure 2-1**). HCV infects human hepatocytes, and we have recently demonstrated the directed differentiation of human iPSCs into hepatocyte-like cells (iHLCs) [82]. iHLCs routinely demonstrate an expected cobblestone morphology (**Figure 2-2A, *left***), and over 80% express both albumin and HNF-3β (**Figure 2-2A, *right***). In addition, iHLCs secrete liver-specific serum proteins such as albumin and alpha 1-antitrypsin at levels 15% and 50% respectively of those of primary human hepatocytes maintained in long-term culture models [187] (**Figure 2-2B, *bottom***). Here, we investigated whether iHLCs express host genes important for HCV infection ("host factors"), are capable of supporting the HCV life cycle, and respond to infection with an appropriate antiviral inflammatory response. We found that iHLCs express known HCV host factors including the liver-specific microRNA-122 (**Figure 2-2B**) and entry factors (CD81, SRBI, claudin-1, and occludin) (**Figure 2-2C,D**); analysis of iPSC and iHLC transcriptional microarrays [82] confirmed that host factors previously identified in an shRNA screen [188] were enriched in iHLCs, and expressed to a greater extent in iHLCs

than iPSCs (**Figure 2-2E**). Although iHLCs exhibit many adult hepatocyte characteristics, their expression of phase 1 and phase 2 enzymes (high CYP3A7, CYP7A1, and GSTA4 and low CYP2C family gene and CYP3A4 gene expression) and coexpression of alpha-fetoprotein and albumin is collectively more consistent with that of a fetal hepatocyte [82, 189, 190]. Experimental evidence suggests that iPSC are fully capable of differentiating into terminally differentiated adult hepatocytes as demonstrated in mouse IPS tetraploid complementation experiments and in mouse and human iHLCs transplantation experiments [82]; however, culture conditions have not yet been established that allow for terminal differentiation.

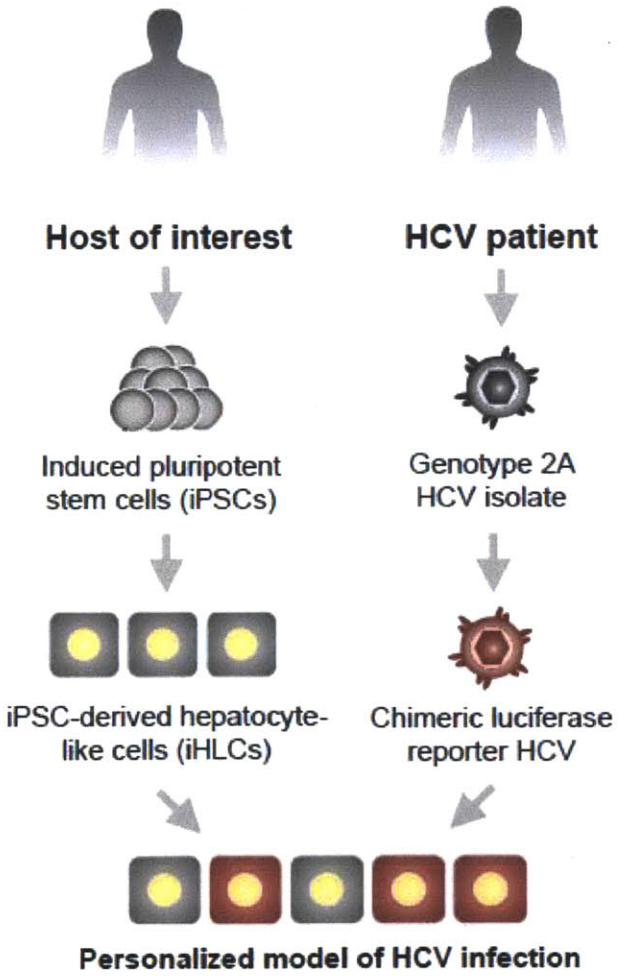

Figure 2-1. Personalized HCV infection model. Induced pluripotent stem cell-derived hepatocytes from one donor are infected with HCV from another.

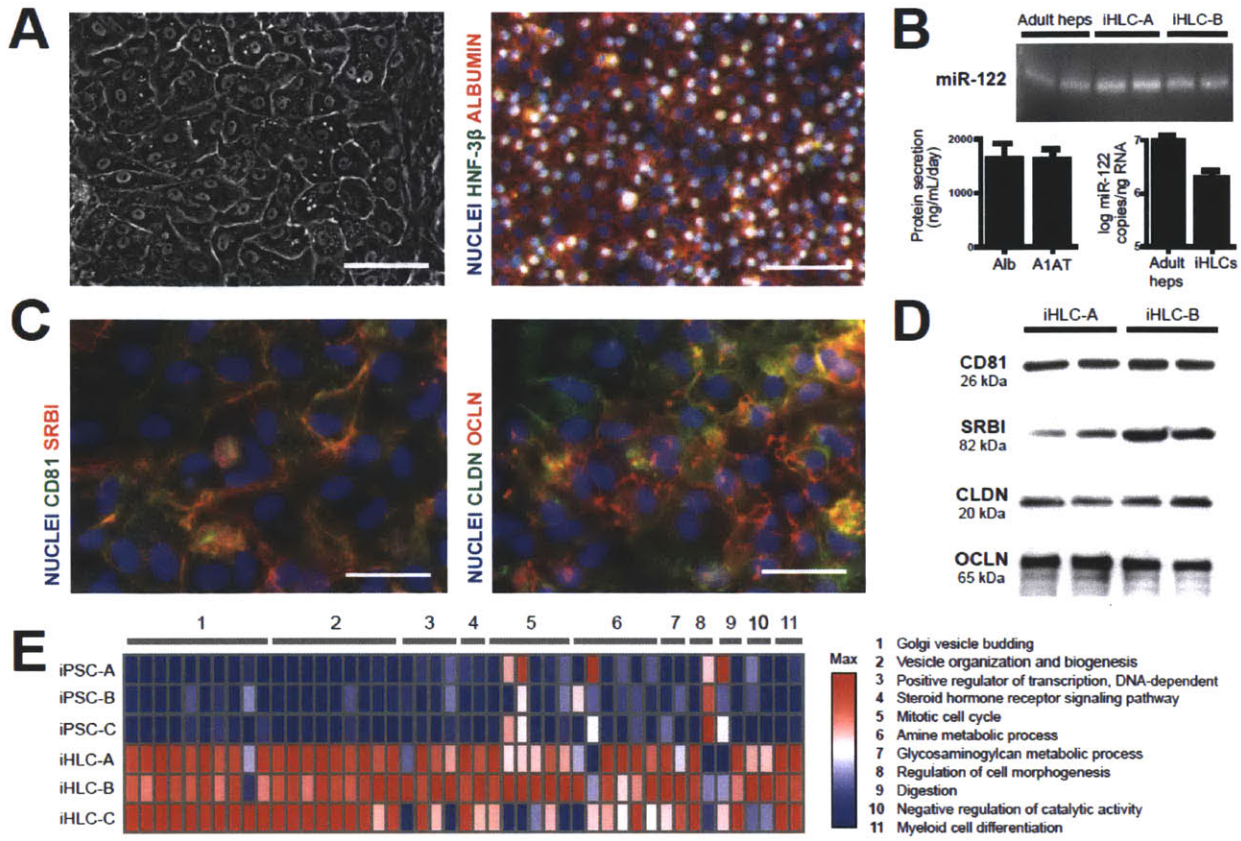

Figure 2-2. Induced pluripotent stem cell (iPSC)-derived hepatocyte-like cells (iHLCs) express known hepatitis C virus (HCV) host factors. (**A**) (***Left***) Phase image of iHLCs. Scale bar = 100 μm. (***Right***) Immunofluorescence imaging of iHLCs for albumin (red), HNF-3β (green), and DAPI (blue). Scale bar = 90 μm. (**B**) Quantification of liver-specific factors in iHLCs. microRNA-122 expression blot (for two typical batches of iHLCs, A and B) and quantification by qPCR. Adult human hepatocytes [187] included as a reference. Albumin (Alb) and alpha 1-antitrypsin (A1AT) secretion by iHLCs as measured by ELISA. Error bars show s.d. (**C**) (***Left***) Immunofluorescence imaging of iHLCs for HCV entry factors scavenger receptor BI (SRBI) (red) and CD81 (green), with DAPI co-staining (blue). Scale bar = 40 μm. (***Right***) Immunofluorescence imaging of iHLCs for HCV entry factors occludin (OCLN) (red) and claudin 1 (CLDN) (green), with DAPI co-staining (blue). Scale bar = 40 μm. (**D**) Western blot for HCV entry receptors CD81, SRBI, CLDN, and OCLN, in two typical batches of iHLCs (A and B) in duplicate samples. (**E**) Relative expression of HCV host factors [188] by three batches of iPSCs and iHLCs as determined through gene microarray [82] (A, B, and C). Host factors organized by gene ontology (GO) biological process terms, including repeats for genes associated with multiple terms.

2.2.2. HLCs support the entire life cycle of hepatitis C virus

To assess HCV replication in iHLCs, we used JFH-1, a genotype 2a HCV reporter virus expressing secreted *Gaussia* luciferase (GLuc) [191]. Persistent elevation of GLuc signal was observed in infected cultures above uninfected ("mock") control (**Figure 2-3A, *top***); further, initiating daily treatment with either the HCV NS5B replicase inhibitor 2'-C-methyladenosine (2'CMA) or the NS3/4A protease inhibitor VX-950 (telaprevir) 7 days post infection (dpi) rapidly abolished GLuc production (**Figure 2-3A, *top***). Further, qRT-PCR on iHLC lysates 14 dpi showed that HCV genomes were significantly more numerous in the absence of antivirals (**Figure 2-3B**), consistent with the GLuc assay. In addition, using a real-time fluorescence reporter of infection [192], we confirmed HCV protease activity in infected iHLCs (**Figure 2-3C**). Together, these results indicate ongoing HCV replication in infected iHLCs. To verify that infected iHLCs produce infectious virions and thus recapitulate the entire viral life cycle, culture supernatants were passaged 13 dpi onto uninfected Huh-7.5 cells which are highly permissive to HCV and thus allow sensitive detection of infectious virions [48]. As shown by GLuc production and HCV NS5A staining (**Figure 2-3A, *bottom***), supernatants from infected iHLCs carried infection to Huh7.5s. Thus, iHLCs support the complete HCV life cycle including replication and release of infectious virions. Therefore iHLCs sustain the entire HCV viral life cycle of at least genotype 2a, consistent with prior reports that have shown that human fetal hepatocytes are capable of sustaining the hepatitis C viral life cycle [193, 194]. Future work towards a fully personalized in vitro model of HCV infection would incorporate both personalized hepatocyte-like cells as well as HCV patient isolates, including the most HCV common genotype 1a.

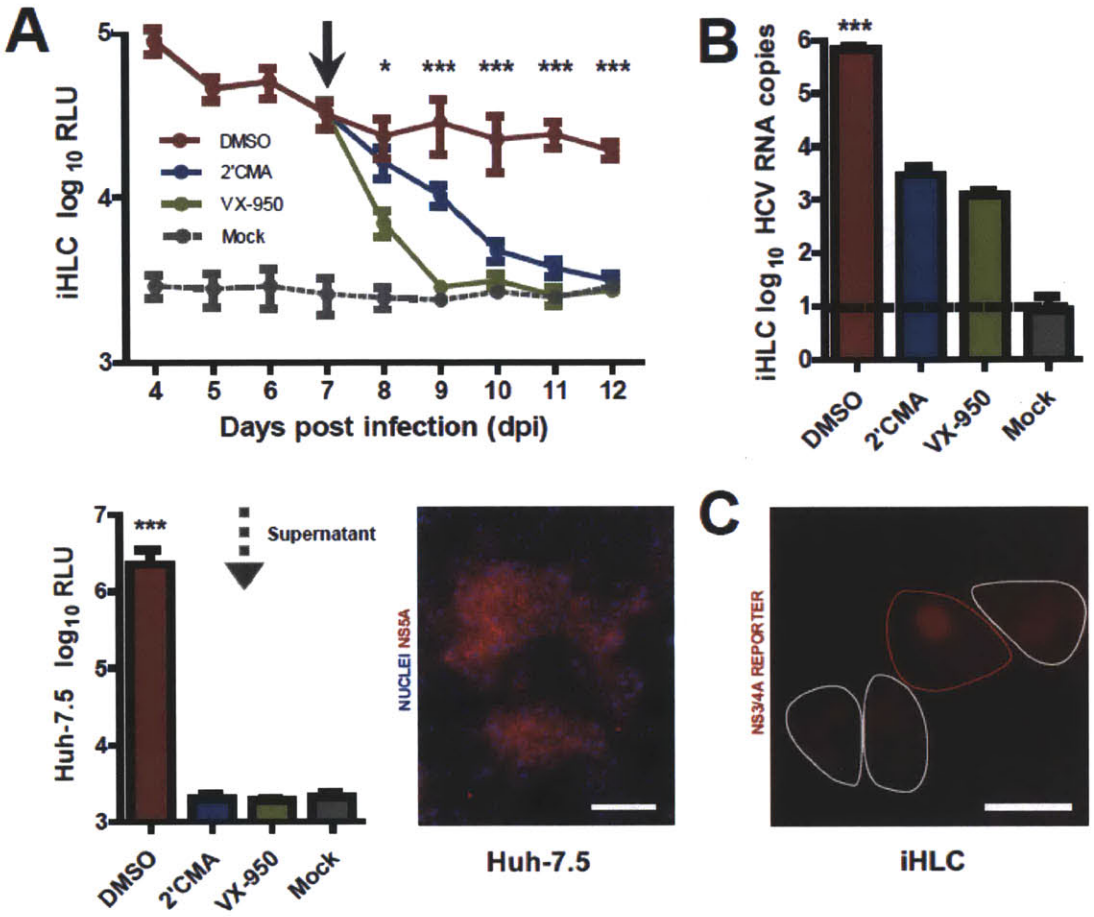

Figure 2-3. iPSC-derived hepatocyte-like cells (iHLCs) as a model for hepatitis C. (**A**) iHLC cultures were either infected with HCV reporter virus expressing secreted *Gaussia* luciferase (GLuc) (n=18) or mock infected (n=6), and subsequently sampled and washed daily. After 7 days (solid gray arrow), infected iHLCs were treated with NS5B polymerase inhibitor 2'CMA (n=6), NS3/4A protease inhibitor VX-950 (n=6), or vehicle DMSO (n=6). Drug treatment was discontinued 12 dpi, and supernatants collected after an additional day of culture were assayed for the presence of infectious virus by passage onto Huh-7.5s. Medium from Huh-7.5 cells was harvested 5 days post passage for GLuc assay. (***Top***) GLuc secretion by iHLCs. RLU = relative light units. DMSO- vs. 2'CMA-treated cultures was statistically significant: $*p < .05$, $***p < .001$ (one way ANOVA with Tukey post test). (***Bottom***) GLuc secretion by Huh-7.5s after passage of iHLC supernatants. DMSO vs. mock was statistically significant: $***p < .001$ (one way ANOVA with Tukey post test). NS5A staining of infected Huh-7.5s post passage. Scale bar = 50 μm. (**B**) iHLCs were lysed 14 dpi. Copies of HCV RNA in lysates were quantified by qRT-PCR. DMSO vs. 2'CMA was statistically significant: $***p < .001$ (one way ANOVA after log transformation with Tukey post test). (**C**) NS3/4A activity imaging of HCV-infected iHLCs [191]. Cells in image delimited by lines (white = uninfected, red = infected). Scale bar = 25 μm. Data in **A-C** are means, error bars show s.d.

2.2.3. HCV infection induces an antiviral inflammatory response from iHLCs

We next determined whether infection induces an antiviral inflammatory response, which is central to the natural history of clinical disease progression but defective in existing *in vitro* models of HCV [52]. qRT-PCR on iHLC lysates 2 or 14 dpi revealed that expression of inflammatory markers was upregulated by infection (**Fig. 4A**), and ELISA on culture supernatants 14dpi verified persistent TNF-α secretion as a result of infection (**Fig. 4B**). These results are characteristic of an ongoing inflammatory response in cells with an intact innate immune axis. Notably, IL-28B, whose gene variation predicts response to hepatitis C treatment in GWAS studies [54], was expressed in response to viral infection 2 dpi but declined over two weeks, underscoring the potential for such a platform to provide clinically relevant insights.

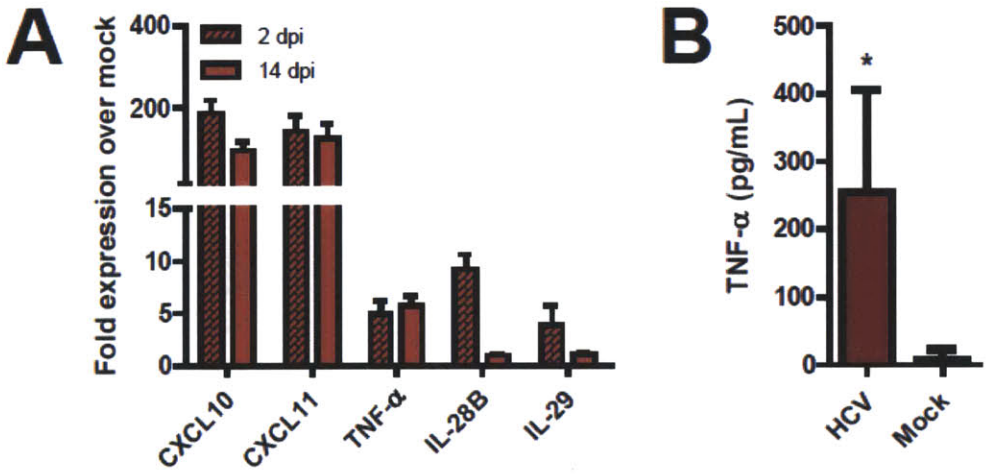

Figure 2-4. iPSC-derived hepatocyte-like cells (iHLCs) demonstrate an inflammatory response to hepatitis C virus infection. (**A**) mRNA expression of innate immune/inflammatory markers in lysates of infected, DMSO-treated iHLCs relative to mock at 2 and 14 dpi as determined by qPCR. (**B**) TNF-α secretion by HCV- and mock-infected iHLCs 14dpi as determined by ELISA. Difference was statistically significant: $*p < .05$. Data in **A** and **B** are means, error bars show s.d.

Existing model systems to study host genetics, such as polymorphisms in IL-28B, are limited to needle biopsies, surgical resection, organ donation and hepatoma cell lines of a single background. We believe that this study lays the foundation for 'personalized' *in vitro* models that can capture genetic variation of both host and pathogen whereby iPSCs can be generated from identified patients with known or unknown genetic defects that impact infection. In this study, we report that hepatocyte-like cells derived from iPSCs support the entire life cycle of hepatitis C virus including inflammatory responses to infection but we believe that in the future, patient derived iHLCs will serve as a new model system to probe the basis of hepatitis viral pathogenesis and can ultimately be extended to other pathogens and tissue systems. Such models will advance our understanding of host-pathogen interactions and help realize the potential of personalized medicine.

2.2.4 Personal contributions to this work

The author of this thesis planned, performed, and interpreted experiments in an equal collaboration with his colleague Dr. Robert Schwartz.

2.3. Materials and methods

Induced pluripotent stem cell culture and hepatocyte-like cell generation

Undifferentiated iPSC were maintained and differentiated into hepatocyte-like cells (iHLCs) as described [82]. In brief, iPSCs were cultured in monolayer on Matrigel (Becton Dickinson) and directed differentiation was achieved by sequential exposure to Activin A, BMP4, bFGF, HGF, and OSM.

HCVcc preparation, infection, luciferase assay, antiviral drugs, and NS3/4A activity imaging

As described [191], *Gaussia* luciferase expressing reporter virus Jc1FLAG2(p7-nsGluc2A) stocks were prepared by electoporating *in vitro* transcribed RNA into Huh-7.5 cells, collection of supernatant, and filter concentration. Fifty percent tissue culture infectious dose ($TCID_{50}$) was determined by titrating on Huh-7.5s to be 10^7 $TCID_{50}$/mL. These stocks were diluted 10x in serum-free, OSM-containing medium and used to inoculate iHLCs for 24h. Cultures were

washed with serum-free medium and propagated in OSM-containing medium. Supernatants were collected and frozen at -80C daily for luciferase quantification. To demonstrate drug-sensitive HCV infection, HCV NS5B polymerase inhibitor 2' C-methyl-adenosine (2'CMA) (EC50=27 nM) and NS3/4A protease inhibitor VX-950 (telaprevir) (EC50=400 nM) were added to culture medium at 50*EC50 and 25*EC50, respectively, at final 0.1% DMSO. 2'CMA was the gift of Drs. D. Olsen and S. Carroll (Merck Research Laboratories, West Point, PA) and also obtained from Carbosynth Limited. VX-950 was obtained from Alembic Limited. Real-time fluorescence reporter of HCV infection by monitoring NS3/4A protease activity was performed as described[8]. Briefly, lentivirus carrying the reporter was used to transduce iPSCs. Infection was carried out five days later, and protease activity was assayed 7 days post infection.

Huh-7.5 culture and infection transmission assay

Huh-7.5s were propagated in a DMEM with L-glutamine (Cellgro)-based medium containing 100 U/mL penicillin and 100 ug/mL streptomycin (Cellgro), and 10% FBS (GIBCO). To test if infected iHLCs produced infectious virions, iHLCs were placed in OSM-containing medium without supplementation with antivirals. Supernatants collected 1 day later were used to inoculate Huh-7.5 cells. After overnight incubation, cells were washed and placed in Huh-7.5 medium for 48h before being washed again. On day 5 post-inoculation, supernatants were assayed for luciferase as described [191]. To assess NS5A antigen expression, Huh-7.5 cells were fixed in methanol, counterstained with Hoechst (Invitrogen), and immunostained with mouse anti-NS5A (9E10) and goat-anti-mouse Alexa Fluor 594 (Invitrogen).

RT-PCR for detection of cytokines and HCV RNA

Total RNA was isolated with RNeasy Plus Mini Kit (Qiagen, Valencia, CA). First-strand cDNA was synthesized using Moloney murine leukemia virus (M-MLV) reverse transcriptase (Biorad). Quantitative PCR for cytokines was carried out with Taq polymerase and SYBR Green in supplier's reaction buffer containing 1.5 mM MgCl2 (Biorad). Oligonucleotide primer sequences are available by request. Amplicons were analyzed by 2% agarose gel electrophoresis. Quantitive PCR on HCV genomes was performed as described [191].

Immunofluorescence analysis for hepatic gene expression and host factor expression

iHLCs were fixed in four percent paraformaldehyde and/or -20oC methanol. Following washing and blocking in 0.1% donkey serum/0.1% Triton X-100 in PBS, cells were incubated in primary antibody overnight at 4C: mouse anti human albumin (Sigma-Aldrich), rabbit anti HNF-3β (Santa Cruz Biotechnology), mouse anti-human CD81 (Becton Dickinson), rabbit anti-CLDN1 (Invitrogen), rabbit anti-SCARB1 (Novus Biologicals), mouse anti human Occludin (Invitrogen). Secondary antibodies were donkey anti mouse DyLight 594-, donkey anti rabbit DyLight 488-, donkey anti mouse DyLight 488-, and donkey anti rabbit DyLight 594-conjugates and counterstained with Hoescht dye (Invitrogen).

Western blot for entry receptors

Total protein was extracted with RIPA lysis buffer, and samples were separated by electrophoresis on 12% polyacrylamide gels and electrophoretically transferred to a polyvinylidene difluoride membrane (Bio-Rad Laboratories). Blots were probed with mouse anti-human CD81 (Millipore), rabbit anti-SCARB1 (NB110-57591, Novus Biologicals), rabbit anti-CLDN1 (51-9000, Invitrogen), and rabbit anti-occludin (40-4700, Invitrogen), followed by horseradish peroxidase-conjugated secondary antibodies, and developed by SuperSignal West Pico substrate (Thermo Scientific).

miR-122 analysis

Total RNA was isolated with miRNeasy Mini Kit (Qiagen). miRNAs were polyadenylated by poly(A) polymerase and cDNA was synthesized using miScript PCR kit (Qiagen). Quantitative real-time PCR on miR-122 was then performed using hsa-miR-122 specific primer (Qiagen) and normalized to RNU6B (Qiagen). Standard curves were performed to obtain absolute levels with synthetic miR-122 (Dharmacon).

Albumin and alpha 1-antitrypsin ELISA

Spent medium was stored at -20 °C. Alpha-1-Antitrypsin and albumin media concentrations were measured using sandwich ELISA technique with horseradish peroxidase detection (Bethyl Laboratories) and 3,3',5,5'-tetramethylbenzidine (Thermo Scientific) as a substrate.

Microarray analysis and host factor expression

Microarray analysis was performed as described[4]. Microarray profiles on iHLCs (http://www.ncbi.nlm.nih.gov/geo/ accession number GSE14897) were analyzed using gene set enrichment analysis v2.0 with a list of previously identified HCV host factors[6]. Enriched genes were determined by random permutation of gene sets and a p-value<0.05. Gene ontology terms and gene associations were obtained using Gene Set Analysis Toolkit v2. Statistical analysis was performed using a hypergeometric distribution to identify terms enriched with two genes and a p-value <0.05, and then connected in a tree hierarchy [195].

Chapter 3. Studying immune control of infection using an engineered liver model

3.1 Introduction

Hepatitis C virus (HCV) remains a major public health problem, affecting approximately 130 million people worldwide. HCV infection can lead to cirrhosis, hepatocellular carcinoma, and end-stage liver disease, as well as extrahepatic complications such as cryoglobulinemia and lymphoma. Preventative and therapeutic options are severely limited; there is no HCV vaccine available, and nonspecific, interferon (IFN)-based treatments are frequently ineffective. Development of targeted antivirals and the advancement of HCV basic biology have been hampered by the lack of robust HCV cell culture systems that reliably predict human responses.

The recent advancement of the HCV cell culture (HCVcc) system [48] has enabled recapitulation of the entire HCV life cycle in human hepatoma cells. Despite the demonstrated value of these models to HCV research programs, these cell lines differ significantly from the natural primary hepatocyte host for HCV, displaying abnormal proliferation, deregulated gene expression, as well as aberrant signaling and endocytic functions [37-40]. Consequently, neither the perturbation of normal hepatocyte biology by infection, nor authentic host responses to HCV, can be studied accurately in culture [37]. Primary hepatocytes are considered a more physiologically relevant system, but are notoriously difficult to maintain in culture as they precipitously decline in viability and phenotype upon isolation from their *in vivo* microenvironment [45]. This rapid deterioration, as well as the lack of HCV detection methods with high specificity and sensitivity, has made it difficult to assess viral replication in primary human cell cultures [193, 196-200]. Over the last few decades, investigators have employed a

plethora of different strategies to preserve liver-specific functions *in vitro* and to extend the lifetime of liver model systems [150]. These strategies typically include extracellular matrix manipulations, defined culture media, fluid flow using bioreactors, or alteration of cell–cell interactions by forming three-dimensional (3D) spheroidal aggregates or co-cultivating with nonparenchymal cell types [34, 45, 121, 150]. Although some of these models provide necessary extracellular matrix cues, they lack crucial heterotypic cell–cell interactions and control over tissue architecture, both of which are known to affect liver-specific functions [45, 150]. Further, in culture techniques using fragile extracellular matrix gels, 3D aggregates, and/or continuous perfusion, scaling down to 96-well and smaller formats appropriate for drug screening remains challenging. Most importantly, it is unclear whether any of these model systems support persistent HCV infection.

First [201], we show the entire HCV life cycle recapitulated in micropatterned co-cultures (MPCCs) of primary human hepatocytes and supportive stroma in a multiwall format. MPCCs form polarized cell layers expressing all known HCV entry factors, and sustain viral replication for approximately two weeks. When coupled with highly sensitive fluorescence- and luminescence-based reporter systems, MPCCs have potential as a high-throughput platform for simultaneous assessment of *in vitro* efficacy and toxicity profiles of anti-HCV therapeutics.

Second, we address the question of why infection is resolved after only two weeks, a finding in our system that deviates from the expectation of a chronic virus. In particular, we test the hypothesis that IFN signaling controls HCV infection in MPCCs. The Huh-7.5 hepatoma cell line [51] used by most investigators suffers from numerous deficiencies including an inhibitory

mutation in RIG-I [52] that incapacitates IFN signaling; indeed, this may explain the robust infection observed in this model. By contrast, natural primary hepatocytes should be capable of mounting an innate immune response to infection. We show that IFN signaling constrains infection, leading to acute resolution of infection in MPCCs after two weeks. Inhibition of IFN signaling rescues the robust and chronic infection characteristic of infection *in vivo*. Finally, we show that a cytokine normally present in the liver microenvironment, interleukin-6 (IL-6), "tolerizes" hepatocytes to infection by inhibiting several components of the IFN/signal transducer and activator of transcription (STAT1) signaling pathway. As such, a refined MPCC model dosed with IL-6 recapitulates the more robust infection normally observed *in vivo*. These findings have implications for the mechanistic basis behind viral persistence *in vivo*.

3.2 Results and discussion

3.2.1. Primary human hepatocytes in micropatterned co-cultures form polarized cell layers and support HCV glycoprotein-mediated entry

We have recently developed a miniaturized, multi-well model of human liver tissue with optimized microscale architecture that maintains phenotypic functions for several weeks *in vitro* [150]. In this cell culture system, primary adult human hepatocytes do not seem to proliferate. Primary hepatocytes are organized into micropatterned colonies of empirically optimized dimensions, and subsequently surrounded by supportive stroma (**Figure 3-1**, **Figure 3-2a,b**). Here, we show that primary human hepatocytes form polarized cell layers in MPCCs. Multidrug resistant protein 2 (MRP2), zona occludens protein 1 (ZO1), and HCV entry factors claudin-1 (CLDN1) [202] and occludin (OCLN) [203, 204], were located in the canalicular domain of tight

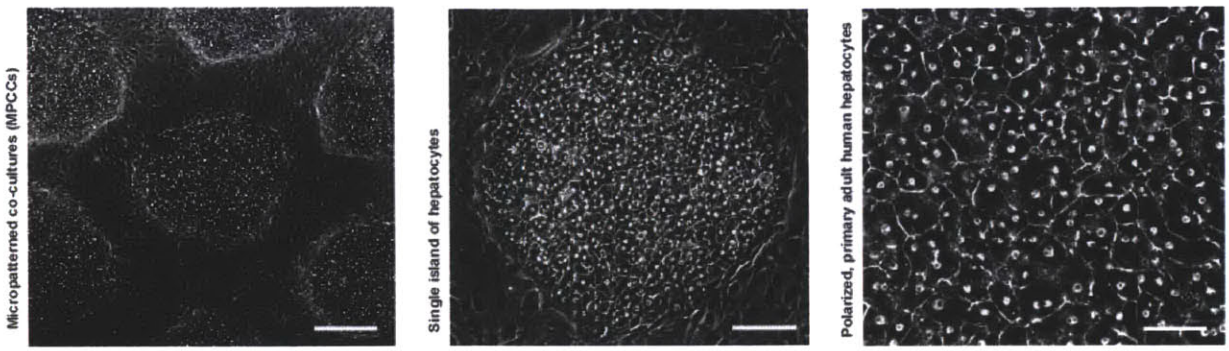

Figure 3-1. Micropatterned co-cultures (MPCCs) of human primary adult hepatocytes and supportive stroma. Progressively magnified phase images of hepatocytes in micro-patterned co-cultures (islands 500 μm in diameter).

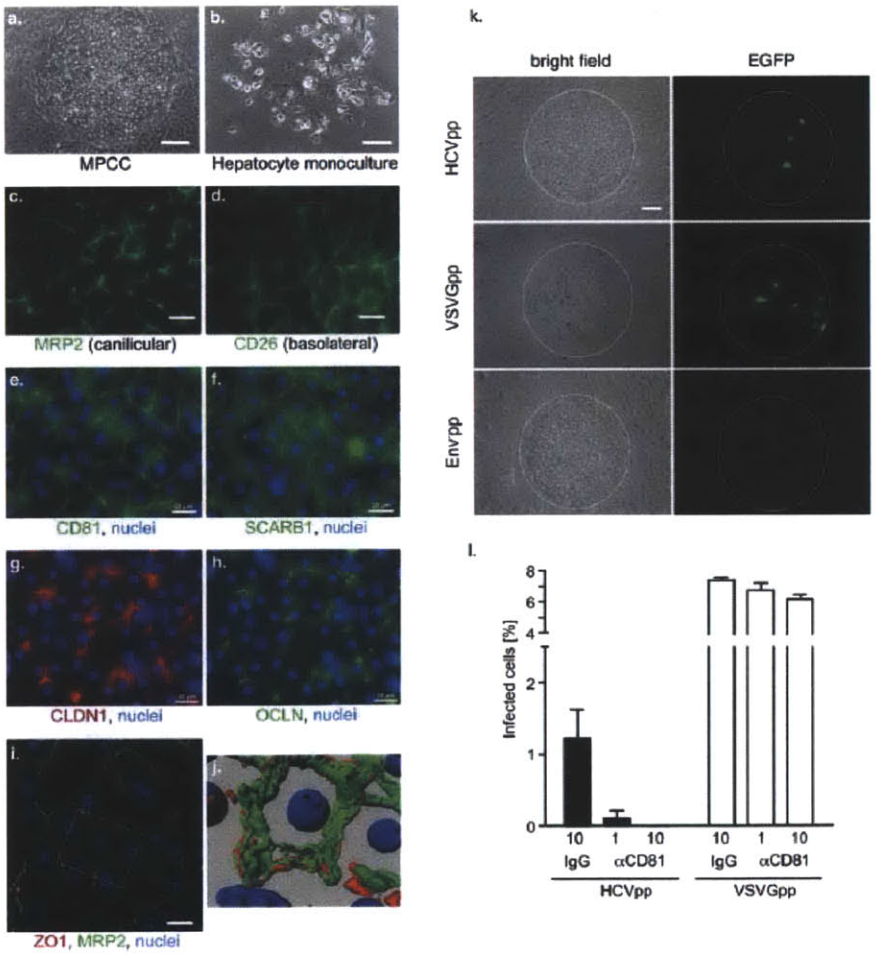

Figure 3-2. Primary human hepatocytes in MPCCs form polarized cell layers, express HCV entry factors, and support HCV glycoprotein-mediated entry. Bright

field images of primary hepatocytes in MPCCs (**a**) and in mono-cultures (**b**). Wide-field fluorescence images of fixed MPCCs stained for the canalicular marker multidrug resistance-associated protein 2 (MPR2) (**c**), and the basolateral marker CD26 (**d**). Nuclear (blue) and antigen-specific staining (green) for CD81 (**e**), scavenger receptor class B member 1 (SCARB1) (**f**), claudin 1 (CLDN1) (red) (**g**), and occludin (OCLN) (**h**) in MPCCs. (**i**) Merged image of primary hepatocytes stained for MRP2 (green), zona occludens protein 1 (ZO1) (red), and nuclei (blue). (**j**) 3D rendering of boxed area in (**i**). (**k**) Infection of MPCCs with retroviral pseudoparticles bearing HCV glycoproteins (HCVpp), vesicular stomatitis virus glycoprotein (VSVGpp), or no glycoproteins (Env-pp), and containing an enhanced green fluorescent protein (EGFP) reporter gene. Representative images are shown for all experiments. (**l**) Anti-CD81 antibody blocks entry of HCVpp (dark bars), but not VSVGpp (white bars). Concentrations of antibody (μg/mL) are noted. Mean and s.d. are shown. Scale bars: 100 μm (**a**, **b**, **k**), 50 μm (**c**, **d**), 20 μm (**e-i**).

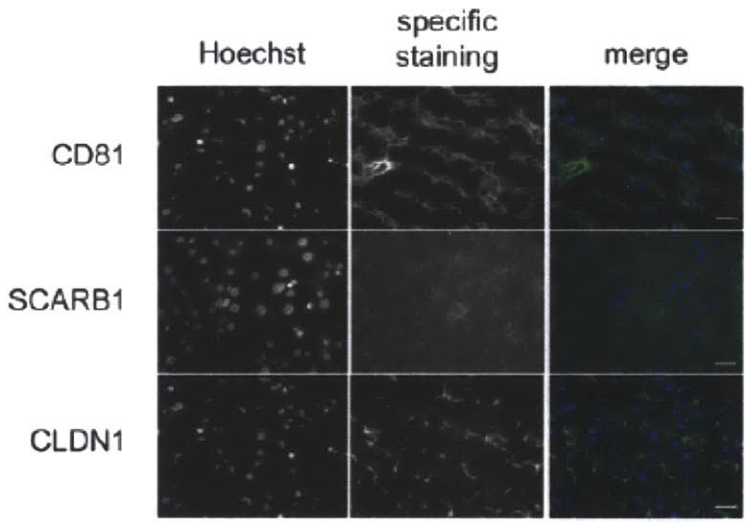

Figure 3-3. HCV entry factor staining in normal human liver. Wide-field fluorescence images of fixed sections of human liver from normal uninfected donors stained nuclei (blue in merged image) and antigen-specific staining (green in merged image) for CD81 (***Upper***), SCARB1 (***Middle***) and CLDN1 (***Lower***). Scale bars: 30 μm.

junction (TJ)-like structures, whereas CD26 was localized on the basolateral domain (**Figure 3-2**). The presence of bile canalicular structures between adjacent hepatocytes was confirmed via 3D renderings of ZO1 and MRP2 (**Figure 3-2i,j**). Compared to human liver tissue, primary

hepatocytes in MPCCs expressed similar patterns of HCV entry factors CD81 [205], scavenger receptor class B type 1 (SCARB1) [206], and CLDN1 [202] (**Figure 3-2**, **Figure 3-3**).

To test whether MPCCs support HCV glycoprotein-mediated entry, we infected cultures with HCV pseudoparticles (HCVpps). HCVpp, which are defective lentiviral particles that display the HCV E1 and E2 envelope glycoproteins, and encode an enhanced green fluorescent protein (EGFP) reporter gene, allow rapid quantification of infection in the absence of replication. Approximately 1–3% of the human hepatocytes in MPCCs, but none of the supporting murine embryonic fibroblasts (3T3-J2), could be infected with HCVpp (**Figure 3-2k,l**). Pseudoparticles lacking glycoproteins did not infect the cultures, although MPCCs were readily infected by pseudoparticles displaying the pan-tropic vesicular stomatitis virus glycoprotein (VSVGpp). A blocking antibody targeting CD81 completely abrogated HCVpp infection but not VSVGpp infection, consistent with HCV-specific dependence on CD81 (**Figure 3-2l**).

3.2.2. HCV persistent replicates in primary human hepatocyte MPCCs

Despite considerable effort, it has not been possible to unequivocally demonstrate HCV replication in primary hepatocyte cultures over prolonged periods of time. Previous studies have relied on quantifying HCV RNA by quantitative reverse transcription polymerase chain reaction (qRT-PCR), a technique that cannot be convincingly used for detecting rare infectious events due to the high background of nonspecifically bound viral RNA. We instead employed a highly sensitive HCVcc reporter virus expressing secreted *Gaussia* luciferase (Gluc), Jc1FLAG2(p7-nsGluc2A) [207]. After inoculation, cultures were washed to remove Gluc carryover, and luciferase secretion was monitored as an indicator of viral replication. We found that several

conventional culture systems – pure hepatocytes on adsorbed collagen, collagen gel sandwich, Matrigel overlay, and randomly distributed co-cultures – could not sustain HCV replication, presumably due to a decline in liver-specific phenotype (**Figure 3-4**) [150]. In contrast, MPCCs in multi-well formats supported HCV replication for at least two weeks (**Figure 3-5A**, **Figure 3-6**). Treatment with HCV nonstructural protein 3/4A (NS3/4A) protease inhibitor ITMN191, nonstructural protein 5B (NS5B) polymerase inhibitor (2'CMA), or IFN-α reduced luciferase activity to background levels (**Figure 3-5A**), indicating that persistent signal was indeed due to ongoing viral replication. Persistent HCV infection was achieved in MPCCs created from freshly isolated or cryopreserved human hepatocytes from several donors, reflecting the reproducibility of the optimized microscale architecture and the concomitant phenotypic stability. We next attempted to quantify HCV RNA and proteins in MPCCs by qRT-PCR, immunofluorescence, and Western

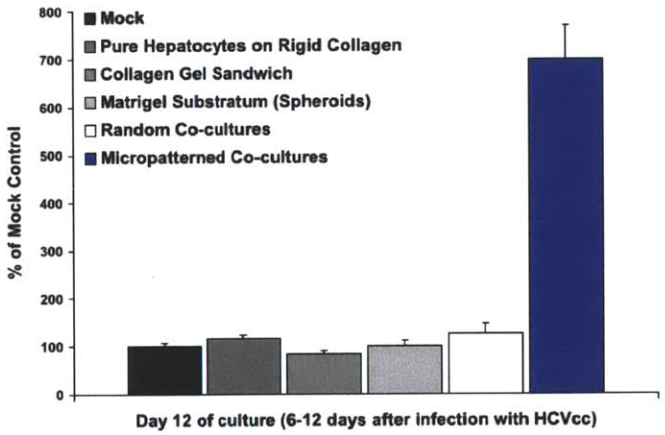

Figure 3-4. Primary hepatocytes in MPCCs maintain HCVcc infection over longer periods of time than conventional hepatocyte systems. Conventional, pure hepatocyte cultures, widely used in the pharmaceutical industry, and MPCCs were created from the same donors. Conventional cultures were infected with HCVcc within 24 h of plating, whereas MPCCs were infected once they achieved functional stability (6 days after plating). Luciferase activity in supernatants was monitored over 2 weeks post-infection. One representative time point (6-12 days post-infection) is shown. Luciferase activity is expressed as percent of mock control.

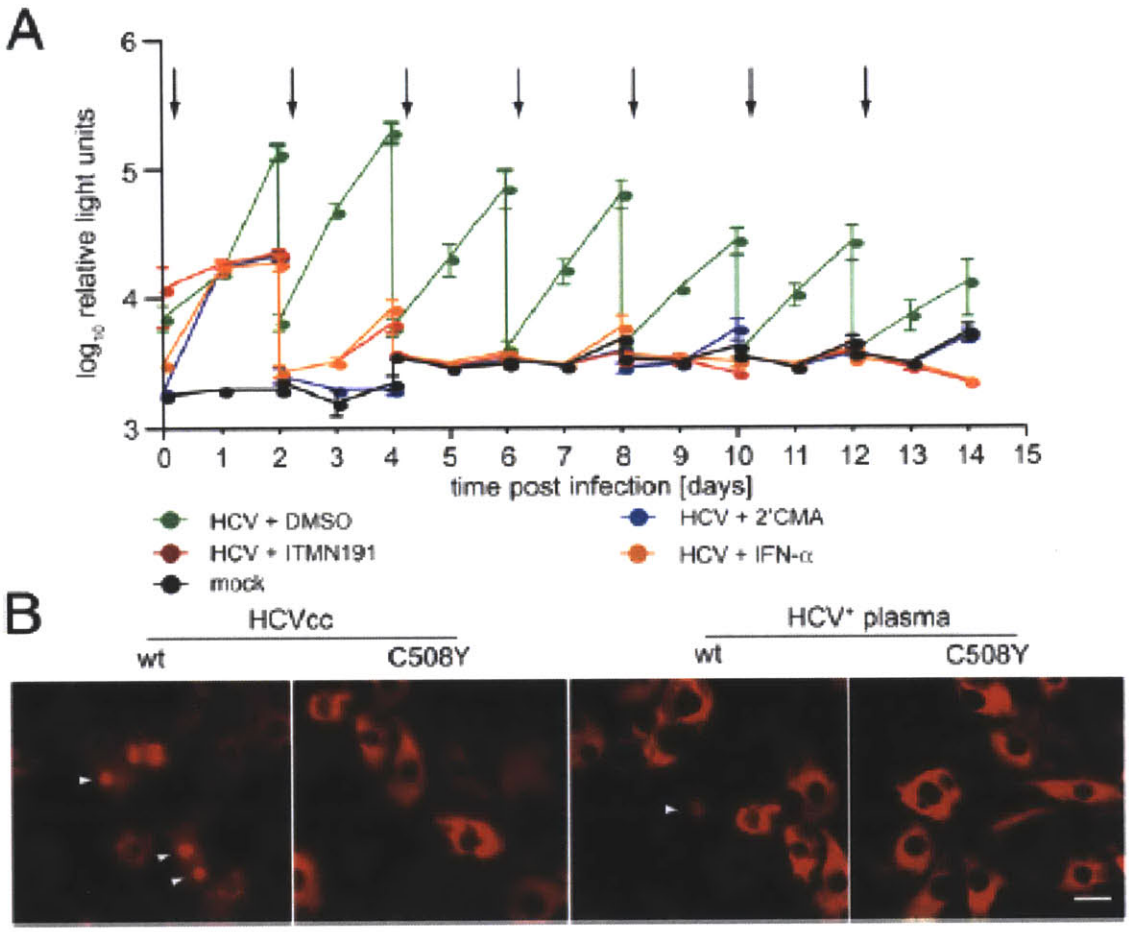

Figure 3-5. Primary human hepatocyte MPCCs are susceptible to HCV. (**A**) Persistent infection of primary human hepatocytes with HCVcc. Primary hepatocytes in MPCC were infected with Jc1FLAG2(p7-nsGluc2A). After 24 h, virus was removed and MPCC medium containing DMSO (0.1%) or the indicated inhibitors was added. All inhibitors were used at approximately 50× IC50 (polymerase inhibitor 2'CMA = 2.16 mM, protease inhibitor ITMN191 = 0.16 mM, IFN-α = 500 U/mL). Samples were taken daily and the media replaced with washing every 48 h. Accumulated luciferase activity in the supernatants is plotted. Arrows indicate the addition of fresh inhibitor. (**B**) Visualization of HCV infection in primary human hepatocytes. MPCCs were transduced with lentiviruses expressing wild-type (wt) or mutant (C508Y) RFP-NLS IPS HCV reporter. 24 h after transduction, MPCCs were infected with Jc1FLAG2(p7-nsGluc2A) or plasma from HCV-infected patients in the presence of heparin (5 IU), CaCl2 (9 mM), and MgCl2 (6 mM). 12 h post-infection, virus was removed and MPCC medium was added. Un-fixed MPCCs were imaged by wide-field fluorescence microscopy at 48 h postinfection. Representative pseudo-colored fluorescent images are shown; white arrow heads show nuclear RFP, indicative of HCV infection. Scale bar: 20 μm.

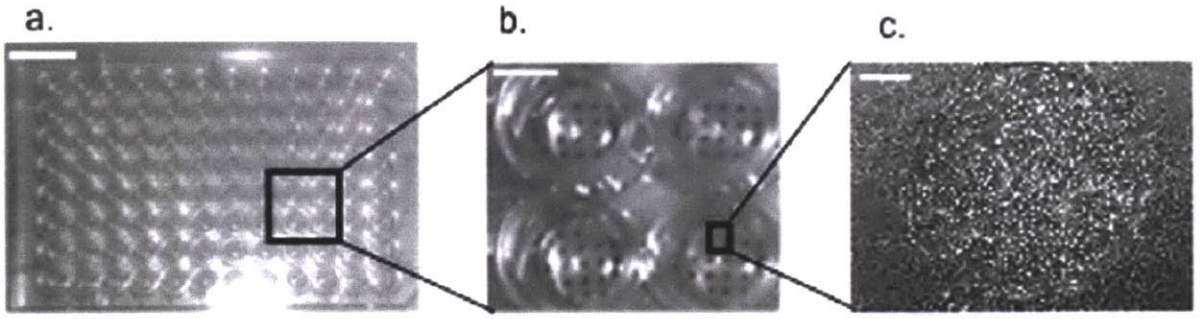

Figure 3-6. Miniaturized 96-well primary hepatocyte MPCCs. (**A**) MPCCs were created in off-the-shelf tissue culture polystyrene plates in formats up to 96-well plates using soft lithographic techniques. (**B**) Each well of a 96-well plate contains 14–15 islands of hepatocytes that are 500 μm in diameter and spaced 1200 μm apart (center-to-center), and (**C**) surrounded by 3T3-J2 murine embryonic fibroblasts to create MPCCs. Scale bars: 2 cm (a), 4 mm (b), 100 μm (c).

blot. In contrast to recent reports [200], we were unable to obtain specific signals above background, reminiscent of failed attempts to detect HCV proteins in infected liver biopsies, probably due to the low number of HCV RNA copies per cell [208].

To demonstrate that HCV actively replicates in the primary hepatocyte component of the MPCCs, we made use of a recently developed fluorescence-based live cell reporter [192]. This system uses a reporter (RFP-NLS-IPS) composed of a red fluorescent protein (RFP), an SV40 nuclear localization sequence (NLS), and a C-terminal mitochondrial targeting domain (IPS) derived from the IFN-β promoter stimulator 1 protein (IPS-1), a known cellular substrate for the HCV NS3/4A protease. The RFP-NLS-IPS substrate was stably expressed in primary hepatocyte MPCCs (**Figure 3-5B**). In HCV-infected cells, RFP-NLS-IPS processing by NS3/4A results in translocation of the cleavage product, RFP-NLS, from mitochondria to the nucleus. This redistribution of fluorescence was detected in approximately 1–5% of hepatocytes in infected MPCCs transduced with wild-type RFP-NLS-IPS; no re-localization was detected after infection of MPCCs harboring a cleavage-resistant reporter (C508Y) or in supporting fibroblasts (**Figure**

3-5B). At very low frequency (approximately 1 in 30,000 cells), we also detected RFP-NLS-IPS cleavage in MPCC cultures infected with plasma or sera from HCV-infected patients (**Figure 3-5B**).

3.2.3. Primary hepatocytes in MPCCs produce infectious virus

To determine whether primary hepatocytes in MPCCs are capable of producing infectious virions, filtered culture supernatants were used to inoculate naïve Huh-7.5 cells, followed by staining for HCV nonstructural protein 5A (NS5A) at 72 h post-infection. Infectious virus was detected in MPCC supernatants harvested at day 4 post-infection and for all time points measured up to day 12 (**Figure 3-7**). Supernatants from MPCCs infected in the presence of specific antiviral inhibitors did not yield NS5A-positive foci in Huh-7.5 cells, indicating that *de novo* virus production, rather than carry-over of the inoculum, was detected. Attempts to passage MPCC-produced virus onto naïve MPCCs were unsuccessful, likely due to the low titers produced by the primary cells which also precluded further biophysical analysis of the virus.

3.2.4. Proof-of-principle for preclinical screening of anti-HCV therapeutics in MPCCs

Persistently infected MPCCs may be a viable and relevant platform for preclinical screening of anti-HCV therapeutics. Antibodies blocking HCV entry factors, in particular CD81 and SCARB1, have proven effective *in vitro* [48, 209, 210] and in small animal models [210]. We tested the ability of monoclonal antibodies against these cellular targets, as well as four antibodies specific for HCV E2, to inhibit HCVcc entry in MPCCs; none of these reagents had previously been tested in primary cell cultures. Anti-CD81 (JS-81) blocked HCVcc entry very efficiently ($IC_{50} < 1$ μg/mL), whereas anti-SCARB1 (C167) did not efficiently block uptake.

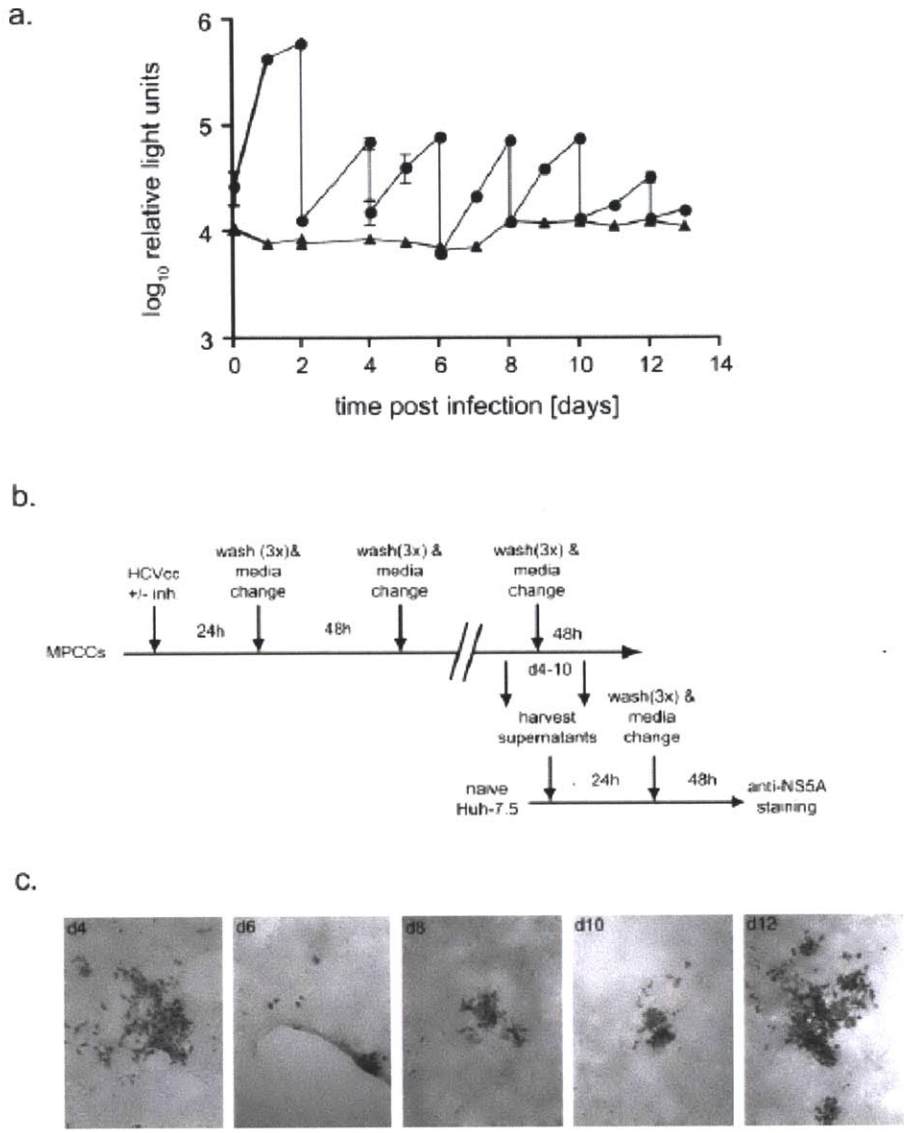

Figure 3-7. Primary human hepatocytes in MPCCs produce infectious virus. (**a**) HCVcc infection kinetics in primary hepatocyte MPCCs. Primary hepatocytes in MPCCs were infected with Jc1FLAG2(p7-nsGluc2A) (circles) or mock infected (triangles). After 24 h, virus was removed and MPCC medium added; samples were taken daily and media replaced with washing three times every 48 h. (**b**) Schematic of the experimental setup. Supernatants collected pre- and post-wash at days 4, 6, 8, 10, and 12 following infection were used to infect naïve Huh-7.5 cells. 24 h post-infection, media were replaced and nonstructural protein 5A (NS5A) staining was performed 72 h post-infection to visualize HCV infection. (**c**) HCV infection of Huh-7.5 cells was visualized by immunocytochemical staining for NS5A. Days indicate the time points when supernatants were taken from the infected MPCC cultures.

All antibodies against E2 were able to inhibit HCVcc infection, although with varying efficiencies (IC_{50} for AP33 > 3/11 > CBH5 > AR3A) (**Figure 3-8A**). A variety of specific antivirals targeting HCV enzymes are also under preclinical development. Unfortunately, *in vitro* models capable of simultaneously assessing drug toxicity and efficacy are not widely available.

We have previously shown the utility of MPCCs in drug metabolism and toxicity screening via assessment of gene expression profiles, phase I/II metabolism, canalicular transport, secretion of liver-specific products, and susceptibility to hepatotoxins [150]. Here, we examined the use of MPCCs in evaluating antiviral efficacy (**Figure 3-8B**). We measured HCV replication by luciferase activity at 4 days post-treatment with protease inhibitors (BILN2061 and ITMN191), polymerase inhibitor (2'CMA), or IFN-α. These compounds inhibited HCV replication in the sub-micromolar range, indicating the relevance of MPCCs for monitoring HCV inhibition. We then evaluated the efficacy of protease inhibitors (SCH-6 and BILN2061) and polymerase inhibitor (2'CMA) in HCVcc-infected MPCCs pretreated for 3 days with compounds known to modulate drug metabolism and other cellular functions *in vivo* (**Figure 3-8C**) [150]. We found that the addition of certain drugs severely reduced the efficacy of SCH-6 and 2'CMA, as compared to DMSO solvent control. Although the mechanisms underlying these adverse drug interactions remain unknown, these observations demonstrate the importance of conducting drug combination studies during *in vitro* efficacy assessment. These studies indicate that MPCCs may be well-suited as a metabolically competent *in vitro* model of the liver, allowing HCV replication to be studied over several days to weeks, and a variety of intervention strategies to be tested for both efficacy and toxicity.

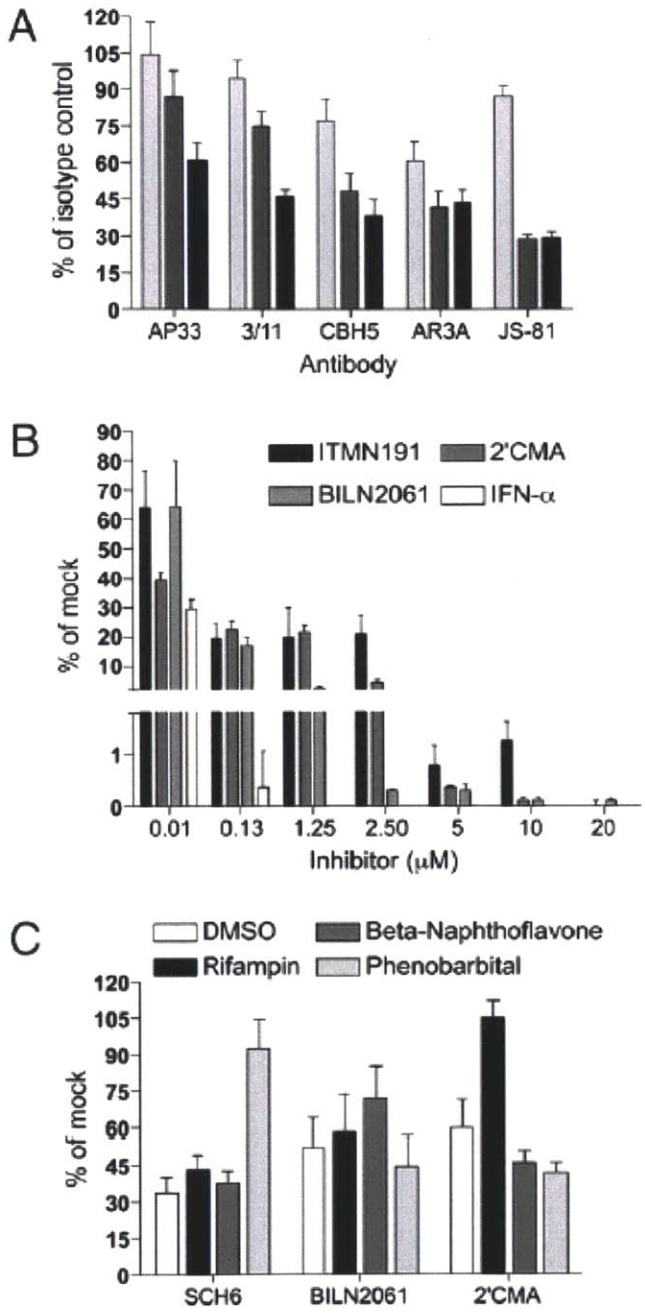

Figure 3-8. Utility of primary human hepatocyte MPCCs in antibody and small molecule screening. (**A**) Dose-dependent inhibition of HCVcc replication in MPCCs treated with antibodies against HCV glycoproteins (AP33, 3/11, CBH5, AR3A) or cellular CD81 (JS-81). Antibody concentrations are 0.1 (light gray), 1 (dark gray), and 10 (black) μg/mL (**B**) Dose-dependent inhibition of HCVcc replication in MPCCs treated with IFN-α (up to 0.13 μM) or small molecules (NS3-4A protease inhibitors, BILN2061 and ITMN191, or polymerase inhibitor, 2'CMA). HCVcc-infected MPCCs were pulse-treated for 2 days with compounds and supernatants were collected at days 2 and 4

(shown) post inhibitor treatment. (**C**) Drug-drug interactions lead to reduced efficacy of small molecules in HCVcc-infected MPCCs. Infected MPCCs were treated for 3 days with prototypical inducers of drug metabolism enzymes [150, 211], followed by treatment of cultures with small molecules for 2 days. In all experiments, HCVcc replication was monitored by luciferase secretion into the supernatants. Mean and standard error of the mean are shown.

3.2.5. Discussion on MPCCs as an *in vitro* model of infection and test-bed for antivirals

Here we have described a microscale primary human hepatocyte *in vitro* culture platform that supports the entire HCV life cycle. Primary hepatocyte MPCCs are stable for several weeks and therefore allow monitoring of human hepatotropic infections over extended periods of time. Although this is an important step forward, limitations remain. Entry of HCVpp and tissue culture-derived virus into MPCC hepatocytes was inefficient. Although the four critical viral entry factors are present on these cells, it is possible that differences in their spatial distribution might account for the low uptake efficiency. Indeed, antibodies block entry into primary hepatocytes at different efficacies than previously reported [212-214], possibly due to limited accessibility of the HCV entry factors on polarized cells. Furthermore, following isolation from the liver and disruption of hepatic polarity, it may be that viral entry factors on the membranes of some MPCC hepatocytes do not reach the threshold quantity and appropriate polarized distribution required for efficient viral uptake. We also did not observe any increase in the number of infected cells over time, arguing for limited spread of HCV in the cultures. Several factors could contribute to this phenomenon, including limited numbers of infectious particles, heterogeneous polarity, or an inherent or acquired refractory nature of a proportion of cells. Furthermore, certain critical host factors may be heterogeneously expressed and therefore limiting in some cells, rendering them resistant to infection or unable to sustain HCV RNA replication. Although our data demonstrate that primary hepatocytes in MPCCs can produce

infectious virus, the titers are low and few infectious virions are available for spread. The low permissiveness of MPCC hepatocytes to HCV may also reflect the *in vivo* reality of chronic hepatitis. Technical challenges have traditionally made it difficult to estimate the number of infected cells in an HCV-positive liver. Recently, however, two-photon microscopy methods have been used to suggest that only a small proportion (7–20%) of patient hepatocytes express viral antigens [215]. Although further improvements in infection efficiency may be possible, our system lays the foundation for preclinical assessment of antiviral therapeutics against human hepatotropic pathogens in a more physiologically relevant microenvironment. Importantly, due to the phenotypic stability of MPCCs, infection processes can be monitored longitudinally, potentially allowing the kinetics of viral spread and antiviral signaling to be characterized at the single cell level. The polarized nature of the MPCC hepatocytes allows HCV entry and uptake inhibitors to be studied in the context of intact tight junction structures. Furthermore, using sera from HCV-infected patients and a very sensitive fluorescent reporter system [192], we were able to detect an extremely low frequency of productive infection, suggesting that a combination of authentic virus and host cells may be achievable. Proof-of-principle studies reported here also demonstrate the value of MPCCs in drug studies. The high baseline activities of drug metabolism enzymes (i.e., cytochrome P450s) and their drug-mediated induction/inhibition in MPCCs [150] allows for simultaneous measurements of drug efficacy, drug-drug interactions, and drug toxicity, thereby providing critical preclinical parameters. These advantages combine to make MPCCs a highly valuable system for studies of HCV biology.

Although low quantities of antigen and HCV RNA in hepatocytes are apparently consistent with *in vivo* pathophysiology, it is still surprising that infection in MPCC hepatocytes is cleared

acutely over two weeks. This is in stark contrast to the standard hepatoma models of infection used by HCV reporters in which infection is robust, progressive, and persistent, with an appreciably greater portion of cells infected. One hypothesis to explain these differences is that primary hepatocytes with intact innate immune signaling are capable of mounting an interferon response characterized by expression of interferon-stimulated genes (ISGs) that curtails viral spread and persistence [216-218].

3.2.6. Interferon signaling clears HCV infection acutely in primary adult hepatocytes

To determine whether interferon signaling constrains infection, we inhibited interferon signaling using three exogenous agents that disrupt various parts of the signaling cascade: a Janus-associated kinase (JAK) inhibitor (JAKi) that is a pyridone-containing tetracycle targeting JAK1, JAK2, JAK3, and tyrosine kinase 2 (Tyk2) [219]; the lentivirally introduced parainfluenza virus 5 V protein (PIV5V) that binds and inhibits melanoma differentiation-associated gene 5 (MDA5) as well as induces proteosomal degradation of signal transducer and activator of transcription 1 (STAT1) [220, 221]; and BX795, an aminopyrimidine-containing inhibitor of tank-binding kinase 1 (TBK1) and IκB kinase ε (IKKε) [222-224]. While luminescent signal from Gluc-expressing HCV dissipates over two weeks post infection (**Figure 3-9A**), inclusion of JAKi, PIV5V, or BX795 lead to a significant increase in luciferase signal by Gluc-expressing HCV as well as qualitative persistence presumably characteristic of infection *in vivo* (**Figure 3-9A, Figure 3-10**). Further, infection frequency of hepatocytes was determined using a fluorescent reporter of HCV nonstructural protein 3/4A (NS3/4A) activity [57]. Suggesting successful viral spread, more NS3/4A+ hepatocytes were detected upon introduction of interferon pathway-interrupting agents (**Figure 3-9B**); NS3/4A+ cells demonstrate a focal pattern (**Figure 3-11**)

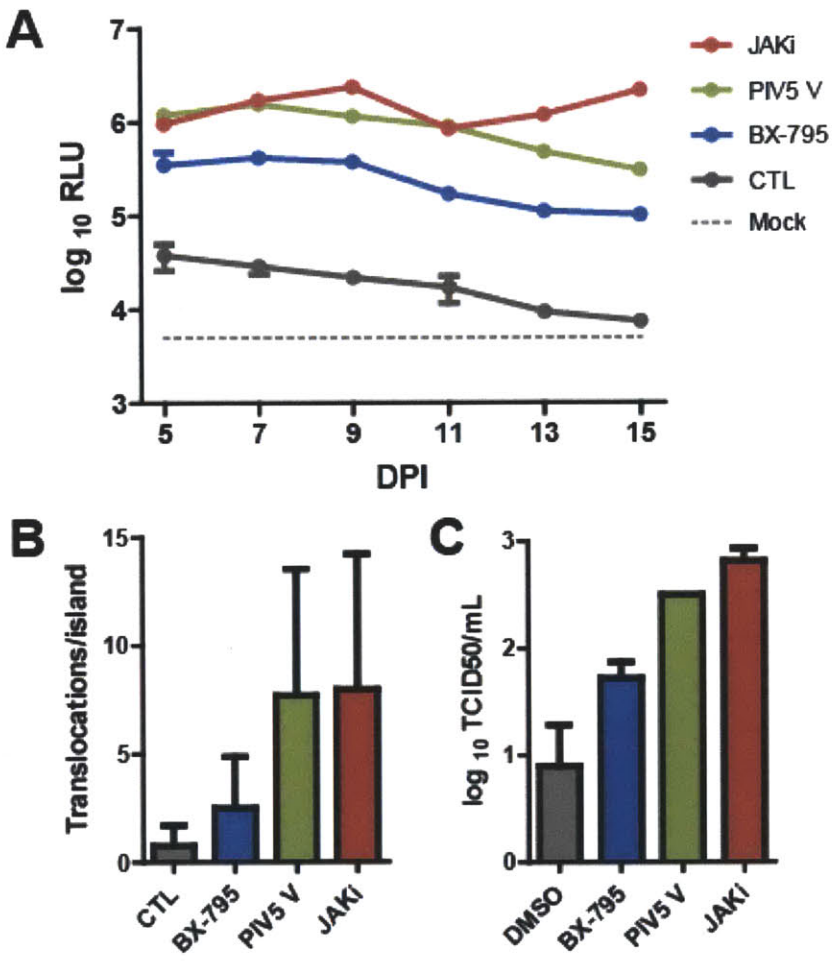

Figure 3-9. Inhibition of interferon (IFN)-signaling rescues hepatitis C virus (HCV) infection. (**A**) JAK inhibitor (JAKi) was dosed (1 μM) starting one day pre-infection and continuously thereafter. Parainfluenza virus 5 V protein (PIV5 V) was lentivirally introduced 3 days pre-infection to give time for expression. BX-795 inhibitor of TBK1 and IKKε was dosed (1 μM) starting one day pre-infection and continuously thereafter. Relative light units (RLU) from Gluc-expressing HCV presented on a logarithmic scale versus days post infection (DPI). Difference between any intervention and control (CTL) was highly significant at all time-points by ANOVA. (**B**) NS3/4A reporter [57] translocations per MPCC island shown 7 dpi (approximately 200 heps/island) ($n > 75$ per condition). Difference between any intervention and CTL significant by ANOVA. (**C**) Viral titer (TCID50/mL) presented on a log scale for 7 dpi as determined by passaging onto naïve Huh-7.5s. Difference between any intervention and CTL significant by ANOVA. Data in (**A**)-(**C**) are presented as $\mu \pm \sigma$.

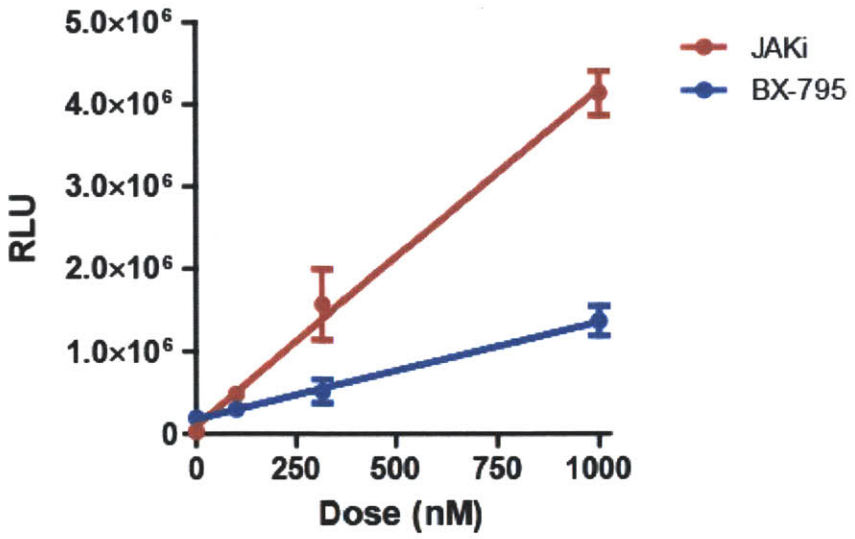

Figure 3-10. Linear range of dose response of JAK inhibitor (JAKi) and BX-795. Compounds were dosed starting one day pre-infection and continuously dosed thereafter. Luminescence produced by Gluc-expressing HCV shown 9 days post-infection for various doses of compound. Linear regression performed on these data sets yielded R^2 = .99 for JAKi and R^2 = .97 for BX-795. Data are plotted as $\mu \pm \sigma$.

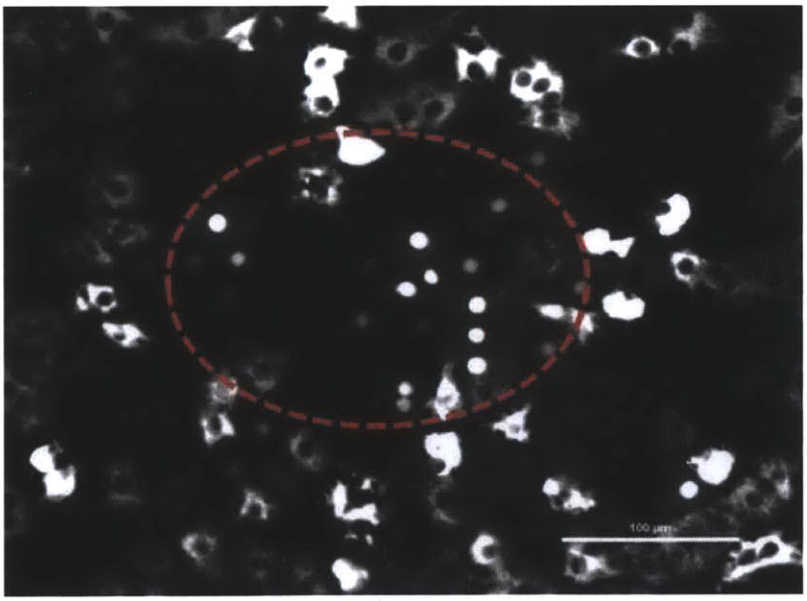

Figure 3-11. Viral spread in interferon-inhibited MPCCs. NS3/4A reporter imaging [57] in infected, JAKi-treated MPCCs reveals large "foci" of proximal infected cells. Representative image taken 9 dpi, focus circled in red dashed line. Scale bar = 100 μm.

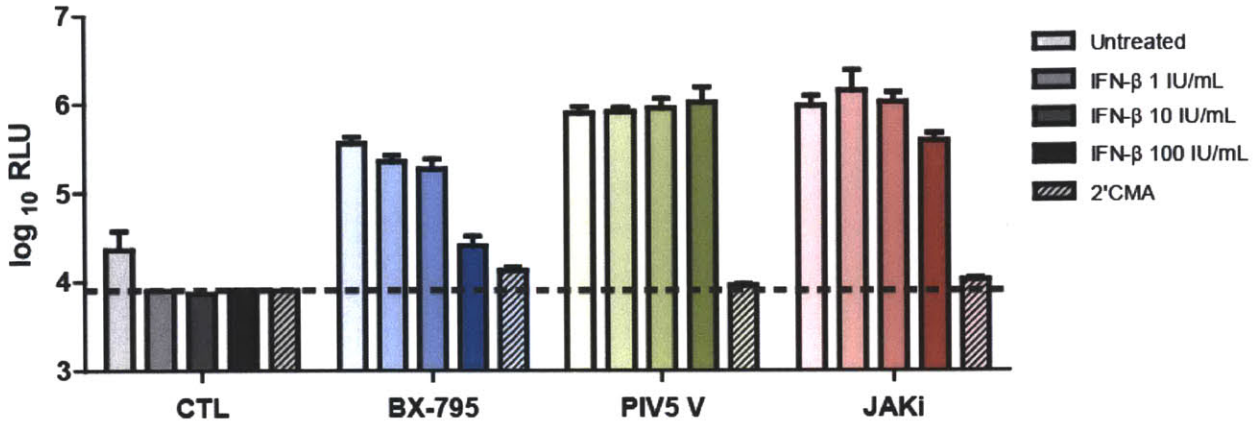

Figure 3-12. Interferon-inhibition-mediated enhancement of infection responds to interferon (IFN) in a mechanistically appropriate manner. Post infection, cultures treated with JAKi, PIV5 V, and BX-795 as described were treated with IFN-β at several doses or the polymerase inhibitor 2'CMA (2.16 μM) for 4 days before luminescence was measured by Gluc-expressing HCV. Relative light units (RLU) presented on a logarithmic scale as $\mu \pm \sigma$.

[225-227]. Passaging to naive hepatoma cultures confirmed that viral titers were also elevated with these interventions (**Figure 3-10C**). Finally, we performed a direct test of the role of IFN signaling in limiting infection – delivery of IFN-β to control infected cultures cleared infection at all doses observed, mimicking the effects of treatment with the antiviral compound 2'-C-methyladenosine (2'CMA) that inhibits the HCV polymerase, nonstructural protein 5B (NS5B) (**Figure 3-12**). Taken together, these data suggest that interferon signaling limits various steps of the viral life cycle.

We performed several assays to study the mechanism of these interferon-disrupting agents. Based on the described functions of these agents, JAKi should inhibit only the response to IFN; PIV5V should inhibit both the production and response to IFN; and BX795 should only inhibit the production of IFN. As such, treatment with JAKi or PIV5V should protect infection from the clearing effects of IFN, but BX795 dosing should not. Consistent with this, we observed that

though all cultures remained sensitive to 2'CMA treatment, only BX795-treated cultures responded significantly to type I IFN (**Figure 3-12**). To explore the possibility that JAKi may operate through non-STAT1 functions of JAK proteins, a screen of small molecules targeting the alternate downstream pathways was performed; consistent with STAT1 signaling being responsible for the rescue of infection, none of these molecules was able to enhance infection (**Figure 3-13**).

To further elucidate viral clearance, we studied the expression of a panel of prototypical ISGs early after infection. ISG upregulation is the ultimate downstream target of IFN signaling, and ISGs are the most direct way to assess activation of an antiviral state. Consistent with detection of HCV pathogen-associated molecular patterns (PAMPs) by pattern recognition receptors (PRRs), infection robustly induced the expression of ISGs over mock uninfected controls (**Figure 3-14**). By contrast, inhibiting IFN signaling using JAKi, PIV5 V, or BX-795 significantly reduces this ISG upregulation post-infection, accordant with IFN-mediated elevation in ISG levels as well as ISG-mediated viral clearance (**Figure 3-14**). Given that HCV has mechanisms to interrupt IFN signaling [8, 228, 229], these data raise the question of whether the ISGs induced are in infected cells themselves or in neighboring cells; though the rapid clearance of infection in untreated MPCCs suggests that ISGs are upregulated in initially infected cells as well, this hypothesis could be tested using single-molecule fluorescence *in situ* hybridization as described earlier in this thesis.

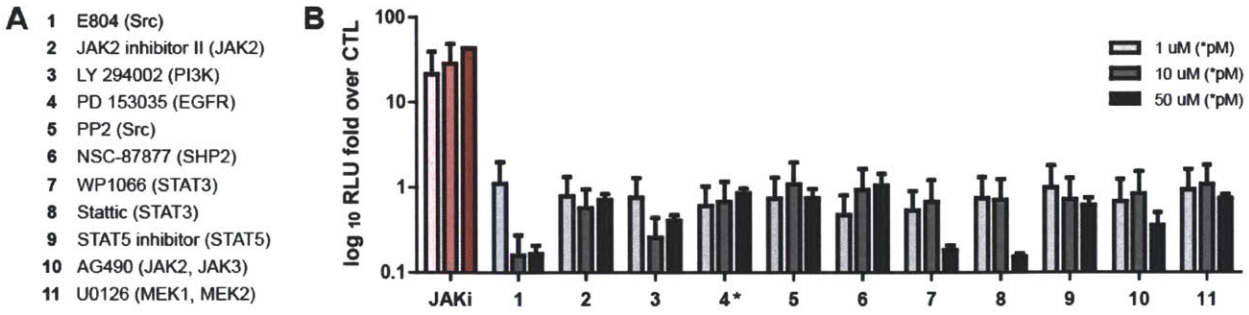

Figure 3-13. Determining specificity of JAKi by testing alternative pathways downstream of JAK signaling. (**A**) Numbered list of compounds (targets listed in parentheses) for various signaling pathways downstream of JAK signaling. (**B**) Numbered compounds were dosed starting one day pre-infection and continuously thereafter at 3 doses as listed (compound 4 was tested at lower doses as listed). Luminescence of Gluc-expressing HCV normalized by untreated infected control and presented on a log scale as $\mu \pm \sigma$. Only JAKi elevates infection statistically significantly.

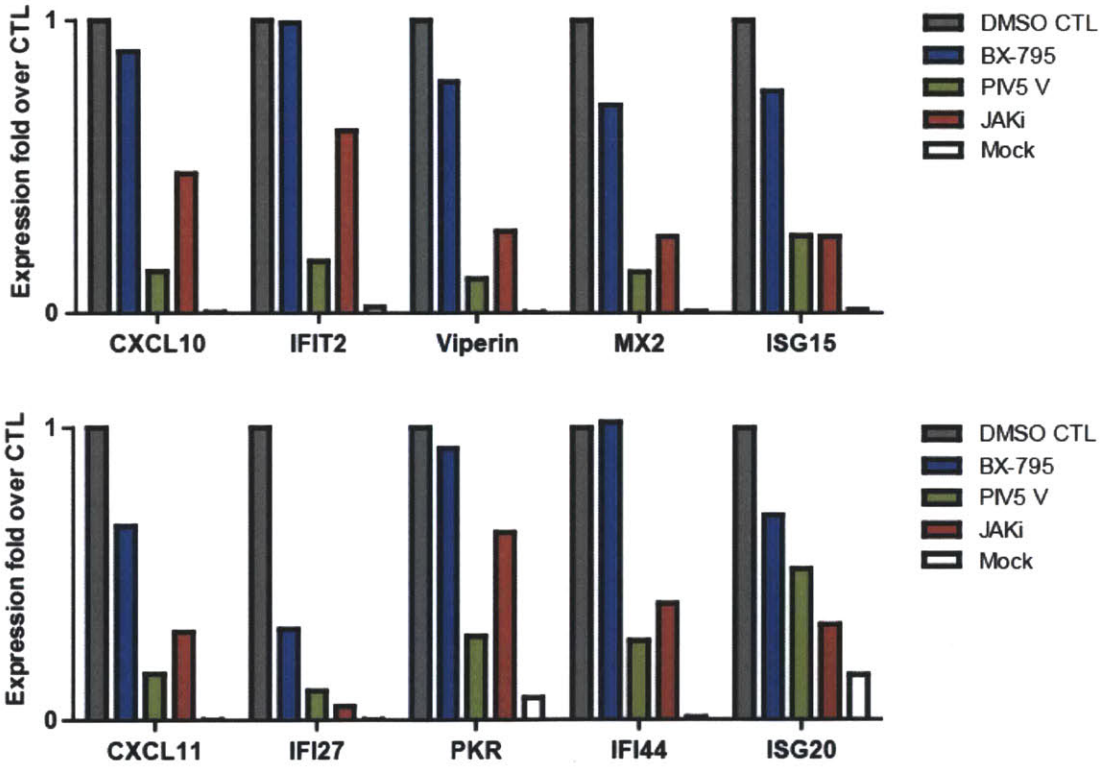

Figure 3-14. Inhibition of interferon-stimulated gene (ISG) induction post hepatitis C virus (HCV) infection upon inhibition of interferon signaling. Infected cultures were lysed 48 hpi, and RT-PCR was performed and normalized by a house-keeper. Expression of prototypical ISGs relative to infected controls is presented for interferon-inhibiting agent treated cultures (dosed as described) as well as mock uninfected cultures.

Collectively, these data suggest that primary adult hepatocytes mount a potent interferon response to infection and thus intrinsically resist HCV infection, contributing to acute clearance of infection. This contrasts significantly from the conceptual model of disease pathogenesis built on observations *in vivo* and in hepatoma cell lines, where the expression of anti-interferon machinery by HCV underlies its remarkable predilection towards chronic infection *in vivo* [8]. Based on these data, we hypothesized that chronicity in hepatoma cell lines may be due to defects in innate immune signaling [41, 230]l; and that while primary adult hepatocytes are a more physiologic host for infection, their state *in vivo* could be significantly different from that *in vitro*. In particular, we hypothesized that liver microenvironmental signals present *in vivo* could "tolerize" hepatocytes to infection by dampening the activity of interferon signaling.

The broader concept that hepatocytes are tolerized to infection has precedence [231-234]. Downstream of the enteric circulation, the liver experiences a constant influx of microbial and other antigens which would theoretically engender a constant state of liver inflammation if unchecked. Several other phenomena suggest the tolerogenic nature of the liver – liver allografts experience surprisingly low immunologic rejection [235]; the "oral tolerance" effect, whereby consumption of allergy-inducing antigens can lead to tolerance, has been partly attributed to the liver based on loss of the effect after shunting the portal circulation across the liver [236]; and the success of cancer metastases that invade the liver. While such tolerogenic properties are known to be exploited by liver pathogens [232], the described mechanisms of tolerance generally involve modulation of the activity of either innate immune effector cells or adaptive immune cells and functions; this modulation is typically achieved by the elaboration of soluble cues by liver nonparenchymal cells. Here, we sought to determine if such signals could also mediate

tolerance by modulating the interferon signaling activity of the primary locus of infection itself, the hepatocyte.

3.2.7. Screen in MPCCs identifies liver microenvironmental immunosuppressive agents that enhance infection of primary adult hepatocytes

Based on the literature [232-234], we identified 10 candidate compounds with general immunosuppressive qualities in the liver, some of which are already known to elicit functions by hepatocytes – interleukin (IL)-1β, IL-4, IL-6, IL-8, IL-10, IL-13, IL-22, transforming growth factor (TGF)-β, tumor necrosis factor (TNF)-α, and prostaglandin E2 (PGE2). We observed that IL-4, IL-6, IL-13, and IL-22 significantly enhanced infection (**Figure 3-15**); IL-6 was particularly potent, enhancing infection 10-30x across several experiments. As such, we chose to further pursue the possible role of IL-6 in hepatocyte immunomodulation.

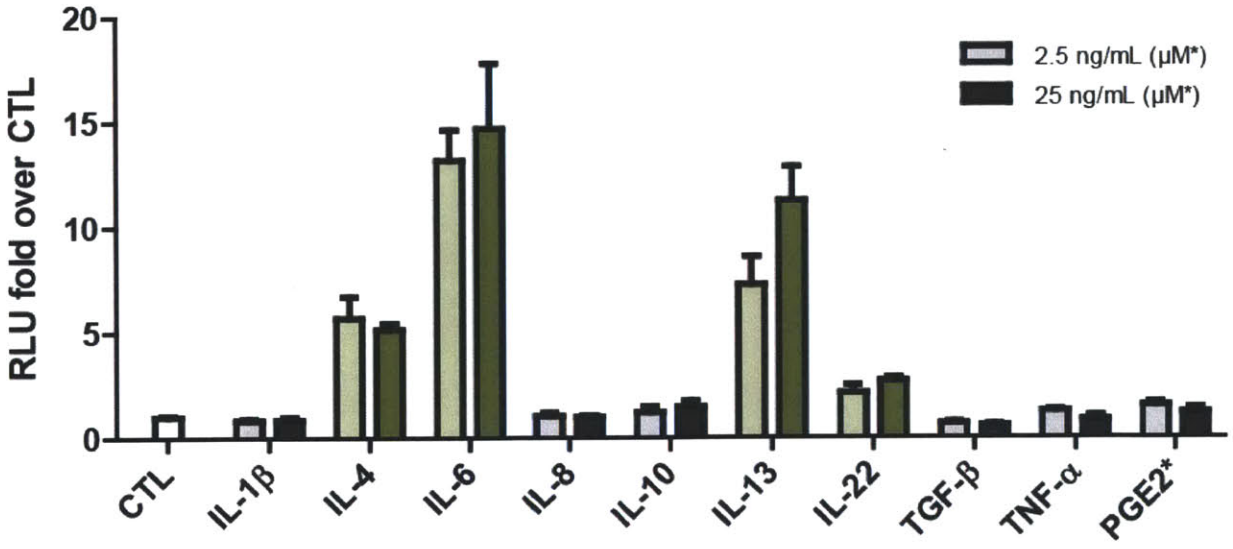

Figure 3-15. Effect of liver compounds on HCV infection. MPCCs were untreated (CTL) or dosed with compounds starting one day pre-infection (with Gluc-expressing HCV) and continuously thereafter. RLU fold over CTL is presented 7 dpi as $\mu \pm \sigma$. Compounds that are significantly above CTL are presented in green ($p < 0.05$ as determined by one-way ANOVA followed by Tukey post-test).

3.2.8. IL-6 inhibits the induction of ISGs post infection via STAT3-mediated inhibition of IFN pathway components

We next sought to determine whether the enhancement in infection by IL-6 could be explained by an inhibition of IFN signaling. MPCCs were infected with and without exposure to IL-6, and ISG induction was measured by RT-PCR. Like the inhibition of HCV-mediated ISG induction using inhibitors of IFN signaling (**Figure 3-14**), IL-6 broadly reduced ISG induction by HCV (**Figure 3-16**), suggesting that IL-6 operates through IFN pathway inhibition. To determine possible targets of inhibition, expression of various IFN pathway components was analyzed by RT-PCR. Consistent with the reduced ISG induction upon infection, various components of the IFN pathway were down-regulated by IL-6 exposure (**Figure 3-17**); inhibition of PAMP detection seems more significantly affected. Finally, we determined whether IL-6-mediated enhancement of infection was dependent on the primary transcription factor activated by IL-6, signal transducer and activator of transcription 3 (STAT3) [237]; consistent with this, the STAT3 inhibitor WP1066 [238] reduced the effect of IL-6 on infection (**Figure 3-18**). While subsequent

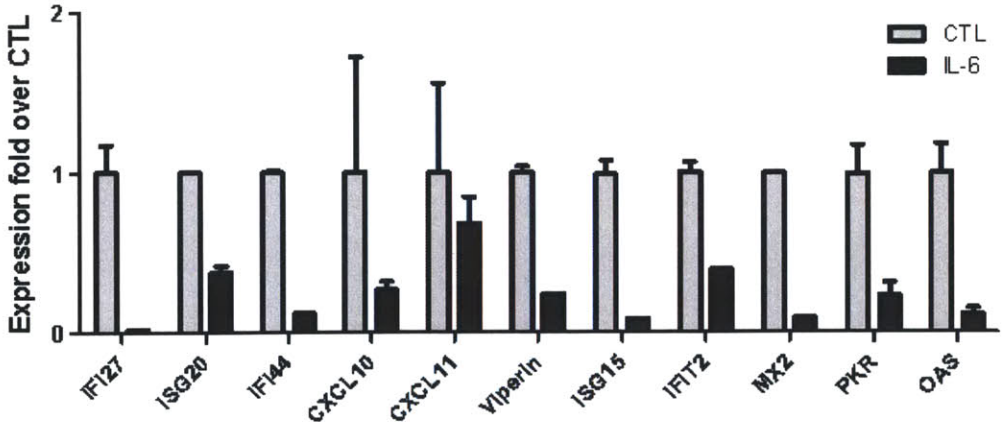

Figure 3-16. Inhibition of induction of interferon-stimulated genes (ISGs) post hepatitis C virus (HCV) infection upon exposure to interleukin (IL)-6. MPCCs were treated with IL-6 (10 ng/mL) or untreated (CTL) starting 2 days pre-HCV infection and continuously thereafter. Cultures were lysed 3 days post infection and RT-PCR for ISGs (with normalization by a house-keeper) was performed. $\mu \pm$ SEM is shown.

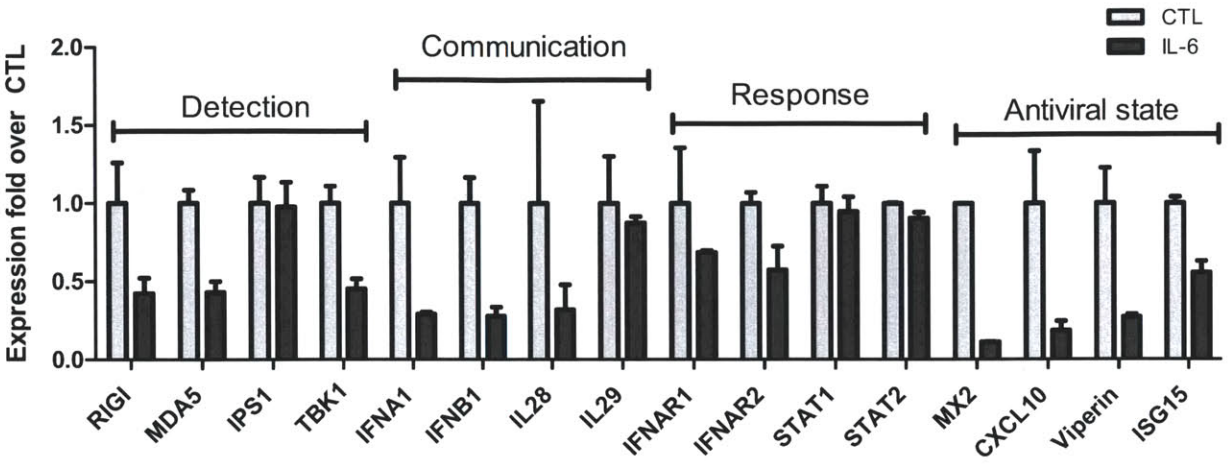

Figure 3-17. Expression of key elements of the IFN cascade after exposure to IL-6. RT-PCR was performed for various groups of the IFN pathway cascade, which demonstrated broadly reduced levels of expression. House-keeper normalized expression for untreated (CTL) and IL-6 (10 ng/mL) presented as expression fold over CTL, $\mu \pm \sigma$.

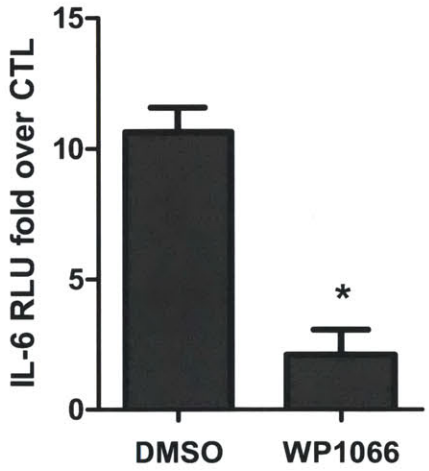

Figure 3-18. IL-6 mediated enhancement of infection is dependent on signal transducer and activator 3 (STAT3) activity. Cultures were dosed with untreated (CTL) or treated by IL-6 (10 ng/mL) starting 2 days pre-infection (by Gluc-expressing HCV), and by carrier control DMSO or by STAT3 inhibitor WP1066 (10 μM) starting 1 day pre-infection and continuously thereafter. Data presented as IL-6 RLU fold over untreated CTL, $\mu \pm$ SEM. Two-sided *t* test confirmed significance (* $p < 0.05$).

investigation will be necessary to fully elucidate the mechanism of infection rescue, these data implicate depression of IFN pathway activity.

3.2.9. Innate immune inhibition enhances the growth of non-JFH-1 strains of HCV

As described earlier in this thesis, a significant problem in the study of HCV is the general inability to cultivate non-JFH-1 strains of HCV [32]. We sought to test the hypothesis that hepatoma cells do not furnish the right environment for the growth of these HCV strains due to aberrations in host factor expression and function, and that primary hepatocytes may be a more appropriate environment for their cultivation. Because curated virions cannot be sourced due to the lack of a culture model, we used synthesized versions of the Con1 (genotype 1b) RNA with an embedded *Gluc* gene. We optimized the transfection of MPCCs using novel "lipidoids" materials which demonstrate successful siRNA delivery in primary hepatocytes *in vivo* [239]. After showing that these materials can deliver JFH-1 genomes to recreate robust infection (data not shown), we transfected Gluc-expressing Con1 into MPCCs. We observed that although MPCCs did not sustain infection in the absence of innate immune inhibition, there was a significant increase in infection after IFN inhibition using either PIV5 V or IL-6 (**Figure 3-19**). While we do not observe robust infection of Con1, disproving the notion that the use of primary hepatocytes is sufficient for robust growth, these data are consistent with an innate immune barrier to growth of HCV Con1 as well.

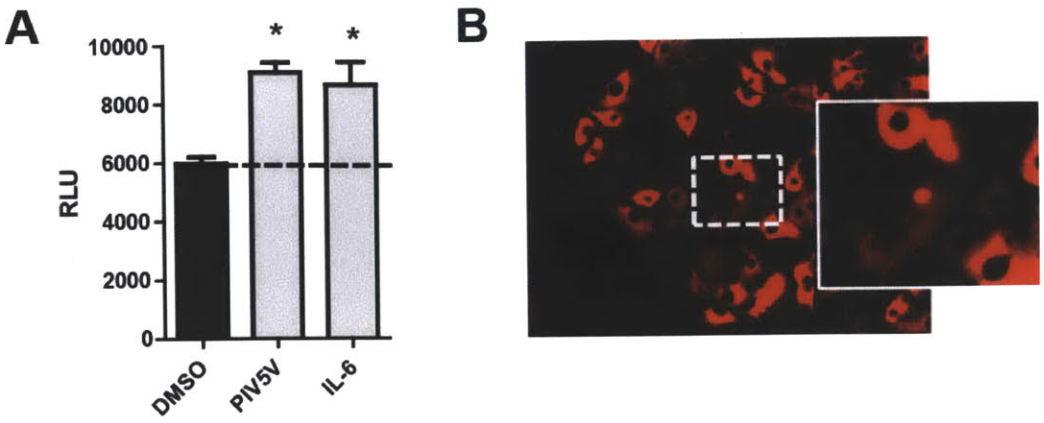

Figure 3-19. Infection by Con1 HCV in MPCCs is increased by innate immune inhibition. (A) Gluc-expressing Con1 RNA was transfected using lipidoids into CTL (DMSO) cultures, PIV5 V transduced cultures, and IL-6 (10 ng/mL) treated cultures. PIV5 V and IL-6 demonstrated significantly higher infection ($p < 0.05$ by one way ANOVA followed by Tukey post-test). Data presented as $\mu \pm \sigma$. **(B)** NS3/4A infection frequency reporter [192] demonstrated sparse positive events only in immunosuppressed cultures.

3.2.10. Innate immune inhibition enhances the growth of liver-stage malaria

Our lab has recently demonstrated the MPCCs can be used to study liver-stage malaria [240]. Here, we sought to determine whether innate immune interferon signaling presents a barrier to infection by malaria as well. We observed that *P. falciparum* infection was significantly enhanced by the inhibition of IFN signaling using JAKi, as measured by both quantity (**Figure 3-20A**) and size (maturity) (**Figure 3-20B**) of exoerythrocytic forms (EEFs). RT-PCR verified that the expression of ISGs after *P. berghei* infection was reduced in the presence of JAKi or IL-6 (**Figure 3-20C**). Notably, while JAKi did not inhibition IFN expression as expected mechanistically, IL-6 inhibited IFN expression as well as ISGs, consistent with IL-6 interfering with pathogen detection by PRRs (**Figure 3-20C**). Collectively, these data suggest that innate immunity mounts a significant barrier to hepatotropic infections broadly; tolerization of hepatocytes in the liver could thus contribute to the success of these infections *in vivo*.

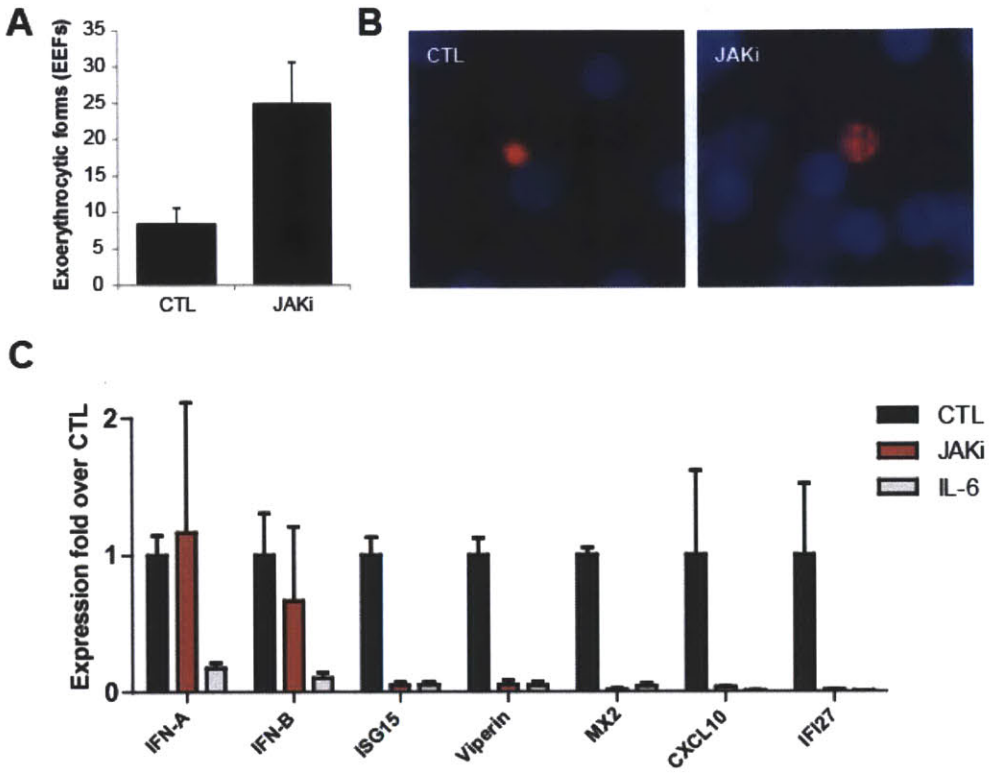

Figure 3-20. Liver-stage malaria infection in MPCCs is increased by innate immune inhibition. (A) Exoerythrocytic forms (EEFs) of *P. falciparum* were quantified in CTL (DMSO) treated cultures and JAKi treated cultures. Difference was statistically significant as verified by *t* test. **(B)** EEFs of *P. falciparum* were larger in the presence of JAKi treatment. **(C)** RT-PCR was used to measure IFN and ISG levels post-infection (by *P. berghei*) in the presence of CTL, JAKi, or IL-6 treated cultures. House-keeper-normalized expression is presented relative to CTL expression as $\mu \pm \sigma$.

3.2.11. Discussion on interferon control of infection by the liver

As described, the development of MPCCs enabled us to study HCV infection in a more physiologic, primary hepatocyte host. Using this model, we made the unexpected finding that primary adult hepatocytes acutely clear infection, in contrast to hepatoma cells. We hypothesized that intact innate immune signaling could explain this, and indeed demonstrated this using exogenous inhibitors if IFN signaling which profoundly enhanced viral infection signal and persistence. This observation raises an important question – how does HCV achieve robust infection and chronicity in the presence of intact IFN signaling? Based on the general notion that

the liver is immune-tolerant from an adaptive and innate immune effector cell perspective, we sought to determine whether endogenous signals present in the liver microenvironment could enhance infection in hepatocytes by tolerizing hepatocyte-intrinsic innate immune signaling. A screen of normally expressed liver cytokines with immunosuppressive qualities as described in the context of immune effector cells revealed hits that significantly boosted infection. In particular, IL-6 enhanced infection 10-30x. We showed that IL-6 does indeed minimize the activation of ISGs concomitant with infection, likely by inhibiting sensing and the response to infection. IL-6 is normally elaborated at a basal level by liver-resident Kupffer cells in response to microbial antigens such as lipopolysaccharide (LPS) entering the liver from the portal circulation [241]. As such, we propose a new working model for another facet of liver tolerization that may operate in parallel with other tolerizing features of the liver [232]. LPS-stimulated Kupffer-cells secrete IL-6 which, itself and likely in conjunction with other liver cytokines, inhibits IFN signaling; this in turn induces tolerization to inflammatory substances and infection in liver hepatocytes that is exploited by hepatotropic pathogens (**Figure 3-21**). Experiments in more complex cellular *in vitro* models (e.g. including Kupffer cells) and *in vivo*, as well as generalization to other hepatotropic pathogens, will be essential for validating and understanding the broader impacts of this conceptual model. Excitingly, inhibiting IL-6 signaling could restore IFN activity and thus be an attractive approach to therapy of hepatotropic pathogens; this is particularly promising since neutralization of IL-6 signaling is already used clinically for other indications [242]. Lastly, from a model development perspective, inhibition of IFN signaling in MPCCs through either exogenous or endogenous agents will enable the study of persistent infection *in vitro*, enhancing our ability to dissect host-virus interactions and to study phenomena of robust infection such as viral spread.

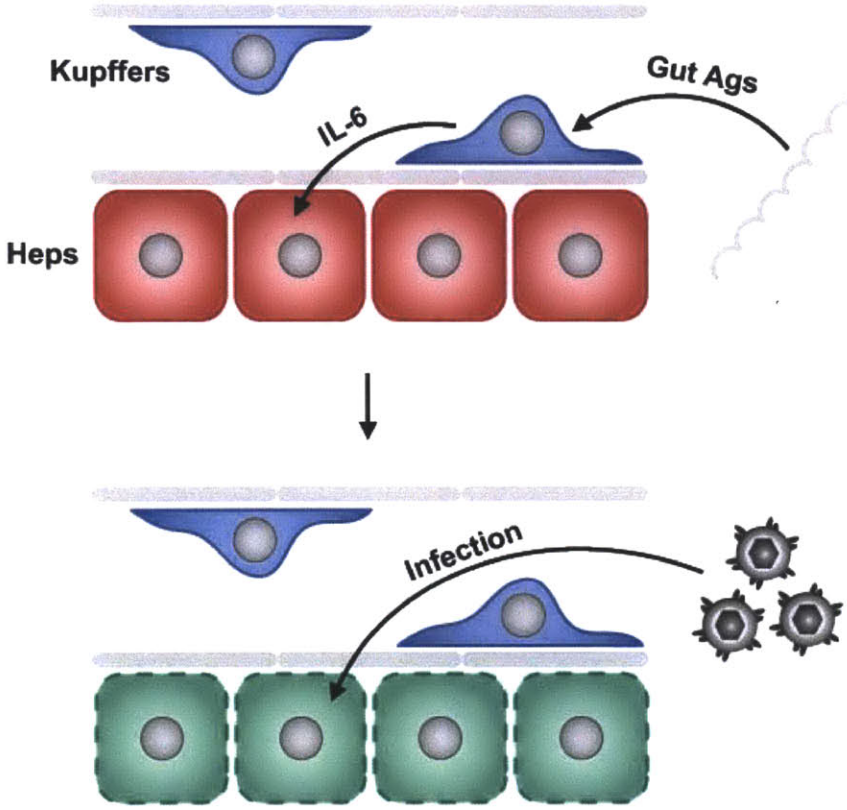

Figure 3-21. Model. Microbial antigens from the gut induce Kupffer cells to produce immunoregulators including interleukin-6 (IL-6) which tolerizes hepatocytes immunologically to inflammatory substances. This dampened surveillance is in turn exploited by pathogens such as hepatitis C virus (HCV), which can mount robust infection as a result.

3.2.11. Personal contributions to this work

This work was divided into two projects – development of the primary hepatocyte model of infection [201], and use of the model to study innate immune signaling. For the first project, the author of this thesis worked in a team lead by Drs. Alexander Ploss and Salman Khetani to assist in experimentation, as well as re-validate, characterize, and explain findings made by others. For the second project, the author of this thesis lead a group of researchers in planning, performing, and interpreting experiments.

3.3 Materials and methods

Virus genomes and stocks

Jc1FLAG2(p7-nsGluc2A) is a fully-infectious HCVcc reporter virus encoding Gaussia luciferase between p7 and NS2 [207]. Virus stocks were created by electroporation and titered by limiting dilution as previously described [48].

Liver sections and hepatocytes

Primary human hepatocytes were purchased from vendors permitted to sell products derived from human organs procured in the United States by federally designated Organ Procurement Organizations. Vendors included: Celsis In vitro Technologies, BD-Gentest and CellzDirect. Human hepatocytes were pelleted by centrifugation at 50–100 xg for 5–10 min at 4 °C, resuspended in hepatocyte culture medium, and assessed for viability using Trypan blue exclusion (typically 70–90%). Liver-derived nonparenchymal cells, as judged by size (<10 μm diameter) and morphology (nonpolygonal), were consistently found to be less than 1% in these preparations. Human liver sections were obtained from the New York Presbyterian Hospital from uninfected donor tissue deemed unacceptable for liver transplantation. Tissue was processed by immediately freezing in OCT compound at -80°C or by fixation in 10% formalin solution for 24 h followed by paraffin embedding. Tissue sections were cut (~5-6 μm) on poly- L-lysine coated slides. Human serum and plasma samples were obtained at Weill Cornell Medical Center. All protocols for human primary material procurement were approved by the Committee on Use of Human Experimental Subjects, MIT, or by the IRB, Rockefeller University and Weill Cornell Medical Center.

Micropatterned co-cultures of primary human hepatocyte sand supportive stromal cells

Off-the-shelf tissue culture polystyrene (24- and 96-) or glass bottom (24-) multi-well plates, coated homogenously with rat tail type I collagen (25–50 μg/ml), were subjected to soft-lithographic techniques [150] to pattern the collagen into micro-domains (islands of 500 μm in diameter with 1200 μm center-to-center spacing). To create MPCCs, hepatocytes were seeded on collagen-patterned plates that mediate selective cell adhesion. The cells were washed with medium 2–3 h later (~3x104 adherent hepatocytes in 96 collagen-coated islands in 24-well plate and ~4.5x103 hepatocytes in 14 islands in 96-well plate) and incubated in hepatocyte medium overnight. Hepatocyte culture medium was DMEM with high glucose, 10% FBS, 0.5 U/ml insulin, 7 ng/ml glucagon, 7.5 μg/ml hydrocortisone and 1% penicillin streptomycin. 3T3-J2 murine embryonic fibroblasts were seeded (9×104 cells in each well of 24-well plate and 1.4×104 cells in each well of 96- well plate) in fibroblast medium (DMEM with high glucose, 10% bovine serum and 1% penicillin-streptomycin) 12–24 h later. Fibroblast to-hepatocyte ratio was estimated to be 4:1, once the fibroblasts reached confluency. Fibroblast culture medium was replaced with hepatocyte culture medium 24 h after fibroblast seeding and subsequently replaced daily. Control conventionally-plated pure hepatocyte cultures (Collagen gel sandwich, Matrigel overlay, Matrigel substratum, and randomly distributed Cocultures of hepatocytes and murine fibroblasts) were created as described previously [150].

Pseudoparticle generation and infection assays

Pseudoparticles were generated by cotransfection of plasmids encoding an EGFP-encoding provirus (CSGW) or provirus encoding transgene (pTRIP), HIV gag-pol, and envelope glycoprotein(s), as previously described [204]. HCVpp were generated using H77 E1/E2 (residues 170–746).

Antibodies, immunostaining, and blocking

For immunostaining, cells or tissue sections were fixed in 1% paraformaldehyde and/or −20 °C methanol. Following washing and blocking in 1% BSA/0.2% milk or 1% BSA/0.3% Triton X-100 in PBS, cells were incubated in primary antibody overnight at 4 °C: mouse anti-human CD81 (clone JS-81, BD Pharmingen; 1:200), rabbit anti-SCARB1 (NB110-57591, Novus Biologicals; 1:100), rabbit anti-CLDN1 (51- 9000, Zymed; 1:200), rabbit anti-ZO1 (61-7300, Zymed; 1:200), mouse anti- OCLN (33-1500, Zymed; 1:200), mouse anti-MRP2 (Clone M2III-6, Kamiya Biomedical; 1:50), mouse anti-EEA1 (clone 14, BD Biosciences; 1:100), mouse anti-NS5A (9E10 [48], 1:2000). Secondary antibodies were goat-anti-mouse or goat-anti-rabbit AlexaFluor488- or AlexaFluor594-conjugates (Invitrogen; 1:1000) for immunofluorescence, or goat-anti-mouse HRP (ImmPress kit, Vector Labs) with DAB+ substrate (Dako) for immunohistochemistry. Nuclei were detected using Hoechst dye (500 ng/mL in PBS, Invitrogen). Images were captured on a Nikon inverted microscope using SPOT image analysis software. Confocal images were captured on a Zeiss LSM 510 inverted microscope at 0.3 μm optical slices using Zeiss software (v3.2). Z-stack files were uploaded into ImageJ64 software with images generated using a "Sum Slices" projection and 3D renderings were done using Imaris software. Final images were assembled using Adobe Photoshop CS3 software. Blocking experiments used human anti-SCARB1 antibody C167 [209], anti-CD81 (clone JS-81; BD Pharmingen), anti-E2 3/11 [243], and antibodies kindly provided by A.H. Patel (University of Glasgow, Scotland) (AP33) [212], S.K. Foung (Stanford University, Palo Alto, CA) (CBH5) [213], and D.R. Burton (The Scripps Research Institute, La Jolla, CA) (AR3A) [214]. Human IgG1 (clone MOPC-21), IgG4 (MOR6391), and rat IgG2a (MCA1124R) isotype control antibodies were purchased from AbD Serotec.

Chapter 4. Illuminating intercellular heterogeneity of viral infection

4.1 Introduction

The heterogeneity amongst single cells in a population has long been appreciated in numerous prokaryotic and eukaryotic cell systems [244]. The advent of quantitative imaging technologies for ascertaining cell-cell variability in molecular composition has revolutionized our understanding of single-cell heterogeneity [158-162], demonstrating how biochemical variations underlie decision-making in diverse processes such as migration, nutrition, and differentiation. Single-molecule RNA imaging in particular has been applied to assessing inter-cell differences in mRNA expression, uncovering extensive gene expression heterogeneity that contributes to phenotypic variation [163-165, 167-172, 245]. One unexplored area for which quantitative, single-molecule RNA imaging has similar potential is in elucidating the single-cell heterogeneity of RNA virus infection. RNA viruses must enter and replicate within individual host cells, and at any time, cells presumably contain different quantities of genomic viral RNA (vRNA) species. While much of this asynchrony likely stems from the stochastic nature of infection, inter-cell variations in host gene expression also underlie such differences [162, 246]; conversely, heterogeneous infection likely engenders single-cell differences in host gene expression as well. Although mastery of the systems biology of RNA virus infection will require a window into this rich single-cell complexity, such information is typically lost with the use of conventional, population assays for infection and for host gene expression.

Single-molecule RNA fluorescence *in situ* hybridization (smFISH) methods have been developed that allow imaging of individual mRNA molecules [164, 168], advancing our appreciation of cellular heterogeneity. smFISH is highly specific and sensitive, enabling

quantification of cell-cell differences; can be performed in numerous cell culture models and tissues without genetically modifying target RNAs or host cells; is amenable to multiplexing several RNA species; is compatible with immunocytochemistry; and is experimentally facile, involving readily available reagents, straightforward protocols, and standard epifluorescence microscopy [173].

Despite significant advances in vRNA imaging [247, 248], to our knowledge very few reports suggest single viral genome imaging [249, 250]; though these studies are of great potential value to investigations of genome trafficking and co-localization with host or viral factors, it is unclear whether the specificity, sensitivity, and resolution of these assays are sufficient to quantify individual viral genomes at the single-cell level. To determine if smFISH permits such imaging, we applied it to hepatitis C virus (HCV). HCV chronically infects the liver hepatocytes of almost 200 million worldwide and is a major cause of end-stage liver disease [2]. HCV drug development has been challenged by the lack of sensitive and quantitative tools for studying infection. It is a single-stranded, positive-sense RNA virus, in that the "positive" (or sense) strands contained in HCV virions replicate through intermediate "negative" (or antisense) strands [11]. Here, we show that smFISH affords specific and sensitive, quantitative detection of individual positive and negative strands of vRNA as diffraction-limited spots. We demonstrate that single-cell multiplexing of positive and negative vRNA strands illuminates the dynamics of positive and negative strand proliferation and can thus enhance our understanding of the viral life cycle. We also apply smFISH to multiplex vRNA with host gene expression and shed light on host-virus interactions, by revealing that the infection load of individual cells correlates with their response to an innate immune cytokine.

4.2 Results and discussion

4.2.1. Specific and sensitive, single-molecule imaging of genomic vRNA

In mRNA smFISH (**Figure 4-1A**) [168], cells are fixed and permeabilized, and fluorophore-labeled probe sets targeting the mRNA of interest are delivered. After hybridization, the aggregate fluorescence intensity at the site of individual mRNA molecules is sufficient to visualize them as diffraction-limited spots using standard epifluorescence microscopy; Z-stacks can be performed to acquire all such spots in the target cells. smFISH is highly sensitive and specific; further, comparison with real-time polymerase chain reaction (RT-PCR) corroborates mRNA transcript enumeration by smFISH spot counting, furnishing a quantitative assay for cell-cell differences in mRNA transcript levels.

We adapted this smFISH method to visualize genomic vRNA by studying HCV infection of the Huh-7.5 hepatoma cell line [51, 251], and to determine whether the assay can be used specifically and sensitively in this setting. We developed two probe sets each for both the HCV positive and negative strands – a Cy5 probe set targeting the 5' half of the strand, and an Alexa594 probe set targeting the 3' half. While smFISH performed on uninfected hepatoma cultures (**Figure 4-2A**) or infected cultures in the absence of probe sets (**Figure 4-2B**) revealed no spots, infected cultures imaged simultaneously with both Cy5 and Alexa594 probe sets for the positive or negative strand revealed diffraction-limited spots in both channels (**Figure 4-1B**). The high co-localization frequency of these spots (>80%) (**Figure 4-1B**) supports imaging specificity and that only one probe set is required to image each strand; further, this frequency is quantitatively similar to what has been observed for mRNAs [168]. Occasional non-co-localizing spots may reflect incomplete vRNA or vRNA with regions of poor accessibility to FISH probes.

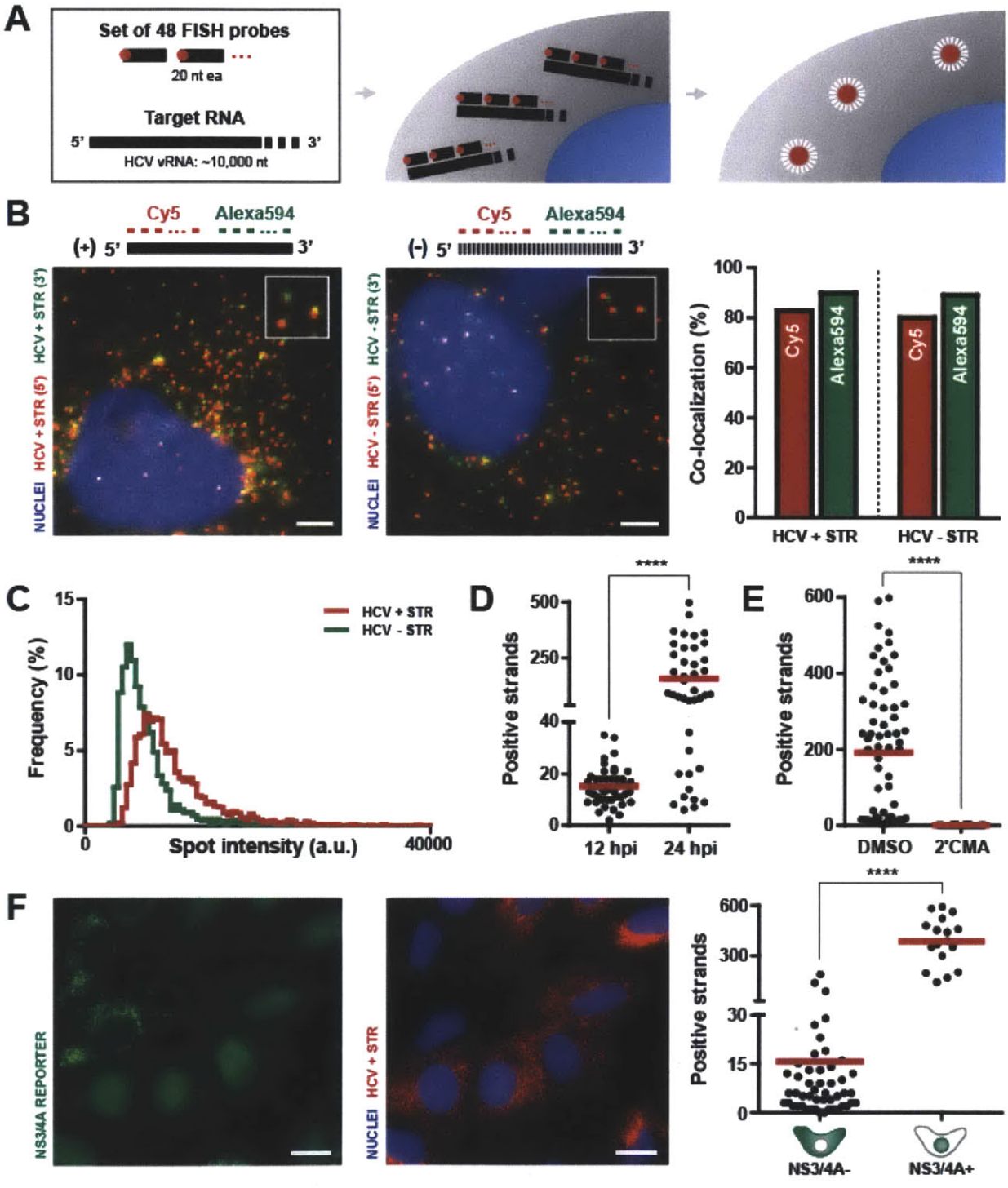

Figure 4-1. Specific and sensitive imaging of individual molecules of genomic viral RNA (vRNA). (**A**) Schematic illustration of single-molecule RNA FISH (smFISH) method [168]. A set of 48 DNA FISH probes (20 nucleotides/probe) that are each end-labeled with one fluorophore targeting non-overlapping portions of the target RNA (***Left***) are introduced to fixed and permeabilized target cells. Hybridization of probes to the

target RNA (***Center***) produces sufficient local fluorescence for the RNA molecule to be visualized as a diffraction-limited spot using standard epifluorescence microscopy (***Right***). As shown previously, spots are detected only once a minimum number of probes bind the target, reducing false positives due to random, off-target probe binding. Z-stacks can be performed to acquire all such spots in target cells. Using custom software, spots can be identified in three dimensions and quantified over a wide dynamic range, ranging two orders of magnitude from zero to several hundred spots per cell; alternatively, for cells with too many spots to identify individually, an estimate can be obtained by integrating the fluorescence intensity in the cell. Comparison with real-time polymerase chain reaction (RT-PCR) corroborates transcript enumeration by smFISH spot counting, showing that smFISH is quantitative. (**B**) Co-localization of diffraction-limited spots in infected Huh-7.5 hepatoma cultures (16 hours post infection) was determined by simultaneously introducing two spectrally distinct probe sets (coupled to Cy5 and Alexa594 respectively) targeting different portions of the same genomic vRNA strand. Typical images of positive (***Left***, Z-stack projection, scale bar $\approx$ 5.0 μm; ***Inset***, ~2x zoom) and negative (***Center***, Z-stack projection, scale bar $\approx$ 4.0 μm; ***Inset***, ~2x zoom) strands shown. Percentage of Cy5 and Alexa594 spots that co-localize with the other channel shown for both strands (***Right***). (**C**) Histogram representation of integrated intensity distribution for spots 24 hours post infection (hpi) for both strands. (**D**) Number of positive strands in individual cells at 12 and 24 hpi (means in red). Difference was statistically significant: ****$p < 0.0001$ (two-tailed t test). (**E**) Number of positive strands in individual cells in DMSO or the HCV NS5B polymerase inhibitor 2'CMA at 24 hpi (means in red). Difference was statistically significant: ****$p < 0.0001$ (two-tailed t test). (**F**) NS3/4A activity reporter [57] deems cells infected based on nuclear fluorescence and uninfected based on cytosolic fluorescence. The Huh-7.5 Clone 8 line which carries this reporter stably was used to compare NS3/4A imaging with smFISH. Sample images from the same field of view for both NS3/4A reporter (***Left***, scale bar $\approx$ 18.5 μm) and smFISH (***Center***, $\approx$ 18.5 μm) are shown. Number of positive strands in NS3/4A- or NS3/4A+ cells 24 hpi are provided (***Right***). Stat. significant diff: ****$p < 0.0001$ (two-tailed t test).

We next determined whether vRNA smFISH spots were indicative of single genomic strands or higher-order aggregates of RNA by integrating the total spot fluorescence for many spots. The spot intensity distribution was unimodal (**Figure 4-1C**), suggesting that spots represent single-molecule events [252]. Infrequent higher-order spots are detected, and may represent clusters of proximal genomes, accordant with many viruses employing organelle-like replication complexes [253-255].

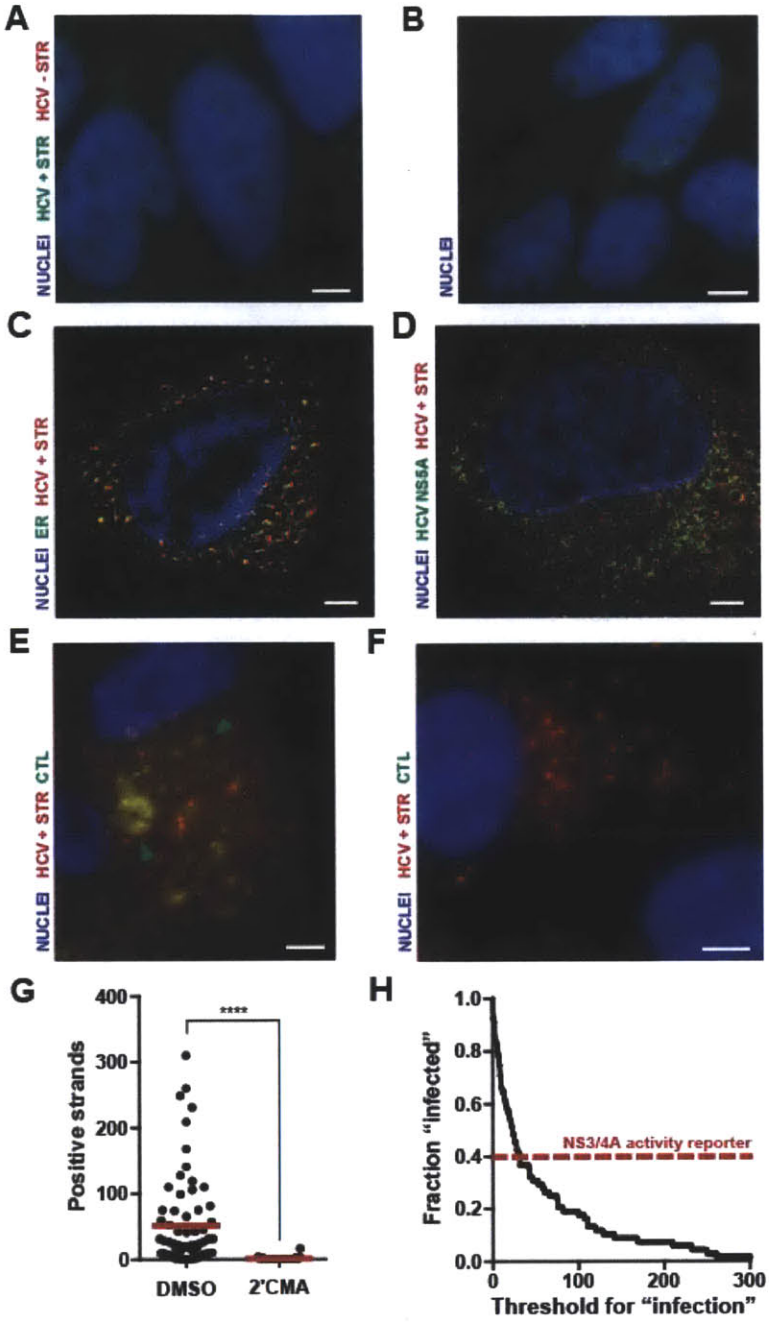

Figure 4-2. Specific and sensitive imaging of viral RNA in hepatoma and primary hepatocyte culture models. (A) Uninfected Huh-7.5 hepatoma cells imaged with probe sets for both the positive and negative strand (Z-stack projection, scale bar ≈ 4.9 μm). **(B)** Infected Huh7.5 cells imaged 24 hours post infection (hpi) on DAPI, Cy5, and Alexa594 channels but without FISH probe sets (Z-stack projection, scale bar ≈ 6.2 μm). **(C)** Structured illumination microscopy (SIM) of HCV (Cy5) and ER (Alexa594) (scale bar ≈ 3.0 μm) in infected Huh-7.5 cells 24 hpi. **(D)** SIM of HCV (Cy5) and HCV NS5A (Alexa594) (scale bar ≈ 3.7 μm) in infected Huh-7.5 cells 48 hpi. **(E)** Primary induced pluripotent stem-cell (iPSC)-derived hepatocyte-like cells imaged 1 week post infection [181] using confocal microscopy (scale bar

≈ 4.7 μm). Alexa594 (green) imaging performed without probe sets as a control to aid in the identification of frequent lipid-like autofluorescent foci (green arrows) distinct from diffraction-limited spots specific to the delivered probe set. **(F)** Primary human fetal liver cells (HFLCs) imaged 48 hpi by the J6/JFH Clone 2 strain of HCV (Z-stack projection, scale bar ≈ 4.2 μm). Alexa594 (green) imaging performed without probe sets also to identify occasional autofluorescent foci (none in this field of view). **(G)** Number of positive strands in individual HFLCs in DMSO or the HCV NS5B polymerase inhibitor 2'CMA at 48 hpi (means in red). Difference was statistically significant: ****$p < 0.0001$ (two-tailed t test). **(H)** Fraction of HFLCs "infected" at 48 hpi depending on the minimum threshold number of genomes for a cell to be deemed infected. NS3/4A activity reporter [57] infection rate estimate on replicate samples provided as a comparison.

Consistent with smFISH specificity and with spots serving as a measure of infection, the number of spots increases with time post infection (**Figure 4-1D**), and the number of spots is greatly reduced by the inclusion of an antiviral compound, the HCV non-structural protein 5B (NS5B) polymerase inhibitor 2'-C-methyladenosine (2'CMA) (**Figure 4-1**Error! Reference source not found.**E**). We also compared vRNA smFISH to a highly sensitive, single-cell fluorescent reporter of HCV infection that discriminates infected from uninfected cells based on HCV non-structural protein 3/4A (NS3/4A) protease activity [57]. In this assay, cytosolic fluorescence is observed in the absence of NS3/4A activity (NS3/4A-), whereas nuclear florescence is induced in cells with active NS3/4A (NS3/4A+). Notably, this method has proven more sensitive than viral antigen immunostaining (data not shown), paralleling the general assumption that enzymatic activity is inherently amplified and thus a highly sensitive indicator of enzyme presence. We observed that smFISH spots are significantly more numerous in NS3/4A+ than NS3/4A- cells (**Figure 4-1F**), verifying that smFISH qualitatively measures functional infection. Notably, even NS3/4A- cells display a wide range of smFISH spot counts, suggesting that vRNA smFISH is sufficiently sensitive to detect infection ahead of an enzymatic reporter, and that vRNA imaging in general is more sensitive than viral protein imaging.

In addition to being specific and sensitive, smFISH maintains spatial information and can be combined with staining for other targets, permitting localization of vRNA with respect to intracellular components. As a proof-of-principle, we performed smFISH using three-dimensional structured illumination microscopy (3D-SIM) [256], which enables fluorescence imaging at sub-diffraction-limit resolution. 3D-SIM reveals HCV positive strands positioned along the endoplasmic reticulum (ER) (**Figure 4-2C**), which may reflect strand replication along ER-derived membranes [257]; further, imaging can be performed alongside immunostaining for the HCV non-structural protein 5A (NS5A) (**Figure 4-2D**). As such, smFISH could assist investigations of vRNA trafficking and association with host or viral factors.

While hepatoma cells as used above have been central to the study of HCV, they have numerous drawbacks including abnormal proliferation, gene expression, innate immune signaling, and polarization [37-42]. Thus, there is interest in studying HCV infection in primary hepatocytes, but infection assays have generally been insufficiently sensitive given the high autofluorescence and low levels of HCV antigens [215, 258]. To determine if sensitive detection of single vRNA strands can overcome these difficulties, we performed smFISH on two primary hepatocyte models of HCV infection – induced pluripotent stem cell (iPS)-derived hepatocyte-like cells (iHLCs) [181] and primary human fetal liver cells (HFLCs) [259]. Infected iHLCs (**Figure 4-2E**) and HFLCs (**Figure 4-2F**) demonstrate positive strand vRNA smFISH spots, with fewer strands detected in the presence of 2'CMA (**Figure 4-2G**). While only 40% of HFLCs were NS3/4A+ using the above-described enzymatic reporter in replicate samples, smFISH spots were detected in most cells (**Figure 4-2H**); indeed, 93% of HFLCs had at least one viral genome. The phenotypic implications of containing viral genomes must thus be understood to define

"infection" at the cellular level, particularly in the setting of intact innate immune signaling where certain cells may successfully control attempts at infection. The ability to detect HCV infection in primary cultures suggests that smFISH will assist in studies ideally performed in primary cultures, including investigations of host-innate immune interactions, the role of hepatocyte polarization in infection, and the focal spreading of infection via cell-to-cell transmission [215, 225, 226]. As smFISH has been performed in tissue samples as well [260], such findings could be extended to *in vivo* studies as well.

4.2.2. Corroboration of smFISH genome quantification using a novel bulk infection assay

As shown, vRNA smFISH enables specific and sensitive visualization of individual viral positive and negative strands as diffraction-limited spots in infected cells. To determine if smFISH is quantitative for positive and negative strands, we would ideally compare such measurements with validated bulk assays of genomic vRNA. Unfortunately, existing PCR assays for vRNA have not demonstrated convincing strand discrimination, with estimates of the negative/positive strand ratio (NPSR) for HCV ranging widely from 1:10 to 1:1000 [261-272]. As such, the negative strand has been conceptually relegated to a qualitative indicator of productive infection in various cell types [262].

To address this shortfall and to corroborate our smFISH quantifications of both positive and negative strands, we developed a SYBR-based, tagged quantitative RT-PCR (qPCR)-based assay of vRNA burden in bulk populations. Total RNA is poly-A tailed, after which a tagged NV-oligo-dT primer is used for reverse transcription off the nascent tail (**Figure 4-3A**); the resulting complementary DNA (cDNA) is then used for qPCR, employing a primer for the tag sequence

and an HCV-specific primer for the 3' end of the target vRNA. This assay differs from previous tagged assays in two main ways – strand specificity is introduced at the PCR stage, and amplicons are generated that straddle the 3' ends of completed products of the viral polymerase. Using standards for both strands individually, we confirmed that the assay is sensitive over 8 logs for both strands (**Figure 4-3B**). To ascertain specificity, we used cross-mixed standards to determine that both strands could be detected unambiguously within a large range (**Figure 4-3C**). We next compared smFISH single-cell quantifications to bulk measurements made by qPCR on replicate samples; both assays yielded a similar fold change in positive or negative strand vRNA between two time-points post infection (**Figure 4-3D, Figure 4-3E**). Taken collectively, these data suggest that smFISH is quantitative for both positive and negative strands, and that these methods can help capture the elusive viral negative strand for HCV and potentially other RNA viruses.

4.2.3. Single-cell, multiplexed quantification of viral positive and negative strands for studying the viral life cycle

Genomic positive and negative strands are central to the fundamental processes of RNA virus infection, including production of viral proteins, replication, and population of new virions. Our understanding of how these functions are coordinated at the systems scale is largely based on bulk assays of infection, which are confounded by the asynchrony and thus single-cell heterogeneity of infection; further, strand discrimination has proven challenging even at the bulk level, as discussed above. We applied smFISH to permit direct, simultaneous enumeration of positive and negative strands in individual cells. Hepatoma cells were incubated in HCV and upon transfer into fresh medium, were fixed at various hours post infection (hpi) (**Figure 4-4A**).

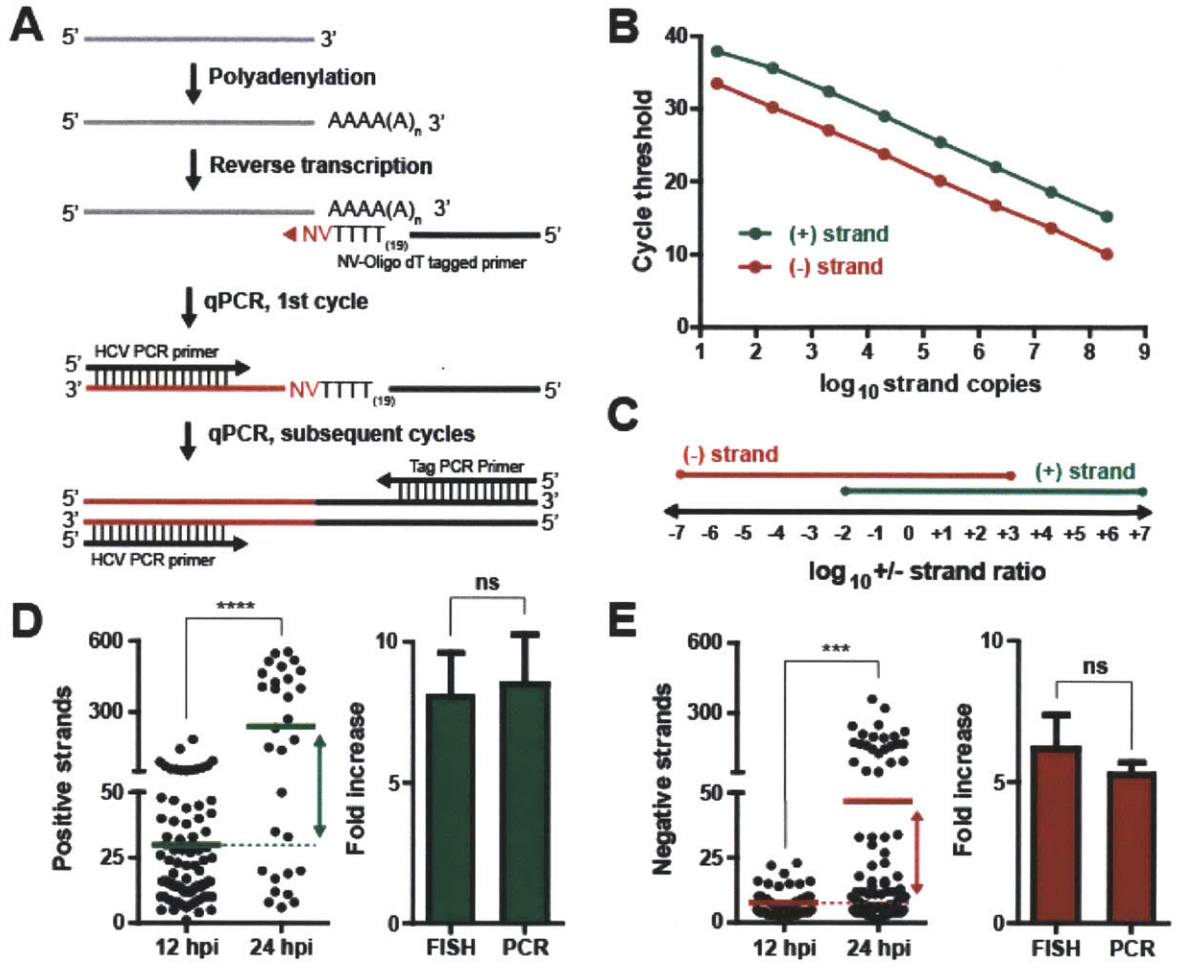

Figure 4-3. Single-molecule RNA FISH (smFISH) is a quantitative assay as verified by a novel bulk assay for quantifying genomic viral RNA (vRNA). (**A**) Schematic of quantitative polymerase chain reaction (qPCR) assay for measuring vRNA strands. Briefly, HCV is polyadenylated before undergoing an RT reaction with a tagged NV-oligo-dT primer. The resulting cDNA is used for qPCR using the exogenous tag primer and a strand-specific HCV primer directed towards the RNA 3' end. (**B**) Sensitivity of method as shown by cycle threshold (Ct) as a function of strand copies. (**C**) Specificity of method as shown by positive/negative strand ratio range within which single, unambiguous PCR products were identified. (**D**) qPCR comparison with smFISH-based quantification of HCV positive strands. Number of positive strands in individual cells shown at 12 hpi and 24 hpi (means in green), with fold increase visualized by green arrow (***Left***). Fold increase measured by both assays (***Right***). Data plotted as mean (μ) ± standard error of the mean (SEM). Difference was not statistically significant (n.s.) ($p > 0.05$) by two-tailed *t* test. (**E**) Assay comparison for negative strands. Number of negative strands in individual cells shown at 12 hpi and 24 hpi (means in red), with fold increase visualized by red arrow (***Left***). Fold increase measured by both assays (***Right***). Data plotted as μ ± SEM. Difference was not statistically significant (n.s.) ($p > 0.05$) by two-tailed *t* test.

Multiplexed imaging was performed using two spectrally distinct probe sets, each targeting a different vRNA strand (**Figure 4-4A**). The resulting images at each time (**Figure 4-4B**) yielded a corresponding single-cell joint distribution of positive and negative strand counts (**Figure 4-4D**). Population-scale replication trends can be obtained by summarizing the strand joint distributions with average metrics – the mean single-cell numbers of positive and negative strands, and the mean single-cell negative/positive strand ratio (NPSR) (**Figure 4-4C**). Taken together, such data portray significant inter-cell heterogeneity in strand counts at each time-point, highlighting the asynchrony inherent in infection that is masked by bulk assays, and reveal the correlation between positive and negative strands at single-cell level; further, they allow us to follow the temporal evolution of infection heterogeneity.

One notable feature of these data relates to the NPSR. In contrast to the prevailing positive-sense RNA virus dogma that positive strands are orders of magnitude more numerous than negative strands [273, 274], the NPSR measured by smFISH in this platform is highly dynamic. We observed that the mean single-cell NPSR starts low at 4 hpi, consistent with early virion unpacking and minimal replication, and exceeds unity, with the negative strands outnumbering positive strands at 12 and 24 hpi, prior to tapering thereafter (**Figure 4-4C, *Inset***). The single-cell strand joint distribution at 48 hpi shows that cells with fewer positive strands have greater NPSR than those with more positive strands (**Figure 4-4D, *Inset***); mirroring the population-scale NPSR trends. This result is consistent with cells earlier in infection initially favoring the production of negative strands before making further positive strands.

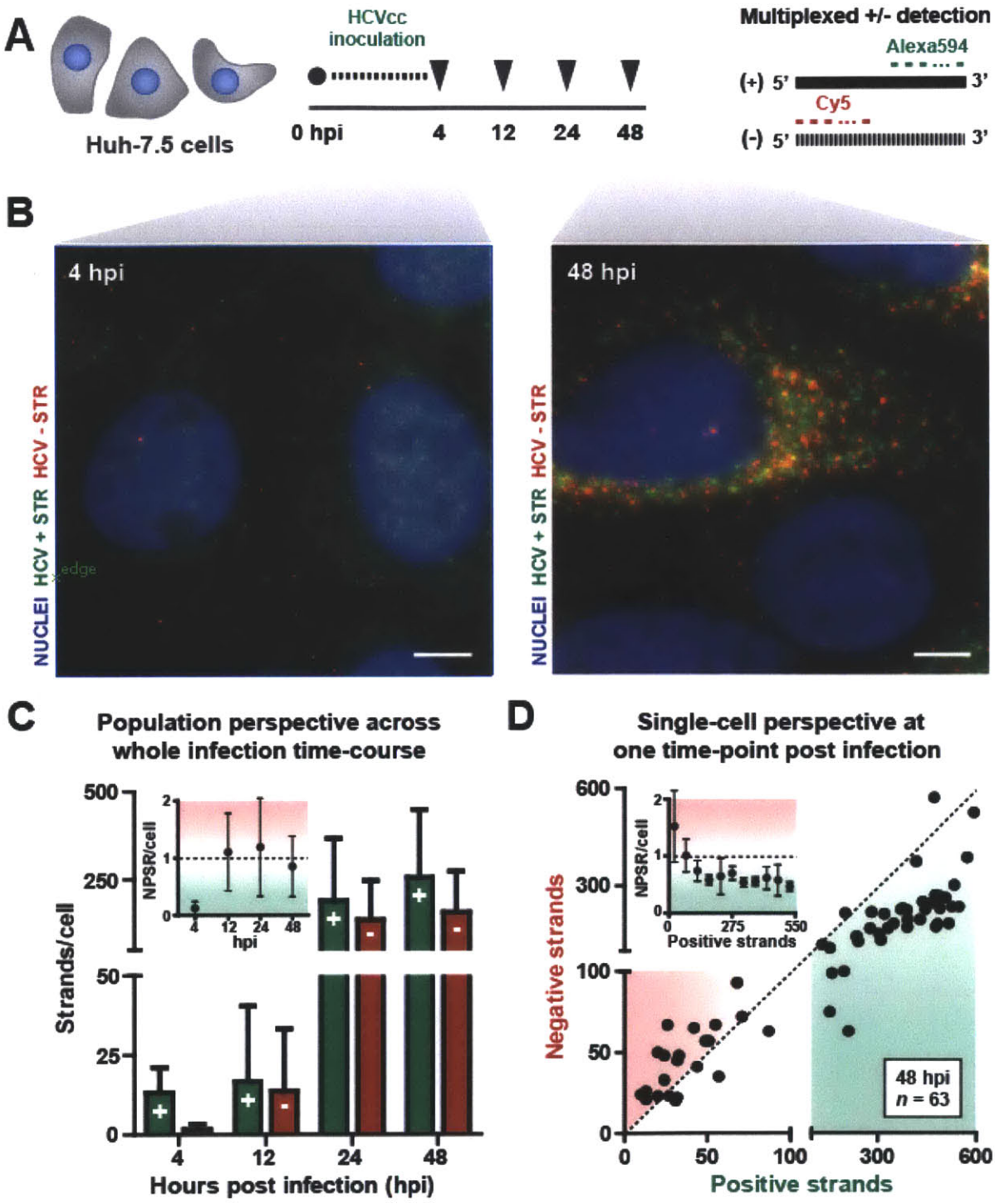

Figure 4-4. Multiplexed quantification of positive and negative viral strands in individual cells for illuminating viral replication. (**A**) Schematic illustration of experiment. Huh-7.5 hepatoma cells were inoculated with HCV for 4 hours, and then fixed for smFISH at various times thereafter (***Left***). Multiplexed imaging was performed by simultaneously employing an Alexa594 probe set for the positive strand and a Cy5 probe set for the negative strand (***Right***). (**B**) Sample images at 4 (***Left,*** Z-stack

projection, scale bar ≈ 7.0 μm) and 48 hpi (***Right***, Z-stack projection, scale bar ≈ 6.0 μm). (**C**) Population-wide perspective across whole infection time-course obtained by averaging the number of observed positive and negative strands for each cell at each time-point (4 hpi: $n = 70$; 12 hpi: $n = 44$; 24 hpi: $n = 67$; 48 hpi: $n = 63$). Data plotted as mean (μ) ± standard deviation (σ). The average single-cell negative-positive strand ratio (NPSR) at each time-point plotted as $\mu \pm \sigma$ (***Inset***). (**D**) Single-cell joint distribution of positive and negative strands for 48 hpi presented as a scatter plot showing the strand counts in individual cells ($n = 63$) (Pearson correlation coefficient $\rho = 0.86$). The dashed line separates the regions in which positive strands are more numerous than negative strands (below, green fill) and vice versa (above, red fill). Binning cells by positive strands and obtaining the average single-cell NPSR for each bin is plotted as $\mu \pm \sigma$ (***Inset***).

Another informative facet of these data is the bimodality of the strand distribution (**Figure 4-5**), with a separation of cells into subpopulations with low or high strand counts. One hypothesis to explain this pattern is that virus entry and early infection are slow, with a relatively gradual increase in strand counts. Upon achieving a threshold, moderate strand count, replication may accelerate, which tracks the rapid growth of strand counts observed between 12 hpi and 24 hpi (**Figure 4-4C**). Finally, single cells may saturate at some maximum number of strands, consistent with the slower strand count growth we see from 24 hpi to 48 hpi. This saturation could be due to the existence of a "carrying capacity" in cells wherein essential host factors are completely saturated [275, 276], or a dynamic equilibrium where strand production is matched by turnover of strands or dissemination of strands via new virions.

Quantitative single-cell analysis of infection heterogeneity has the potential to illuminate the systems biology of viral replication, particularly in association with mathematical models that could enable inference and testing of specific hypotheses given the access to such rich data [277-284]. Such experiments will be informative with the variation of parameters such as multiplicity of infection (MOI), and particularly enlightening in the presence of perturbations to normal infection physiology, such as the use of mutant viral strains with uncharacterized behaviors, the

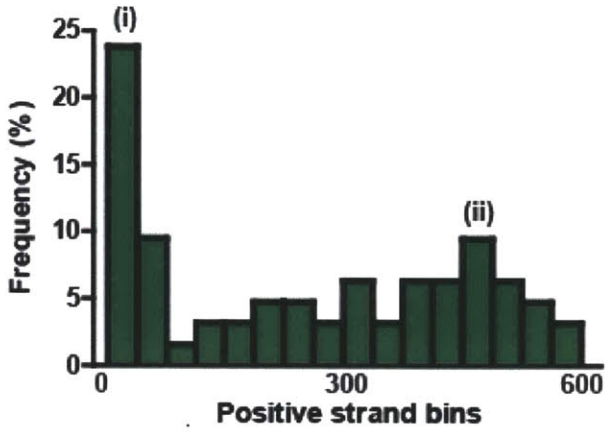

Figure 4-5. Bimodal distribution of infection. Positive strand marginal distribution shown as a frequency histogram at 48 hpi. Bimodality of such distributions is typically observed, with (i) a poorly infected mode and a (ii) highly infected mode.

infection of genetically manipulated host cells, and in the presence of compounds that bind specific viral or host targets.

4.2.4. Single-cell, multiplexed imaging of viral strands and host genes for understanding host-virus interactions

Variability in host cell gene expression likely contributes to the heterogeneity of RNA virus infection, and conversely, infection itself induces gene expression differences in virus-bearing cells. Elucidating this interplay between host genes and infection is central to the study of host-virus interactions, but correlating infection with bulk measurements of host transcript levels – typically made by RT-PCR or transcriptional microarrays – obscures single-cell level correlations. Ideally, single cells should be stratified two-dimensionally by grade of infection and by host factor expression, to provide a visual map of the infection-gene expression relationship. In principle, the use of smFISH can fill this gap, as it can quantitatively visualize cellular mRNAs [168] and image viral genomes in a quantitative manner (**Figure 4-6A**). To demonstrate this capability, we investigated how inter-cell variability in infection modulates the single-cell

response to Type I interferon (IFN). IFN stimulation initiates JAK/STAT signaling that culminates in the induction of antiviral interferon-stimulated genes (ISGs) [216-218], and it is believed that HCV may interrupt this cascade [8, 228, 229]. We developed smFISH probe sets that target mRNA transcripts for two prototypical ISGs: *EIF2AK2* and *ISG15*. Uninfected hepatoma cells were fixed for smFISH immediately before or after IFN-β exposure (**Figure 4-6B**). Imaging cells with probe sets for *EIF2AK2* and *ISG15* shows a baseline quantity of diffraction-limited spots that increases significantly upon administration of IFN-β (**Figure 4-7A, Figure 4-7B, Figure 4-6D**); these post-treatment ISG levels are stable from 6 to 24 h (**Figure 4-7B**). Notably, despite uniform IFN-β stimulation, ISG expression varies dramatically in individual cells, mirroring the stochastic production of IFN-β in response to infection [285]; this observed pattern raises questions as to how liver tissue coordinates an antiviral response to infection.

Similarly, infected hepatoma cells were fixed for imaging before or after a 12 h exposure to IFN-β (**Figure 4-6B**). Multiplexed smFISH was performed to obtain joint distributions of HCV vRNA with *ISG15* and with *EIF2AK2*. This duration of IFN-β treatment did not significantly reduce HCV strand counts (**Figure 4-7C**), arguing against IFN-mediated viral clearance during this interval. Infected hepatoma cells did not upregulate ISG mRNAs in the absence of IFN-β (**Figure 4-6D**), consistent with defective innate immune signaling in Huh-7.5s [41]; further, no correlation between ISG mRNA and HCV strands was observed (**Figure 4-6D**). However, after treatment with exogenous IFN-β, ISG mRNAs were strongly correlated with HCV infection load (**Figure 4-6C, Figure 4-6D**). ISG levels in poorly infected cells were similar to those in uninfected controls, consistent with minimal perturbation to normal cell physiology in these cells

(**Figure 4-6D**); indeed, separating cells into "low" and "high" infection modes based on underlying infection bimodality (**Figure 4-7D**) shows that only highly infected cells harbor significantly more ISG mRNAs than uninfected controls (**Figure 4-7E**). These data seemingly contradict infection-mediated inhibition of IFN signaling under the experimental conditions investigated, which would predict an inverse correlation between ISG transcripts and infection. One possible explanation is that negative feedback regulators of IFN signaling, such as suppressor of cytokine signaling (SOCS) proteins and ubiquitin specific peptidase 18 (USP18), are less efficiently produced in infected cells [286-288], causing ISG levels to exceed physiologic levels. This model is consistent with the recent finding that infection induces PKR-mediated inhibition of host translation [289]. It will be informative to study how such correlations differ in primary hepatocytes with intact innate immune signaling, and how they vary across types of IFN, concentrations, and dosing schedules.

In summary, we have demonstrated that multiplexed imaging of vRNA and host transcripts at the single-cell level can yield unprecedented insights into host-virus interactions. The generalizability of smFISH to imaging arbitrary mRNAs will enable researchers to determine the gene expression-infection interrelationship in numerous experimental settings.

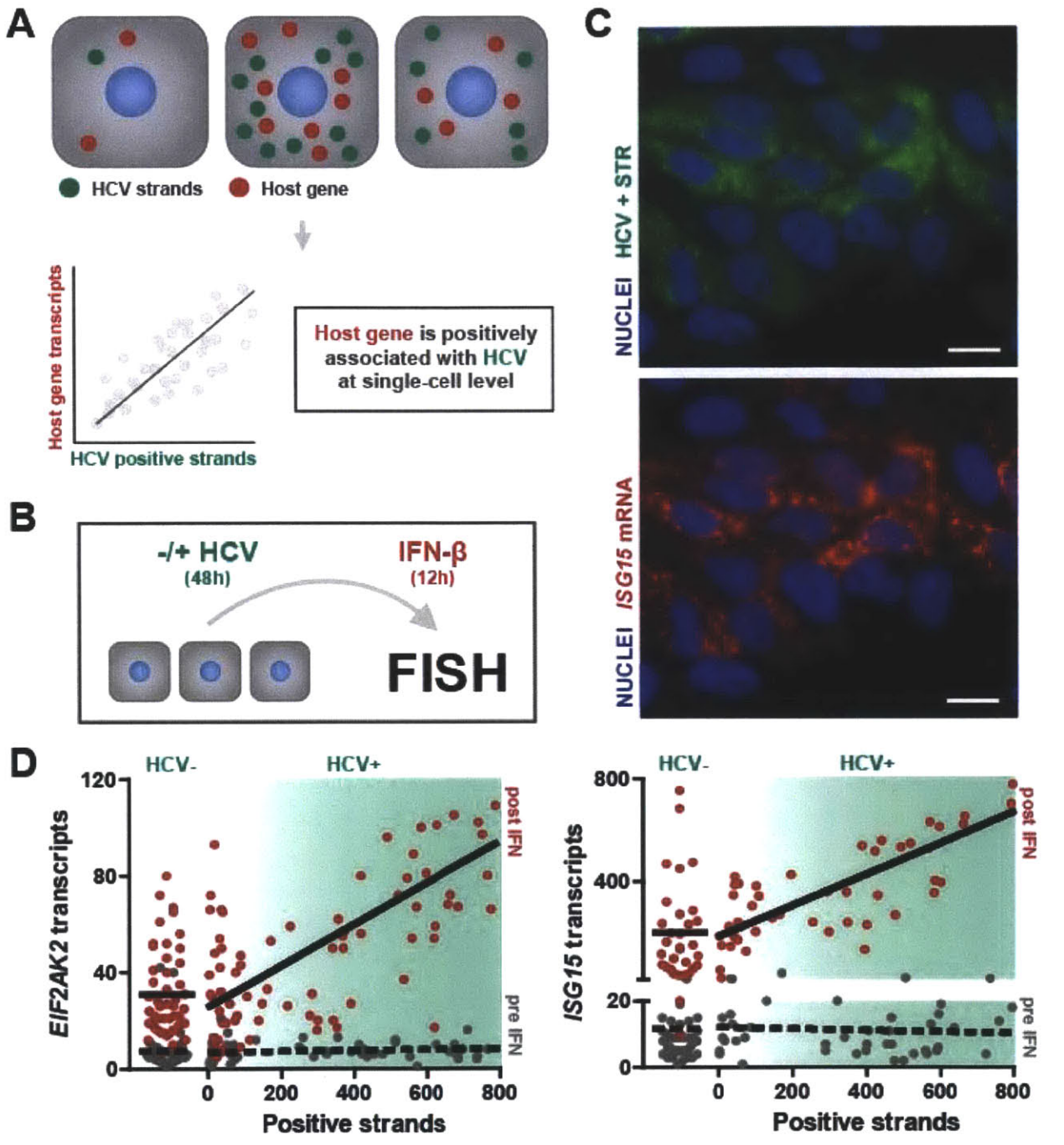

Figure 4-6. Multiplexed quantification of viral positive strands and host mRNA transcripts in individual cells for dissecting host-virus interactions. (**A**) Schematic of concept. A relationship between infection and host gene expression at the single-cell level (***Top***) can be identified using multiplexed smFISH to yield a single-cell joint distribution for these two parameters (***Bottom Left***); statistics can be performed to evaluate the association between these parameters, leading to a conclusion that can assist in addressing hypotheses about host-virus interactions (***Bottom Right***). (**B**) Schematic describing experiment to ascertain relationship between hepatitis C virus (HCV) infection

and interferon-stimulated gene (ISG) expression by dosing with the Type I interferon (IFN), IFN-β. Infected (48 hpi) or uninfected cells are dosed with 10 U/mL IFN-β for 12 hours before performing multiplexed smFISH for HCV positive strands and either *EIF2AK2* or *ISG15*. (**C**) Typical multiplexed images showing the same field of view 12 hours post dosing of IFN-β in terms of HCV positive strand (*Top,* scale bar ≈ 17.0 μm) and *ISG15* mRNA (***Bottom,*** scale bar ≈ 17.0 μm). (**D**) Joint distributions for *EIF2AK2*/HCV (***Left***) and *ISG15*/HCV (***Right***) visualized as scatter plots. In each plot, the results of the uninfected experiment are presented on the left (HCV-) where each point represents the number of ISG mRNA transcripts of individual cells, and on the right are the results of the pre-infected experiment (HCV+) where each point represents both the number of HCV positive strands and the number of ISG mRNA transcripts; progressively more infected cells are rightwards on each plot (green gradient). Gray points are results pre-IFN treatment (dashed mean and best-fit lines), and red points are results post-IFN treatment (solid mean and best-fit line). For uninfected cells, increase post-IFN was statistically significant for *EIF2AK2* (****$p < 0.0001$) and for *ISG15* (****$p < 0.0001$) using two-tailed t test. For infected cells before IFN treatment, there was no positive correlation between ISG mRNA expression and HCV positive strands for both *EIF2AK2* ($p > 0.05$) and *ISG15* ($p > 0.05$) as determined by F test on linear regression parameters. For infected cells after IFN treatment, there was a strong positive correlation between ISG mRNA expression and HCV positive strands for both *EIF2AK2* (****$p < 0.0001$) and *ISG15* (****$p < 0.0001$) as determined by F test on linear regression parameters.

4.2.5. Conclusion

In summary, smFISH permits quantitative visualization of individual genomic strands of HCV, revealing significant virus and host heterogeneity in the process of infection with implications for viral pathogenesis. The study of this heterogeneity will be particularly illuminating in the setting of primary cultures and patient tissue samples. We hypothesize that other RNA viruses are also amenable to smFISH, and given the ideal features of smFISH that encourage adoption, use of this technique could significantly enhance the study of RNA viruses more generally.

4.2.6. Personal contributions to this work

The author of this thesis lead a group of researchers in planning, performing, and interpreting experiments.

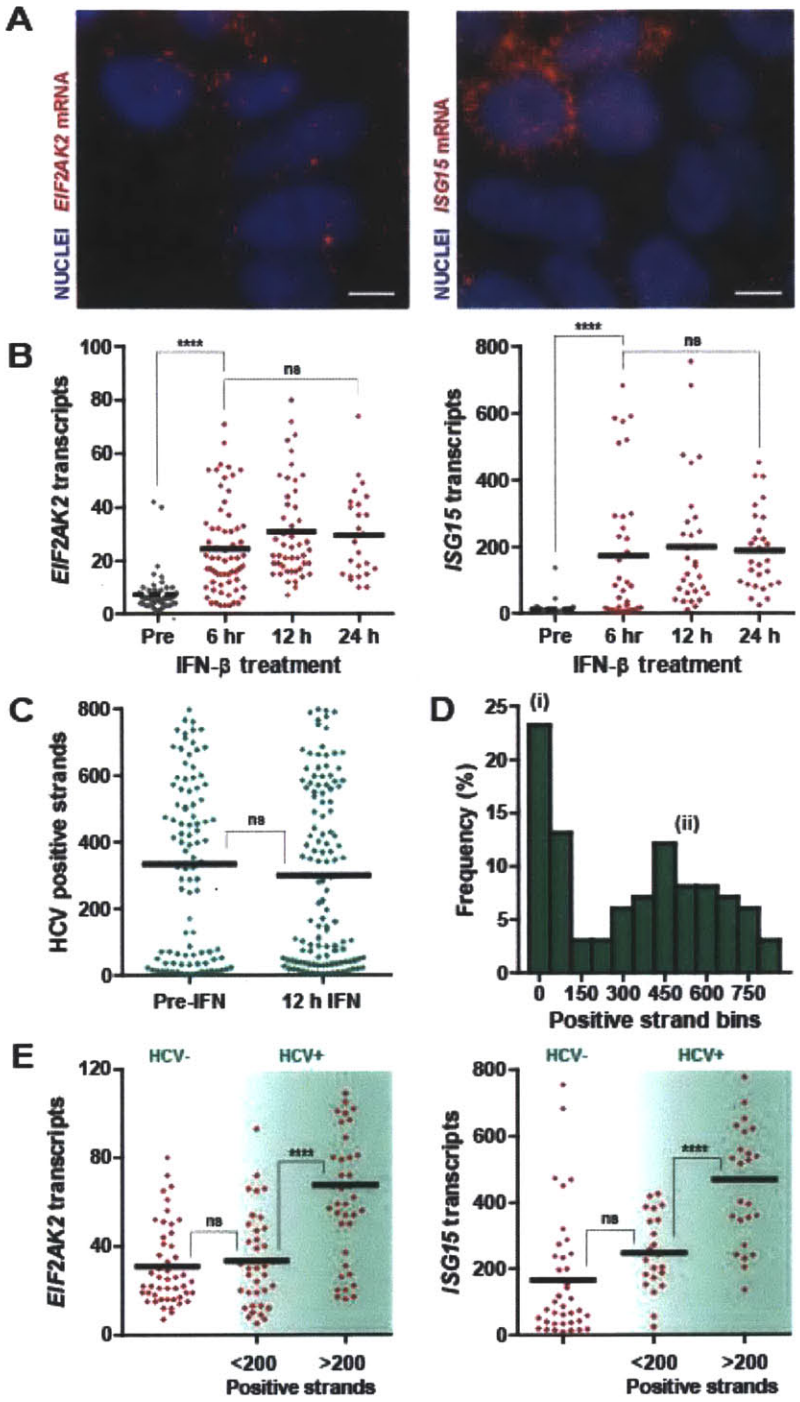

Figure 4-7. Association between viral infection and interferon-stimulated gene (ISG) expression. (A) Typical smFISH images of *EIF2AK2* (*Left*, Z-stack projection, scale bar ≈ 9.5 μm) and *ISG15* (*Right*, Z-stack projection, scale bar ≈ 9.5 μm) post IFN-β-treatment (100 U/mL, 48 hours). **(B)** Number of ISG mRNA transcripts in individual cells pre-IFN (gray) or at various times post-IFN-β treatment (10 U/mL) (red) for *EIF2AK2* (*Left*) and *ISG15* (*Right*). Means are shown as dashed or solid lines for pre- and post-IFN treatment, respectively. Difference between pre-IFN and 6 hours post-IFN are

statistically significant for both *EIF2AK2* (****$p < 0.0001$) and *ISG15* (****$p < 0.0001$). All differences between post-treatment IFN time-points are non-significant (n.s.) for both *EIF2AK2* and *ISG15* ($p > 0.05$) as determined by one-way ANOVA with Tukey's post-test. **(C)** Number of HCV positive strands in individual cells pre-IFN-β and post-IFN-β (10 U/mL) for 12 h (means in black). Difference was n.s. by two-tailed *t* test ($p > 0.05$). **(D)** Single-cell distribution of number of positive strands visualized as frequency histogram reveals bimodality with (i) poorly infected and (ii) highly infected modes. **(E)** Number of ISG transcripts in individual cells for both *EIF2AK2* (*Left*) and *ISG15* (*Right*) (means in black). On each plot, the number of transcripts in uninfected cells is shown (HCV-), and on the right (HCV+), the number of transcripts is presented for each cell after splitting cells into a poorly and highly infected bin based on the number of positive strands (using 200 strands as a threshold). The difference in ISG expression between uninfected cells and poorly infected cells is n.s. for both *EIF2AK2* and *ISG15* ($p > 0.05$) as determined by two-tailed *t* test. The difference in ISG expression between poorly and highly infected cells is highly significant for both *EIF2AK2* (****$p < 0.0001$) and *ISG15* (****$p < 0.0001$) by two-tailed *t* test.

4.3 Materials and methods

Cell culture

Huh-7 [46], Huh-7.5 [51], and a clone of Huh-7.5 stably integrating the NS3/4A activity reporter [57] were all propagated in a DMEM with L-glutamine (Cellgro)-based medium containing 100 U/mL penicillin, 100 μg/mL streptomycin (Cellgro), and 10% FBS (GIBCO). Primary human fetal liver cells (HFLCs) were isolated and plated as described [259]. Cultures were maintained in Hepatocyte Defined Medium (HDM) (BD Biosciences) plus L-glutamine and antibiotics. Induced pluripotent stem cell (iPSC)-derived hepatocyte-like cells (iHLCs) were derived and cultured as described [82, 181]. For smFISH experiments, cultures were grown on 12 mm, circular, No. 1 glass coverslips (VWR) in 24-well plates. For Huh-7.5s, attachment to coverslips was improved by coating with rat tail collagen I (BD Biosciences) at 50 μg/mL in water for 1 hour at 37°C and then rinsing prior to seeding. HFLC attachment was enhanced by first coating with collagen and subsequently with poly-L-lysine hydrobromide (Sigma) at 100 μg/mL for 45 minutes at room temperature and then rinsing prior to seeding. To put iHLCs on coverslips, they were treated with accutase (Millipore) for 15-20 minutes until they balled up. Gentle pipetting was performed to remove the cells, and they were then plated onto Matrigel-coated coverslips.

Hepatitis C virus infection, antiviral treatment, and interferon treatment

Hepatoma and iHLC infections were performed with a *Gaussia* luciferase-expressing reporter virus based on the efficient Jc1 HCV construct [290]; stocks of this reporter were obtained as described [207]. HFLC infections were performed either with this Jc1 reporter or with an adapted HCV called J6/JFH Clone 2 [291]. Titration on naïve Huh-7.5s was used to determine 50% tissue culture infectious dose ($TCID_{50}$) of stocks of these strains of HCV. For infection experiments, we employed three standard models of HCV infection: the Huh-7.5 hepatoma cell line (as

well as the associated Huh-7 cell line and the clone of Huh-7.5 stably expressing the NS3/4A activity reporter as described below) [251], primary human fetal hepatocytes [259], and induced pluripotent stem cell-derived hepatocyte-like cells [181]. Stocks were diluted in the appropriate culture medium to make an inoculum with final titer typically in the 10^5-10^6 $TCID_{50}$/mL range. Cultures to be infected were incubated in inoculum for varying durations depending on the experiment. Subsequently, medium was typically changed every 24-48 hours unless otherwise noted, and cultures were washed with culture medium three times between medium changes. To demonstrate that smFISH imaging of HCV genomes is replication-dependent, the HCV non-structural protein 5B (NS5B) polymerase inhibitor 2'-C-methyladenosine (2'CMA), with EC_{50} = 27 nM [251], was used to supplement both the inoculum and subsequent fresh medium at a concentration of 80*EC_{50} (final 0.1% DMSO) and compared to a DMSO-only control. Human interferon β (IFN-β) (Calbiochem) was used to treat cells as described.

Single-molecule RNA FISH (smFISH)

smFISH on culture samples is performed as described in detail [168]. All protocols are also available online at http://www.singlemoleculefish.com. Briefly, culture samples on coverslips are fixed in 4% w/v paraformaldehyde (Electron Microscopy Sciences) in PBS for 10 minutes. After washing with PBS, samples can be maintained in PBS for at least one week at 4°C. Six hours prior to hybridization with probes, samples are permeabilized by placing in 70% EtOH in water at 4°C. Coverslips are incubated in hybridization buffer containing a probe set targeting the RNA species of interest (BioSearch Technologies; http://www.singlemoleculefish.com; probe sets were designed targeting the *Gaussia*-luciferase-expressing HCV reporter described above), each probe of which is coupled to desired fluorescent molecule (typically Alexa594 or Cy5). Multiple probe sets coupled to spectrally distinct probe sets can be hybridized to sample simultaneous for multiplexed imaging. Finally, samples are washed, during which time fluorescent molecules targeting antigens of interest or immunofluorescence antibodies can be incorporated as described [168], and subsequently mounted for imaging. In this study, endoplasmic reticulum staining was performed using the ER-ID Green assay kit (Enzo Life Sciences), and HCV non-structural protein 5A (NS5A) immunostaining was performed using mouse anti-NS5A (9E10) and goat anti-mouse Alexa Fluor 594 (Invitrogen).

Microscopy and image analysis

Standard epifluorescence microscopy can ascertain smFISH spots as described [168]. All images were taken with a Nikon Ti-E inverted fluorescence microscope equipped with a 100X oil-immersion objective and a Photometrics Pixis 1024 CCD camera using MetaMorph software (Molecular Devices, Downington, PA). Z-stacks were obtained as described [168]; typically, 20-30 planes separated by 0.4 μm was sufficient to comprehensively cover the target cells. Images presented as slices from the Z-stack or maximum intensity projections as described. Images were analyzed to extract data we show using custom software written in MATLAB (The MathWorks), which can identify spots on individual channels, assess co-localization, and quantify spots. Quantification has an upper-bound for each cell that depends on cell volume (height and cross-section), subcellular distribution of target RNA, quality of imaging, and signal-to-noise ratio. At later time-points post infection (~48 hours), the number of positive strands as visualized using an Alexa594 fluorophore probe set typically was deemed too large to be counted computationally

without significant error in a small portion of the cells. For these cells, an estimate was obtained by integrating the fluorescence intensity in a sum projection of the Z-stack for the cell and subtracting the local background, and comparing this quantity with that of countable cells to extrapolate an estimate [170]. In order to obtain spot intensity distributions, we used custom-written MATLAB software to reduce the stacked images to two-dimensional images by maximum projection, and fitted the fluorescent spots to a 2D Gaussian as the model for the point spread function. Single transcript intensity was defined as the integrated intensity of the spot using the two-dimensional Gaussian mask algorithm.

HCV non-structural protein 3/4A (NS3/4A) activity reporter

As previously described [57], we developed a real-time fluorescence reporter of HCV infection based on monitoring NS3/4A protease activity. A clone of Huh-7.5 stably expressing the RFP-NLS-IPS was used to determine the correlation between smFISH imaging of HCV genomes and NS3/4A protease activity.

Strand specific qPCR of HCV RNA

Non-infectious positive strand standards were constructed by digesting a plasmid containing J6/JFH1 "Clone 2" virus (Walters, et al. 2009) with SacI (NEB) and religating the backbone. After XbaI digestion, this DNA was used in a T7 transcription reaction to yield a 3516nt RNA standard with intact 5' and 3' ends. For minus strand standard synthesis, we employed an overlap PCR approach to flip the orientation of the positive strand standard. Generated RNA stocks of both strands were equilibrated via nanodrop to a calculated concentration of 10^{10} copies/ul. Standard curves were generated by serially diluting the RNA standards in the presence of fixed 50ng amounts of total RNA from uninfected Huh-7.5 cells. For qPCR of unknown samples, RNA was isolated using the RNeasy Plus Mini kit (Qiagen, Valencia, CA) from infected Huh-7.5 cells. Approx 50ng of total RNA was then used for PolyAdenylation using E. coli PolyA Polymerase (New England Biolabs, Ipswich, MA) using 1mM ATP, 3U E-PAP and 7.5U RNAsin Plus RNAse inhibitor (Promega, Madison, WS) in a 5ul total reaction volume, and incubated for 10 minutes at 37°C followed by 20 minutes at 65°C to inactivate the enzyme. The resulting RNA underwent reverse transcription using Superscript III (Life Technologies, Carlsbad, CA) following the manufacturers' instructions and using the tagged RT primer (5'-...TTTTTTTTTTTTTTTTTTTVN-3') at a final concentration of 2.5uM. Approx 2ng of the resulting cDNA was used per subsequent qPCR reaction using 2x FastStart SYBRGreen qPCR mix (Roche) following the manufacturer's instructions and using a 2.5uM primer for the tag sequence (GAATCGAGCACCAGTTACGCATG) and either the positive strand primer (CTGGTCTCTCTGCAGATCATGT) or the negative strand primer (CTGCGTGAAGACAGTAGTTCCTCA) also at 2.5uM. For convenience in many experiments, we adapted the miScript RT kit (Qiagen) which employs a polyA-tailing and RT step with the above RT primer in a single reaction, to produce the necessary input for subsequent qPCR using HCV specific primers and the tag primer. qPCR was carried out using iQ5 thermal cyclers (BioRad) using the following cycling paramters: 95°C for 10minutes, 40x (95°C for 15s, 58°C for 15s, 72°C for 20s collecting fluorescence), 95°C for 2 minutes, 55°C for 2 minutes followed by fluorescence measurement for each 0.5°C interval increase to 95°C to generate melt curves.

Statistical analysis

Error bars plotted as standard deviation (σ) or as standard error of the mean (SEM) as noted. Statistical analysis performed as described – two-tailed *t* test, one-way ANOVA with Tukey's post-test, linear regression, and *F* test for determining positivity of slope performed using GraphPad Prism 5 (GraphPad Software). Pearson correlation coefficients obtained using MATLAB (The MathWorks).

Chapter 5. Perspectives and future directions

Viruses are responsible for substantial global morbidity and mortality, with a significant percentage of the world suffering from infection by one of hepatitis C virus (HCV), hepatitis B virus (HBV), and human immunodeficiency virus (HIV). As in disease broadly, improvements in experimental methodologies directly accelerate translational research; to this end, the goal of this thesis was to develop technologies for the study of viral infection and to demonstrate their use. Though this thesis focused specifically on the study of HCV, the techniques, analyses, and concepts introduced here can likely be extended to other viruses and microbes more generally. Here, we reflect on our results and discuss future trajectories for these projects.

We first envisioned a system for "personalizing" the study of infection, by obtaining patient-specific somatic cells; reprogramming them into induced pluripotent stem cells (iPSCs); differentiating them into an adult tissue (in this case, hepatocytes) that is permissive to a pathogen of interest (in this case, HCV); and infecting them with the pathogen. Such a paradigm would enable the investigation of patient-specific natural history of infection and treatment response, bringing us closer to realizing personalized medicine. While researchers have developed numerous models of genetic disease employing iPSCs from individuals with genetic mutations, this approach has not been pursued in the study of infection. Technical barriers have in general forced researchers to perform studies in a small number of host models, raising the question of generalizability of findings to the broader population. Research is gradually revealing how important the host background is; in hepatitis C for example, it has long been known that only some patients respond to interferon regimens, and genome-wide association studies (GWAS) have determined that a polymorphism in the interleukin-28b (*IL-28b*) is predictive of

this response. However, while these and other genetic factors are known to influence infection phenomena, we do not mechanistically understand how they underlie such differential responses. Obtaining such an understanding necessitates an *in vitro* model of infection that captures host genetics, and the emergence of iPSC technology enables the sourcing of such models. By showing in this thesis that iPSC-derived adult tissue can be permissive to a pathogen, we have demonstrated the feasibility of "personalizing" the study of infection.

This work opens the door to numerous investigations. First, it is now possible to systematically obtain iPSC lines from numerous patients with backgrounds of interest, and to study infection in these different contexts. For HCV in particular, iPSC lines can be acquired from individuals with *IL-28b* polymorphisms and with known mutations in genes relevant to viral pathogenesis such as signal transducer and activator 1 (*STAT1*) and low-density lipoprotein receptor (*LDLR*). It will be particularly exciting to study patients with unique clinical trajectories but for which no known genetic mutations have yet been ascribed, such as fulminant hepatitis patients. The study of how infection in these different genetic backgrounds responds to therapy differentially will be especially valuable, paving the way for "customized treatment" of individual patients. Second, we are determining whether it is possible to develop personalized animal models of infection. Though animal models are a mainstay in the development of therapy and in illuminating systems pathophysiology, animal models of HCV infection have been elusive largely due to the primate tropism of HCV. Our lab has recently described the development of robust, "humanized" mice [292], in which a tissue-engineered "organoid" carrying hepatocytes is transplanted intraperitoneally; these organoids integrate with mouse vasculature, through which they can serve as ectopic livers. It will be fruitful to determine whether iPSC-derived hepatocytes can be

cultivated in these organoids and subsequently transplanted into animals, furnishing a personalized, humanized mouse that could be used to study patient-specific infection *in vivo*. Third, the ability to coax iPSCs from the pluripotent stage to hepatocytes makes it possible to study the onset of HCV-permissiveness throughout this maturation; thus can enable us to both identify the minimal host factor machinery necessary for infection, and study the development of the innate immune response to infection which may progress after the fetal hepatocyte stage [293]. Finally, it will be natural to show that the paradigm of personalized studies of infection can be applied beyond HCV.

The second project we described sought to address another major hindrance to the HCV field – the lack of a primary adult hepatocyte *in vitro* model of infection. Instead, the HCV research community and indeed scientists studying liver biology in general have relied extensively on hepatoma cell lines which suffer from defective signaling, gene expression, proliferation, and polarization. Partly due to its exceptional permissiveness to HCV, the Huh-7.5 hepatoma cell line has proven invaluable for HCV basic research and for antiviral screening. Despite this progress, deviations from expected physiology in this model have cultivated great interest in studying HCV infection in a more physiologic, primary adult hepatocyte model. Though the stable culture of primary hepatocytes *in vitro* has been notoriously challenging, our lab has employed tissue engineering methodologies to develop a micropatterned co-culture (MPCC) of hepatocytes and supportive stroma that exhibits long-term liver phenotype maintenance [150]. In this thesis, we demonstrated that MPCCs are permissive to HCV infection, enabling researchers to begin studying HCV infection in its native host.

One unexpected finding in this model was that "isolated" primary adult hepatocytes – hepatocytes in the absence of liver microenvironmental stimuli – acutely resolve HCV infection. HCV *in vivo* has a remarkable tendency to chronicity, partly due to its ability to blunt IFN signaling; however, despite the absence in MPCCs of innate and adaptive immune effectors, infection was more rapidly cleared *in vitro*. By comparison with Huh-7.5s which lack effective intrinsic innate immunity, we hypothesized that IFN signaling in primary hepatocytes may constrain HCV infection and showed that this was the case using various methods to interrupt the IFN pathway. So why is IFN signaling able to eliminate infection only in these "isolated" primary adult hepatocytes but not *in vivo*? We hypothesized that signals in the liver microenvironment may "tolerize" hepatocytes to infection by dampening IFN signaling. It has long been appreciated that the liver is a remarkably tolerant environment in which innate and adaptive immune effector cells are exposed to anti-inflammatory agents that mitigate their immune functions. However, our hypothesis was that the hepatocytes themselves, which are the primary site of infection, are also exposed to cues that tolerize their IFN signaling. To this end, we performed a screen of candidate anti-inflammatory compounds in MPCCs which identified several hits that enhance infection; interleukin (IL)-6 was the most potent, able to enhance infection 10-30 fold. We confirmed mechanistically that IL-6 blunts the IFN response to infection, which likely explains its capacity to boost infection so dramatically. IL-6 is normally secreted by the liver-resident macrophages known as Kupffer cells as a result of their continuous exposure to lipopolysaccharide (LPS) introduced through the intestinal circulation. It is believed that this influx of LPS and other microbial antigens would require anti-inflammatory compensation to prevent the liver from being constantly inflamed. In line with this, we suggest a model in which LPS-provoked Kupffer cells produce IL-6 that encourages hepatocytes to

become immunologically inert to avoid inflammation; this quiescence is in turn exploited by HCV, malaria, and potentially other pathogens, which can establish themselves in a host with lessened surveillance. Proper elucidation and generalization of this concept will benefit from the "bottom-up" development of more complex MPCC models incorporating nonparenchymal cell types such as Kupffer cells to determine how they modulate infection; it is likely that numerous liver cell types modulate infection in various ways, and we have indeed shown that human liver fibroblasts, liver sinusoidal endothelial cells (LSECs), mesenchymal stem cells (MSCs), and an unrefined collection of rat liver nonparenchymal cells (NPCs) all enhance HCV infection. Finally, it will be possible to verify these findings *in vivo* using small animal models of hepatotropic infection, which our lab and others are developing; initial steps towards this could involve encapsulation of primary hepatocytes in organoids and infection post implantation into mice. Validation of this concept *in vivo* would raise the exciting possibility of using inhibition of IL-6 signaling for hepatotropic pathogens broadly.

The availability of a primary hepatocyte model will be particularly exciting for research where Huh-7.5s deviate most significantly from normal physiology. Aside from innate immune signaling, hepatocyte polarity is another such area, with Huh-7.5s being non-polarized. Unlike simple epithelia, natural hepatocytes demonstrate complex polarization consisting of irregular apical (bile canalicular) and basolateral (space of Disse) domains separated by tight junctions. This is relevant to HCV infection. The entry receptors for HCV – CD81, scavenger receptor BI (SR-BI), and the tight junction proteins claudin 1 (CLDN) and occludin (OCLN) – have distinct localization profiles on hepatocyte membranes. CD81 and SRBI are primarily basolateral, whereas CLDN and OCLN are present in the tight junctions at the periphery of the basolateral

domain. As such, HCV entry is shaped by receptor interactions that are very different on polarized and non-polarized cells. Further, polarization is intimately correlated with the means of viral spread. Viruses are thought to have two primary means of spreading from infected to uninfected cells: "cell-free" transmission whereby virions secreted by an infected cell eventually infect uninfected cells, and "cell-cell" transmission through which infected cells can somehow shuttle virions to uninfected cells. It is hypothesized that HCV may exhibit cell-cell spread as well, with virions being secreted apically into bile canaliculi, through which they can rapidly enter nearby cells while evading humoral immunity. Polarized primary hepatocytes will be necessary to test this hypothesis. Using our real-time reporter of infection [192] we have observed "foci" of infection in MPCCs that start from an initial infectious event (**Figure 3-11**); the use of depolarizing agents or micromechanical tools [145] to physically manipulate cells over small length scales will help determine whether this is truly cell-cell spread as opposed to cell-free spread with highly local virion diffusion.

A related question to the study of polarization is how cell-cell interactions more generally shape viral infection. As discussed, homotypic hepatocyte-hepatocyte contact may accelerate viral spread, but there are far more intercellular signals present, including soluble cues such as IFN signaling; hepatocyte-fibroblast interactions that encourage local differences between hepatocytes on the islands (we have shown that peripheral hepatocytes on patterned islands are indeed more susceptible to viral entry); gap junctional components that may spread inflammatory signals [294]; cadherins that activate IL-6 signaling [295]; and so on. As the behavior of infection is likely influenced by these factors, the result of an infection experiment in MPCCs integrates the complex network of cell-cell interactions present in the decided architecture [246].

Fortunately, hepatocytes in MPCCs are intentionally patterned into a desired architecture. Though the current scheme – islands of a fixed diameter patterned into an array – was empirically determined to maximize albumin out per cell, it is still possible to produce functional cultures from a wide array of hepatocyte architectures. It is thus possible to: modulate architecture; ascertain the resulting infection system using as many sources of information as possible (viral luciferase reporter, smFISH, reporters of signaling pathway activity, etc.); build mathematical models predictive of the infection system given an input architecture and the associated cell-cell interaction network; and use the insights revealed by the mathematical model to make mechanistic hypotheses implicating particular cell-cell interactions in infection.

The last project was motivated by the scarcity of quantitative, single-cell assays of viral infection. Aside from having limited specificity and sensitivity that preclude investigations in low signal-to-noise host systems, typical assays do not provide single-cell data; further, they generally provide limited information, such as binary assessments of infection. Cellular *in situ* imaging has the potential to overcome these limitations, furnishing a high-content source of information that is drastically enhancing screening as well as basic science. To this end, we developed an imaging assay for visualizing individual viral genomes that relies on single-molecule RNA fluorescence *in situ* hybridization (smFISH) [168]; we showed that smFISH can be applied in numerous manifestations to extract various quantitative descriptors of infection, including the single-cell heterogeneity of infection. Like the genomics revolution in molecular biology that resulted from access to rich data, we envision that our understanding of viral infection will be fundamentally improved by assays that simultaneously illuminate features of both virus and host. Single-cell assays are particularly rewarding. For example, one major

question has been whether interferon-stimulated genes (ISGs) elicited by infection are upregulated in infected cells or their neighbors; it is believed that HCV diminishes IFN signaling, in which case infected cells may not be the source of ISGs. Bulk assays of RNA can only detect whole-tissue changes, with no predictions for the single-cell level. We showed using smFISH that single-cell infection is correlated with ISG elevation in response to type I interferon (IFN) stimulation, suggesting that ISG upregulation is not exclusive to uninfected cells. While smFISH can thus be qualitatively powerful, the resulting rich data can also enable researchers to be quantitative. For example, several research groups perform theoretical and computational modeling of the viral life cycle, but the lack of rich data has stymied the fitting of these model parameters, often relegating these models to being solely descriptive; the access to quantitative data by assays such as smFISH will empower these models to make accurate predictions, ultimately enabling hypothesis testing and true inference about infection. To this end, smFISH could be used to understand viral replication by studying the relative dynamics of HCV positive and negative strand proliferation. Another promising area for use of smFISH is in the classification of antiviral mechanism. There are at least two applications in this vein. One application is the determination of mechanism of an identified antiviral hit. There are no systematic ways of determining antiviral mechanism, and assays that can reveal numerous features of infection such as smFISH can act as powerful classifiers of antiviral function. A second application is in empowering small-molecule screens to find compounds with unique antiviral functions. Most known antiviral compounds typically fall into a small number of functional categories (e.g. polymerase inhibitors), and because it is believed that the genetic barrier to resistance emergence is maximized using functionally orthogonal antivirals, it is of great interest to diversify our antiviral portfolios. Assays such as smFISH that yield unique

descriptors of infection will help execute high-throughput screens for compounds that perform novel functions. Another valuable study will involve employing smFISH for detecting HCV in tissue sections. Assays for HCV infection in liver tissue have generally proven ineffective, possibly due to low viral signals combined with the high intrinsic autofluorescent background in liver sections; as smFISH has been demonstrated in tissue sections for mRNA imaging, it is likely to be fruitful in the study of HCV-infected liver samples as well. Finally, it will be of immediate interest to utilize smFISH to study other viruses as well, to both benefit the investigation of these viruses and evaluate RNA virus comparative biology.

One important HCV *in vitro* model development challenge remains. Despite significant research, for reasons that are unclear, only strains of HCV based on one genotype 2a isolate from a fulminant hepatitis patient – Japanese Fulminant Hepatitis 1 (JFH-1) – are robustly infectious *in vitro*. As such, it is impossible to study the differential pathogenesis and treatment responses of various HCV strains; this is particularly concerning because the strain predominant to the Western World, genotype 1a, is far more resistant to IFN therapy. While most researchers tackling this problem focus on determining the unique features of JFH-1 that permit replication *in vitro* and imbuing other viral strains with these features [32], we suggest an alternate approach – as all these strains are obviously infectious *in vivo*, it may be worthwhile asking which important *in vivo* features are absent in our models and adding these features to our *in vitro* models. One hypothesis is that the standard host cells, Huh-7.5s, have abnormalities inconsistent with non-JFH-1 strain viability. However, preliminary experiments have demonstrated that these strains infect abortively in MPCCs as well. Interestingly, inhibition of IFN signaling using the methods described above, including IL-6, boost infection albeit transiently. This is consistent

with IFN signaling presenting a barrier to infection, but that innate immunity does not fully explain their lack of growth in primary hepatocytes. It will be worthwhile adding other liver nonparenchymal cell types with or without spatial patterning, recapitulating other known soluble signals present in the liver, trying experiments in 3D cultures, adding flow or mechanical shear using microfluidics, and so on. Studying the nature of the abortive infection of non-JFH-1 strains, for example using smFISH or reporters of pathway activity, will help yield insights regarding what stages of infection these strains fail to complete. This work is an open frontier for future research in HCV model development.

References

1. Lauer, G.M. and B.D. Walker, *Hepatitis C Virus Infection.* New England Journal of Medicine, 2001. **345**(1): p. 41-52.
2. Shepard, C.W., L. Finelli, and M.J. Alter, *Global epidemiology of hepatitis C virus infection.* Lancet Infect Dis., 2005. **5**(9): p. 558-567.
3. Ghany, M.G., et al., *Diagnosis, management, and treatment of hepatitis C: An update.* Hepatology, 2009. **49**(4): p. 1335-1374.
4. Choo, Q., et al., *Isolation of a cDNA clone derived from a blood-borne non-A, non-B viral hepatitis genome.* Science, 1989. **244**(4902): p. 359-362.
5. Kuo, G., et al., *An assay for circulating antibodies to a major etiologic virus of human non-A, non-B hepatitis.* Science, 1989. **244**(4902): p. 362-364.
6. Liang, T.J., et al., *Pathogenesis, Natural History, Treatment, and Prevention of Hepatitis C.* Annals of Internal Medicine, 2000. **132**(4): p. 296-305.
7. Seeff, L.B., *Natural history of chronic hepatitis C.* Hepatology, 2002. **36**(5B): p. s35-s46.
8. Horner, S.M. and M. Gale, *Intracellular innate immune cascades and interferon defenses that control hepatitis C virus.* J. Interferon Cytokine Res., 2009. **29**(9): p. 489-498.
9. Alter, M.J., et al., *The Prevalence of Hepatitis C Virus Infection in the United States, 1988 through 1994.* New England Journal of Medicine, 1999. **341**(8): p. 556-562.
10. Hoofnagle, J.H. and A.M. Di Bisceglie, *The Treatment of Chronic Viral Hepatitis.* New England Journal of Medicine, 1997. **336**(5): p. 347-356.
11. Moradpour, D., F. Penin, and C.M. Rice, *Replication of hepatitis C virus.* Nat. Rev. Micro., 2007. **5**(6): p. 453-463.

12. Kim, W.R., *The burden of hepatitis C in the United States.* Hepatology, 2002. **36**(5B): p. s30-s34.

13. Sharma, P. and A. Lok, *Viral Hepatitis and Liver Transplantation.* Semin Liver Dis, 2006. **26**(03): p. 285,297.

14. Houghton, M. and S. Abrignani, *Prospects for a vaccine against the hepatitis C virus.* Nature, 2005. **436**(7053): p. 961-966.

15. Feld, J.J. and J.H. Hoofnagle, *Mechanism of action of interferon and ribavirin in treatment of hepatitis C.* Nature, 2005. **436**(7053): p. 967-972.

16. Lavanchy, D., *The global burden of hepatitis C.* Liver International, 2009. **29**: p. 74-81.

17. De Francesco, R. and G. Migliaccio, *Challenges and successes in developing new therapies for hepatitis C.* Nature, 2005. **436**(7053): p. 953-960.

18. Yee, H.S., et al., *Update on the Management and Treatment of Hepatitis C Virus Infection: Recommendations from the Department of Veterans Affairs Hepatitis C Resource Center Program and the National Hepatitis C Program Office.* Am J Gastroenterol, 2012.

19. Garber, K., *Hepatitis C: move over interferon.* Nat Biotech, 2011. **29**(11): p. 963-966.

20. Rice, C., *Perspective: Miles to go before we sleep.* Nature, 2011. **474**(7350): p. S8-S8.

21. Knipe, D. and P. Howley, *Fields Virology*. 2007: Lippincott Williams & Wilkins.

22. Robertson, B., et al., *Classification, nomenclature, and database development for hepatitis C virus (HCV) and related viruses: proposals for standardization.* Archives of Virology, 1998. **143**(12): p. 2493-2503.

23. Gottwein, J.M. and J. Bukh, *Chapter 2 Cutting the Gordian Knot-Development and Biological Relevance of Hepatitis C Virus Cell Culture Systems*, in *Advances in Virus*

Research, A.J.S. Karl Maramorosch and A.M. Frederick, Editors. 2008, Academic Press. p. 51-133.

24. Spahn, C.M.T., et al., *Hepatitis C Virus IRES RNA-Induced Changes in the Conformation of the 40S Ribosomal Subunit.* Science, 2001. **291**(5510): p. 1959-1962.

25. Bukh, J., *A critical role for the chimpanzee model in the study of hepatitis C.* Hepatology, 2004. **39**(6): p. 1469-1475.

26. de Jong, Y.P., C.M. Rice, and A. Ploss, *New horizons for studying human hepatotropic infections.* The Journal of Clinical Investigation, 2010. **120**(3): p. 650-653.

27. Ploss, A. and C.M. Rice, *Towards a small animal model for hepatitis C.* EMBO Rep, 2009. **10**(11): p. 1220-1227.

28. Bartenschlager, R. and S. Sparacio, *Hepatitis C virus molecular clones and their replication capacity in vivo and in cell culture.* Virus Research, 2007. **127**(2): p. 195-207.

29. Boonstra, A., et al., *Experimental models for hepatitis C viral infection.* Hepatology, 2009. **50**(5): p. 1646-1655.

30. Bartenschlager, R. and V. Lohmann, *Novel cell culture systems for the hepatitis C virus.* Antiviral Research, 2001. **52**(1): p. 1-17.

31. Bartenschlager, R., *Hepatitis C virus molecular clones: from cDNA to infectious virus particles in cell culture.* Current Opinion in Microbiology, 2006. **9**(4): p. 416-422.

32. Murray, C.L. and C.M. Rice, *Turning Hepatitis C into a Real Virus.* Annual Review of Microbiology, 2011. **65**(1): p. 307-327.

33. Guillouzo, A., *Liver cell models in in vitro toxicology.* Environ Health Perspect, 1998. **106**: p. 511-532.

34. Sivaraman, A., et al., *A microscale in vitro physiological model of the liver: Predictive screens for drug metabolism and enzyme induction.* Current Drug Metabolism, 2005. **6**(6): p. 569-591.

35. Hewitt, N.J., et al., *Primary Hepatocytes: Current Understanding of the Regulation of Metabolic Enzymes and Transporter Proteins, and Pharmaceutical Practice for the Use of Hepatocytes in Metabolism, Enzyme Induction, Transporter, Clearance, and Hepatotoxicity Studies.* Drug Metabolism Reviews, 2007. **39**(1): p. 159-234.

36. Gebhardt, R., et al., *New Hepatocyte In Vitro Systems for Drug Metabolism: Metabolic Capacity and Recommendations for Application in Basic Research and Drug Development, Standard Operation Procedures.* Drug Metabolism Reviews, 2003. **35**(2-3): p. 145-213.

37. Durantel, D. and F. Zoulim, *Going towards more relevant cell culture models to study the in vitro replication of serum-derived hepatitis C virus and virus/host cell interactions?* J. Hepatol., 2007. **46**(1): p. 1-5.

38. Hsu, I.C., et al., *p53 gene mutation and integrated hepatitis B viral DNA sequences in human liver cancer cell lines.* Carcinogenesis, 1993. **14**(5): p. 987-992.

39. Nagao, K., et al., *Expression of hTERT mRNA in a mortal liver cell line during S phase without detectable telomerase activity.* Int. J. Mol. Med., 2005. **15**(4): p. 683-688.

40. Yokoo, H., et al., *Proteomic signature corresponding to alpha fetoprotein expression in liver cancer cells.* Hepatology, 2004. **40**(3): p. 609-617.

41. Sumpter, R., et al., *Regulating Intracellular Antiviral Defense and Permissiveness to Hepatitis C Virus RNA Replication through a Cellular RNA Helicase, RIG-I.* J. Virol., 2005. **79**(5): p. 2689-2699.

42. Mee, C.J., et al., *Effect of Cell Polarization on Hepatitis C Virus Entry.* J. Virol., 2008. **82**(1): p. 461-470.

43. Akira, S., S. Uematsu, and O. Takeuchi, *Pathogen Recognition and Innate Immunity.* Cell, 2006. **124**(4): p. 783-801.

44. Jung, C.-R., et al., *Adenovirus-mediated transfer of siRNA against PTTG1 inhibits liver cancer cell growth in vitro and in vivo.* Hepatology, 2006. **43**(5): p. 1042-1052.

45. Bhatia, S.N., et al., *Effect of cell-cell interactions in preservation of cellular phenotype: cocultivation of hepatocytes and nonparenchymal cells.* The FASEB Journal, 1999. **13**(14): p. 1883-1900.

46. Nakabayashi, H., et al., *Growth of Human Hepatoma Cell Lines with Differentiated Functions in Chemically Defined Medium.* Cancer Res., 1982. **42**(9): p. 3858-3863.

47. Kato, T., et al., *Sequence analysis of hepatitis C virus isolated from a fulminant hepatitis patient*.* Journal of Medical Virology, 2001. **64**(3): p. 334-339.

48. Lindenbach, B.D., et al., *Complete replication of hepatitis C virus in cell culture.* Science, 2005. **309**(5734): p. 623-6.

49. Zhong, J., et al., *Robust hepatitis C virus infection in vitro.* Proceedings of the National Academy of Sciences of the United States of America, 2005. **102**(26): p. 9294-9299.

50. Wakita, T., et al., *Production of infectious hepatitis C virus in tissue culture from a cloned viral genome.* Nat Med, 2005. **11**(7): p. 791-796.

51. Blight, K.J., J.A. McKeating, and C.M. Rice, *Highly Permissive Cell Lines for Subgenomic and Genomic Hepatitis C Virus RNA Replication.* J. Virol., 2002. **76**(24): p. 13001-13014.

52. Sumpter, R., Jr., et al., *Regulating intracellular antiviral defense and permissiveness to hepatitis C virus RNA replication through a cellular RNA helicase, RIG-I.* J Virol, 2005. **79**(5): p. 2689-99.

53. Wilkening, S., F. Stahl, and A. Bader, *Comparison of primary human hepatocytes and hepatoma cell line HepG2 with regard to their biotransformation properties.* Drug Metabolism and Disposition, 2003. **31**(8): p. 1035-1042.

54. Ge, D., et al., *Genetic variation in IL28B predicts hepatitis C treatment-induced viral clearance.* Nature, 2009. **461**(7262): p. 399-401.

55. Thomas, D.L., et al., *Genetic variation in IL28B and spontaneous clearance of hepatitis C virus.* Nature, 2009. **461**(7265): p. 798-801.

56. Suppiah, V. and M. Moldovan, *IL28B is associated with response to chronic hepatitis C interferon-[alpha] and ribavirin therapy.* Nat Genet, 2009. **41**(10): p. 1100-1104.

57. Jones, C.T., et al., *Real-time imaging of hepatitis C virus infection using a fluorescent cell-based reporter system.* Nat. Biotech., 2010. **28**(2): p. 167-171.

58. Higgins, G. and R. Anderson, *Experimental pathology of liver: restoration of liver in white rat following partial surgical removal.* Arch Pathol, 1931. **12**: p. 186-202.

59. Stocker, E., H. Wullstein, and G. Brau, *Capacity of regeneration in liver epithelia of juvenile, repeated partially hepatectomized rats. Autogradiographic sturies after continuous infusion of 3H-thymidine.* Virchows Arch B Cell Pathol, 1973.

60. Overturf, K., M. AlDhalimy, and R. Tanguay, *Hepatocytes corrected by gene therapy are selected in vivo in a murine model of hereditary tyrosinaemia type I.* Nat Genet, 1996. **12**(3): p. 266-73.

61. Grompe, M., et al., *Serial transplantation reveals stem cell like regenerative potential in parenchymal mouse hepatocytes.* Hepatology, 1996. **24**.

62. Hamazaki, T., et al., *Hepatic maturation in differentiating embryonic stem cells in vitro.* FEBS Letters, 2001. **497**(1): p. 15-19.

63. Chinzei, R., et al., *Embryoid-body cells derived from a mouse embryonic stem cell line show differentiation into functional hepatocytes.* Hepatology, 2002. **36**(1): p. 22-29.

64. Yamada, T., et al., *In Vitro Differentiation of Embryonic Stem Cells into Hepatocyte-Like Cells Identified by Cellular Uptake of Indocyanine Green.* STEM CELLS, 2002. **20**(2): p. 146-154.

65. Cho, C.H., et al., *Homogeneous differentiation of hepatocyte-like cells from embryonic stem cells: applications for the treatment of liver failure.* The FASEB Journal, 2008. **22**(3): p. 898-909.

66. Gouon-Evans, V., et al., *BMP-4 is required for hepatic specification of mouse embryonic stem cell-derived definitive endoderm.* Nat Biotech, 2006. **24**(11): p. 1402-1411.

67. Soto-Gutierrez, A., et al., *Reversal of mouse hepatic failure using an implanted liver-assist device containing ES cell-derived hepatocytes.* Nat Biotech, 2006. **24**(11): p. 1412-1419.

68. Wandzioch, E. and K.S. Zaret, *Dynamic Signaling Network for the Specification of Embryonic Pancreas and Liver Progenitors.* Science, 2009. **324**(5935): p. 1707-1710.

69. Lemaigre, F. and K.S. Zaret, *Liver development update: new embryo models, cell lineage control, and morphogenesis.* Current Opinion in Genetics & Development, 2004. **14**(5): p. 582-590.

70. Schmelzer, E., et al., *Human hepatic stem cells from fetal and postnatal donors.* The Journal of Experimental Medicine, 2007. **204**(8): p. 1973-1987.

71. Zhang, L., et al., *The stem cell niche of human livers: Symmetry between development and regeneration.* Hepatology, 2008. **48**(5): p. 1598-1607.

72. Oh, S.-H., H.M. Hatch, and B.E. Petersen, *Hepatic oval 'stem' cell in liver regeneration.* Seminars in Cell & Developmental Biology, 2002. **13**(6): p. 405-409.

73. Sell, S., *The role of progenitor cells in repair of liver injury and in liver transplantation.* Wound Repair and Regeneration, 2001. **9**(6): p. 467-482.

74. Strick-Marchand, H. and M.C. Weiss, *Inducible differentiation and morphogenesis of bipotential liver cell lines from wild-type mouse embryos.* Hepatology, 2002. **36**(4): p. 794-804.

75. Strick-Marchand, H., et al., *Bipotential mouse embryonic liver stem cell lines contribute to liver regeneration and differentiate as bile ducts and hepatocytes.* Proceedings of the National Academy of Sciences of the United States of America, 2004. **101**(22): p. 8360-8365.

76. Duncan, A.W., C. Dorrell, and M. Grompe, *Stem Cells and Liver Regeneration.* Gastroenterology, 2009. **137**(2): p. 466-481.

77. Lowry, W.E., et al., *Generation of human induced pluripotent stem cells from dermal fibroblasts.* Proceedings of the National Academy of Sciences, 2008. **105**(8): p. 2883-2888.

78. Park, I.-H., et al., *Reprogramming of human somatic cells to pluripotency with defined factors.* Nature, 2008. **451**(7175): p. 141-146.

79. Takahashi, K. and S. Yamanaka, *Induction of Pluripotent Stem Cells from Mouse Embryonic and Adult Fibroblast Cultures by Defined Factors.* Cell, 2006. **126**(4): p. 663-676.

80. Takahashi, K., et al., *Induction of Pluripotent Stem Cells from Adult Human Fibroblasts by Defined Factors.* Cell, 2007. **131**(5): p. 861-872.

81. Yu, J., et al., *Induced Pluripotent Stem Cell Lines Derived from Human Somatic Cells.* Science, 2007. **318**(5858): p. 1917-1920.

82. Si-Tayeb, K., et al., *Highly efficient generation of human hepatocyte–like cells from induced pluripotent stem cells.* Hepatology, 2010. **51**(1): p. 297-305.

83. Song, Z., et al., *Efficient generation of hepatocyte-like cells from human induced pluripotent stem cells.* Cell Res, 2009. **19**(11): p. 1233-1242.

84. Sullivan, G.J., et al., *Generation of functional human hepatic endoderm from human induced pluripotent stem cells.* Hepatology, 2010. **51**(1): p. 329-335.

85. Langer, R. and J. Vacanti, *Tissue engineering.* Science, 1993. **260**(5110): p. 920-926.

86. Chow, L.T. and T.R. Broker, *In vitro experimental systems for HPV: Epithelial raft cultures for investigations of viral reproduction and pathogenesis and for genetic analyses of viral proteins and regulatory sequences.* Clinics in Dermatology, 1997. **15**(2): p. 217-227.

87. Griffith, L.G. and M.A. Swartz, *Capturing complex 3D tissue physiology in vitro.* Nat Rev Mol Cell Biol, 2006. **7**(3): p. 211-224.

88. Yamada, K.M. and E. Cukierman, *Modeling Tissue Morphogenesis and Cancer in 3D.* Cell, 2007. **130**(4): p. 601-610.

89. Grosse-Siestrup, C., et al., *The isolated perfused liver: a new model using autologous blood and porcine slaughterhouse organs.* Journal of Pharmacological and Toxicological Methods, 2001. **46**(3): p. 163-168.

90. Thohan, S. and G.M. Rosen, *Liver slice technology as an in vitro model for metabolic and toxicity studies.* Methods in Molecular Biology, 2002. **196**: p. 291-303.

91. Donato, M.T., et al., *Fluorescence-based assays for screening nine cytochrome P450 (P450) activities in intact cells expressing individual human P450 enzymes.* Drug Metabolism and Disposition, 2004. **32**(7): p. 699-706.

92. Venkatakrishnan, K., L.L. von Moltke, and D.J. Greenblatt, *Evaluation of SupermixTM as an in vitro model of human liver microsomal drug metabolism.* Biopharmaceutics & Drug Disposition, 2002. **23**(5): p. 183-190.

93. Cederbaum, A.I., et al., *CYP2E1-dependent toxicity and oxidative stress in HepG2 cells.* Free Radical Biology and Medicine, 2001. **31**(12): p. 1539-1543.

94. Fukaya, K.-I., et al., *Establishment of a human hepatocyte line (OUMS-29) having CYP 1A1 and 1A2 activities from fetal liver tissue by transfection of SV40 LT.* In Vitro Cellular & Developmental Biology - Animal, 2001. **37**(5): p. 266-269.

95. Liu, J., J. Pan, and S. Naik, *Characterization and evaluation of detoxification functions of a nontumorigenic immortalized porcine hepatocyte cell line (HepLiu).* Cell Transplant., 1999. **8**(3): p. 219-32.

96. Mills, J.B., et al., *Induction of Drug Metabolism Enzymes and MDR1 Using a Novel Human Hepatocyte Cell Line.* Journal of Pharmacology and Experimental Therapeutics, 2004. **309**(1): p. 303-309.

97. Enat, R., et al., *Hepatocyte proliferation in vitro: its dependence on the use of serum-free hormonally defined medium and substrata of extracellular matrix.* Proceedings of the National Academy of Sciences, 1984. **81**(5): p. 1411-1415.

98. Laishes, B. and W. GM, *Conditions affecting primary-cell cultures of functional adult rat hepatocytes.* In Vitro, 1976. **12**(7): p. 521-532.

99. Jindal, R., et al., *Amino acid-mediated heterotypic interaction governs performance of a hepatic tissue model.* The FASEB Journal, 2009. **23**(7): p. 2288-2298.

100. Isom, H.C., et al., *Maintenance of differentiated rat hepatocytes in primary culture.* Proceedings of the National Academy of Sciences, 1985. **82**(10): p. 3252-3256.

101. Miyazaki, M., et al., *Long-term survival of functional hepatocytes from adult rat in the presence of phenobarbital in primary culture.* Experimental Cell Research, 1985. **159**(1): p. 176-190.

102. Kidambi, S., et al., *Oxygen-mediated enhancement of primary hepatocyte metabolism, functional polarization, gene expression, and drug clearance.* Proceedings of the National Academy of Sciences, 2009. **106**(37): p. 15714-15719.

103. Dunn, J., et al., *Hepatocyte function and extracellular matrix geometry: long-term culture in a sandwich configuration [published erratum appears in FASEB J 1989 May;3(7):1873].* The FASEB Journal, 1989. **3**(2): p. 174-177.

104. LeCluyse, E.L., P. Bullock, and A. Parkinson, *Strategies for restoration and maintenance of normal hepatic structure and function in long-term cultures of rat hepatocytes.* Adv Drug Deliv Rev, 1996. **22**: p. 133-86.

105. Lin, P., et al., *Assessing porcine liver-derived biomatrix for hepatic tissue engineering.* Tissue Eng, 2004. **10**: p. 1046-53.

106. Flaim, C.J., S. Chien, and S.N. Bhatia, *An extracellular matrix microarray for probing cellular differentiation.* Nat Meth, 2005. **2**(2): p. 119-125.

107. LeCluyse, E.L., K.L. Audus, and J.H. Hochman, *Formation of extensive canalicular networks by rat hepatocytes cultured in collagen-sandwich configuration.* American Journal of Physiology - Cell Physiology, 1994. **266**(6): p. C1764-C1774.

108. Richert, L., et al., *Evaluation of the effect of culture configuration on morphology, survival time, antioxidant status and metabolic capacities of cultured rat hepatocytes.* Toxicology in Vitro, 2002. **16**(1): p. 89-99.

109. Chen, A.A., et al., *Modulation of hepatocyte phenotype in vitro via chemomechanical tuning of polyelectrolyte multilayers.* Biomaterials, 2009. **30**(6): p. 1113-1120.

110. Janorkar, A.V., et al., *The use of elastin-like polypeptide–polyelectrolyte complexes to control hepatocyte morphology and function in vitro.* Biomaterials, 2008. **29**(6): p. 625-632.

111. Guguen-Guillouzo, C., et al., *Maintenance and reversibility of active albumin secretion by adult rat hepatocytes co-cultured with another liver epithelial cell type.* Experimental Cell Research, 1983. **143**(1): p. 47-54.

112. Hansen, L., C. Hisao, and J. Friend, *Enhanced morphology and function in heaptocyte spheroids: a model of tissue self-assembly.* Tissue Eng, 1998. **4**(1): p. 65-74.

113. Koide, N., K. Sakaguchi, and Y. Koide, *Formation of multicellular spheroids composed of adult-rat hepatocytes in dishes with positively charged surfaces and under other nonadherent environments.* Exp Cell Res, 1990. **186**(2): p. 227-35.

114. Peshwa, M., F. Wu, and H. Sharp, *Mechanistics of formation and ultrastructural evaluation of hepatocyte spheroids.* 32, 1996. **4**(197-203).

115. Wu, F., J. Friend, and R. Remmel, *Enhanced cytochrome P450IA1 activity of self-assembled rat hepatocyte spheroids.* Cell Transplant., 1999. **8**(3): p. 233-46.

116. Yagi, K., K. Tsuda, and M. Serada, *Rapid formation of multicellular spheroids of adult-rat hepatocytes by rotation culture and their immobilization within calcium alginate.* Artif Organs, 1993. **17**(11): p. 929-34.

117. Yuasa, C., et al., *Importance of cell aggregation for expression of liver functions and regeneration demonstrated with primary cultured hepatocytes.* Journal of Cellular Physiology, 1993. **156**(3): p. 522-530.

118. Landry, J., et al., *Spheroidal aggregate culture of rat liver cells: histotypic reorganization, biomatrix deposition, and maintenance of functional activities.* The Journal of Cell Biology, 1985. **101**(3): p. 914-923.

119. Roberts, R.A. and A.R. Soames, *Hepatocyte Spheroids: Prolonged Hepatocyte Viability for in Vitro Modeling of Nongenotoxic Carcinogenesis.* Fundamental and Applied Toxicology, 1993. **21**(2): p. 149-158.

120. Bissell, D.M., et al., *Support of cultured hepatocytes by a laminin-rich gel. Evidence for a functionally significant subendothelial matrix in normal rat liver.* The Journal of Clinical Investigation, 1987. **79**(3): p. 801-812.

121. LeCluyse, E.L., *Human hepatocyte culture systems for the in vitro evaluation of cytochrome P450 expression and regulation.* European Journal of Pharmaceutical Sciences, 2001. **13**(4): p. 343-368.

122. Vukicevic, S., et al., *Identification of multiple active growth factors in basement membrane matrigel suggests caution in interpretation of cellular activity related to extracellular matrix components.* Experimental Cell Research, 1992. **202**(1): p. 1-8.

123. Hsiao, C., J. Friend, and F. Wu, *Receding cytochrome P450 activity in disassembling hepatocyte spheroids.* Tissue Eng, 1999. **5**(3): p. 207-21.

124. Kojima, R., et al., *Spheroid array of fetal mouse liver cells constructed on a PEG-gel micropatterned surface: upregulation of hepatic functions by co-culture with nonparenchymal liver cells.* Lab on a Chip, 2009. **9**(14): p. 1991-1993.

125. Powers, M.J., et al., *A microfabricated array bioreactor for perfused 3D liver culture.* Biotechnology and Bioengineering, 2002. **78**(3): p. 257-269.

126. Brophy, C.M., et al., *Rat hepatocyte spheroids formed by rocked technique maintain differentiated hepatocyte gene expression and function.* Hepatology, 2009. **49**(2): p. 578-586.

127. Chia, S., K. Leong, and J. Li, *Hepatocyte encapsulation for enhanced cellular functions.* Tissue Eng, 2000. **6**(5): p. 481-95.

128. Eschbach, E., et al., *Microstructured scaffolds for liver tissue cultures of high cell density: Morphological and biochemical characterization of tissue aggregates.* Journal of Cellular Biochemistry, 2005. **95**(2): p. 243-255.

129. Knedlitschek, G., F. Schneider, and E. Gottwald, *A tissue-like culture system using microstructures: influence of extracellular matrix material on cell adhesion and aggregation.* J Biomech Eng, 1999. **121**(1): p. 35-9.

130. Park, J.-k. and D.-h. Lee, *Bioartificial liver systems: current status and future perspective.* Journal of Bioscience and Bioengineering, 2005. **99**(4): p. 311-319.

131. Allen, J.W., S.R. Khetani, and S.N. Bhatia, *In Vitro Zonation and Toxicity in a Hepatocyte Bioreactor.* Toxicological Sciences, 2005. **84**(1): p. 110-119.

132. Domansky, K., et al., *Perfused multiwell plate for 3D liver tissue engineering.* Lab on a Chip, 2010. **10**(1): p. 51-58.

133. Tilles, A.W., et al., *Effects of oxygenation and flow on the viability and function of rat hepatocytes cocultured in a microchannel flat-plate bioreactor.* Biotechnology and Bioengineering, 2001. **73**(5): p. 379-389.

134. Park, J., et al., *Microfabricated grooved substrates as platforms for bioartificial liver reactors.* Biotechnology and Bioengineering, 2005. **90**(5): p. 632-644.

135. Roy, P., et al., *Analysis of Oxygen Transport to Hepatocytes in a Flat-Plate Microchannel Bioreactor.* Annals of Biomedical Engineering, 2001. **29**(11): p. 947-955.

136. Park, J., et al., *Radial flow hepatocyte bioreactor using stacked microfabricated grooved substrates.* Biotechnology and Bioengineering, 2008. **99**(2): p. 455-467.

137. Yates, C., et al., *Novel Three-Dimensional Organotypic Liver Bioreactor to Directly Visualize Early Events in Metastatic Progression*, in *Advances in Cancer Research*, F.V.W. George and K. George, Editors. 2007, Academic Press. p. 225-246.

138. Gerlach, J., *Development of a hybrid liver support system: a review.* Int J Artif Organs, 1996. **19**(11): p. 645-54.

139. Catapano, G., J. Patzer, and J. Gerlach, *Transport Advances in Disposable Bioreactors for Liver Tissue Engineering*

Disposable Bioreactors, R. Eibl and D. Eibl, Editors. 2010, Springer Berlin / Heidelberg. p. 117-143.

140. Macdonald, J., S. Wolfe, and B. Gupta, *Tissue engineering liver in a novel multi-coaxial hollow fiber bioreactor.* Free Radic Biol, 2001.

141. Khetani, S.R. and S.N. Bhatia, *Engineering tissues for in vitro applications.* Current Opinion in Biotechnology, 2006. **17**(5): p. 524-531.

142. Folch, A. and M. Toner, *Microengineering of cellular interactions.* Annual Review of Biomedical Engineering, 2000. **2**(1): p. 227-256.

143. Chen, C.S., et al., *Geometric Control of Cell Life and Death.* Science, 1997. **276**(5317): p. 1425-1428.

144. Singhvi, R., et al., *Engineering cell shape and function.* Science, 1994. **264**(5159): p. 696-698.

145. Hui, E.E. and S.N. Bhatia, *Micromechanical control of cell–cell interactions.* Proceedings of the National Academy of Sciences, 2007. **104**(14): p. 5722-5726.

146. Lipshutz, R., et al., *High density synthetic oligonucleotide arrays.* Nat Genet, 1999. **21**: p. 20-4.

147. Chao, P., et al., *Evaluation of a microfluidic based cell culture platform with primary human hepatocytes for the prediction of hepatic clearance in human.* Biochemical Pharmacology, 2009. **78**(6): p. 625-632.

148. Fukuda, J., Y. Sakai, and K. Nakazawa, *Novel hepatocyte culture system developed using microfabrication and collagen/polyethylene glycol microcontact printing.* Biomaterials, 2006. **27**(7): p. 1061-1070.

149. Ohashi, K., et al., *Engineering functional two- and three-dimensional liver systems in vivo using hepatic tissue sheets.* Nat Med, 2007. **13**(7): p. 880-885.

150. Khetani, S.R. and S.N. Bhatia, *Microscale culture of human liver cells for drug development.* Nature Biotechnology, 2008. **26**(1): p. 120-126.

151. Neumann, B., et al., *High-throughput RNAi screening by time-lapse imaging of live human cells.* Nat Meth, 2006. **3**(5): p. 385-390.

152. Collinet, C., et al., *Systems survey of endocytosis by multiparametric image analysis.* Nature, 2010. **464**(7286): p. 243-249.

153. Moffat, J., et al., *A lentiviral RNAi library for human and mouse genes applied to an arrayed viral high-content screen.* Cell, 2006. **124**(6): p. 1283-1298.

154. Abraham, V.C., D.L. Taylor, and J.R. Haskins, *High content screening applied to large-scale cell biology.* Trends in Biotechnology, 2004. **22**(1): p. 15-22.

155. Lang, P., et al., *Cellular imaging in drug discovery.* Nat Rev Drug Discov, 2006. **5**(4): p. 343-356.

156. Yarrow, J.C., et al., *A high-throughput cell migration assay using scratch wound healing, a comparison of image-based readout methods.* Bmc Biotechnology, 2004. **4**.

157. Young, D.W., et al., *Integrating high-content screening and ligand-target prediction to identify mechanism of action.* Nat Chem Biol, 2008. **4**(1): p. 59-68.

158. Balázsi, G., A. van Oudenaarden, and James J. Collins, *Cellular Decision Making and Biological Noise: From Microbes to Mammals.* Cell, 2011. **144**(6): p. 910-925.

159. Eldar, A. and M.B. Elowitz, *Functional roles for noise in genetic circuits.* Nature, 2010. **467**(7312): p. 167-173.

160. Li, G.-W. and X.S. Xie, *Central dogma at the single-molecule level in living cells.* Nature, 2011. **475**(7356): p. 308-315.

161. Raj, A. and A. van Oudenaarden, *Nature, Nurture, or Chance: Stochastic Gene Expression and Its Consequences.* Cell, 2008. **135**(2): p. 216-226.

162. Snijder, B. and L. Pelkmans, *Origins of regulated cell-to-cell variability.* Nat Rev Mol Cell Biol, 2011. **12**(2): p. 119-125.

163. Bumgarner, Stacie L., et al., *Single-Cell Analysis Reveals that Noncoding RNAs Contribute to Clonal Heterogeneity by Modulating Transcription Factor Recruitment.* Molecular cell, 2012. **45**(4): p. 470-482.

164. Femino, A.M., et al., *Visualization of Single RNA Transcripts in Situ.* Science, 1998. **280**(5363): p. 585-590.

165. Gandhi, S.J., et al., *Transcription of functionally related constitutive genes is not coordinated.* Nat Struct Mol Biol, 2011. **18**(1): p. 27-34.

166. Raj, A., et al., *Stochastic mRNA synthesis in mammalian cells.* PLoS Biol, 2006. **4**: p. e309.

167. Raj, A., et al., *Variability in gene expression underlies incomplete penetrance.* Nature, 2010. **463**(7283): p. 913-918.

168. Raj, A., et al., *Imaging individual mRNA molecules using multiple singly labeled probes.* Nat. Meth., 2008. **5**(10): p. 877-879.

169. So, L.-h., et al., *General properties of transcriptional time series in Escherichia coli.* Nat Genet, 2011. **43**(6): p. 554-560.

170. Tan, R.Z. and A. van Oudenaarden, *Transcript counting in single cells reveals dynamics of rDNA transcription.* Mol. Syst. Biol., 2010. **6**.

171. Zenklusen, D., D.R. Larson, and R.H. Singer, *Single-RNA counting reveals alternative modes of gene expression in yeast.* Nat Struct Mol Biol, 2008. **15**(12): p. 1263-1271.

172. Golding, I., et al., *Real-Time Kinetics of Gene Activity in Individual Bacteria.* Cell, 2005. **123**(6): p. 1025-1036.

173. Itzkovitz, S. and A. van Oudenaarden, *Validating transcripts with probes and imaging technology.* Nat. Meth., 2011. **8**(4s): p. S12-S19.

174. Saha, K. and R. Jaenisch, *Technical challenges in using human induced pluripotent stem cells to model disease.* Cell Stem Cell, 2009. **5**(6): p. 584-95.

175. Muller, L.U., G.Q. Daley, and D.A. Williams, *Upping the ante: recent advances in direct reprogramming.* Mol Ther, 2009. **17**(6): p. 947-53.

176. Carvajal-Vergara, X., et al., *Patient-specific induced pluripotent stem-cell-derived models of LEOPARD syndrome.* Nature, 2010. **465**(7299): p. 808-12.

177. Kim, K.Y., E. Hysolli, and I.H. Park, *Neuronal maturation defect in induced pluripotent stem cells from patients with Rett syndrome.* Proc Natl Acad Sci U S A, 2011.

178. Ku, S., et al., *Friedreich's ataxia induced pluripotent stem cells model intergenerational GAATTC triplet repeat instability.* Cell Stem Cell, 2010. **7**(5): p. 631-7.

179. Moretti, A., et al., *Patient-specific induced pluripotent stem-cell models for long-QT syndrome.* N Engl J Med, 2010. **363**(15): p. 1397-409.

180. Rashid, S.T., et al., *Modeling inherited metabolic disorders of the liver using human induced pluripotent stem cells.* J Clin Invest, 2010. **120**(9): p. 3127-36.

181. Schwartz, R., et al., *Modeling hepatitis C virus infection using human induced pluripotent stem cells.* Proc. Natl. Acad. Sci., 2012.

182. Evans, M.J., et al., *Claudin-1 is a hepatitis C virus co-receptor required for a late step in entry.* Nature, 2007. **446**(7137): p. 801-5.

183. Germi, R., et al., *Cellular glycosaminoglycans and low density lipoprotein receptor are involved in hepatitis C virus adsorption.* J Med Virol, 2002. **68**(2): p. 206-15.

184. Pileri, P., et al., *Binding of hepatitis C virus to CD81.* Science, 1998. **282**(5390): p. 938-41.

185. Ploss, A., et al., *Human occludin is a hepatitis C virus entry factor required for infection of mouse cells.* Nature, 2009. **457**(7231): p. 882-6.

186. Scarselli, E., et al., *The human scavenger receptor class B type I is a novel candidate receptor for the hepatitis C virus.* EMBO J, 2002. **21**(19): p. 5017-25.

187. Khetani, S.R. and S.N. Bhatia, *Microscale culture of human liver cells for drug development.* Nat Biotechnol, 2008. **26**(1): p. 120-6.

188. Tai, A.W., et al., *A functional genomic screen identifies cellular cofactors of hepatitis C virus replication.* Cell Host Microbe, 2009. **5**(3): p. 298-307.

189. Phillips, I.R. and E.A. Shephard, *Cytochrome P450 protocols*. 2nd ed. Methods in molecular biology. 2006, Totowa, N.J.: Humana Press. xiii, 363 p.

190. Ahlström, M., *Cytochrome P450, metabolism and inhibition : computational and experimental studies*. 2007, Göteborg: Göteborg University. 1 v. (various pagings).

191. Marukian, S., et al., *Cell Culture-Produced Hepatitis C Virus Does Not Infect Peripheral Blood Mononuclear Cells.* Hepatology, 2008. **48**(6): p. 1843-1850.

192. Jones, C.T., et al., *Real-time imaging of hepatitis C virus infection using a fluorescent cell-based reporter system.* Nat Biotechnol, 2010. **28**(2): p. 167-71.

193. Lazaro, C.A., et al., *Hepatitis C virus replication in transfected and serum-infected cultured human fetal hepatocytes.* Am J Pathol, 2007. **170**(2): p. 478-89.

194. Andrus, L., et al., *Expression of paramyxovirus V proteins promotes replication and spread of hepatitis C virus in cultures of primary human fetal liver cells.* Hepatology, 2011. **In Press**

195. Zhang, B., S. Kirov, and J. Snoddy, *WebGestalt: an integrated system for exploring gene sets in various biological contexts.* Nucleic Acids Res, 2005. **33**(Web Server issue): p. W741-8.

196. Fournier, C., et al., *In vitro infection of adult normal human hepatocytes in primary culture by hepatitis C virus.* Journal of General Virology, 1998. **79**(10): p. 2367-74.

197. Carloni, G., et al., *Susceptibility of human liver cell cultures to hepatitis C virus infection.* Arch Virol Suppl, 1993. **8**: p. 31-9.

198. Iacovacci, S., et al., *Replication and multiplication of hepatitis C virus genome in human foetal liver cells.* Res Virol, 1993. **144**(4): p. 275-279.

199. Rumin, S., et al., *Dynamic analysis of hepatitis C virus replication and quasispecies selection in long-term cultures of adult human hepatocytes infected in vitro.* Journal of General Virology, 1999. **80**(11): p. 3007-3018.

200. Buck, M., *Direct Infection and Replication of Naturally Occurring Hepatitis C Virus Genotypes 1, 2, 3 and 4 in Normal Human Hepatocyte Cultures.* PLoS ONE, 2008. **3**(7): p. e2660.

201. Ploss, A., et al., *Persistent hepatitis C virus infection in microscale primary human hepatocyte cultures.* Proc. Natl. Acad. Sci., 2010. **107**(7): p. 3141-3145.

202. Evans, M.J., et al., *Claudin-1 is a hepatitis C virus co-receptor required for a late step in entry.* Nature, 2007. **446**(7137): p. 801-805.

203. Liu, S., et al., *Tight Junction Proteins Claudin-1 and Occludin Control Hepatitis C Virus Entry and Are Downregulated during Infection To Prevent Superinfection.* Journal of Virology, 2009. **83**(4): p. 2011-2014.

204. Ploss, A., et al., *Human occludin is a hepatitis C virus entry factor required for infection of mouse cells.* Nature, 2009. **457**(7231): p. 882-886.

205. Pileri, P., et al., *Binding of Hepatitis C Virus to CD81.* Science, 1998. **282**(5390): p. 938-941.

206. Scarselli, E., et al., *The human scavenger receptor class B type I is a novel candidate receptor for the hepatitis C virus.* Embo Journal, 2002. **21**(19): p. 5017-5025.

207. Marukian, S., et al., *Cell culture–produced hepatitis C virus does not infect peripheral blood mononuclear cells.* Hepatology, 2008. **48**(6): p. 1843-1850.

208. Stiffler, J.D., et al., *Focal Distribution of Hepatitis C Virus RNA in Infected Livers.* PLoS ONE, 2009. **4**(8): p. e6661.

209. Catanese, M.T., et al., *High-Avidity Monoclonal Antibodies against the Human Scavenger Class B Type I Receptor Efficiently Block Hepatitis C Virus Infection in the Presence of High-Density Lipoprotein.* Journal of Virology, 2007. **81**(15): p. 8063-8071.

210. Meuleman, P., et al., *Anti-CD81 Antibodies Can Prevent a Hepatitis C Virus Infection In Vivo.* Hepatology, 2008. **48**(6): p. 1761-1768.

211. Madan, A., et al., *Effects of Prototypical Microsomal Enzyme Inducers on Cytochrome P450 Expression in Cultured Human Hepatocytes.* Drug Metabolism and Disposition, 2003. **31**(4): p. 421-431.

212. Owsianka, A., et al., *Monoclonal Antibody AP33 Defines a Broadly Neutralizing Epitope on the Hepatitis C Virus E2 Envelope Glycoprotein.* Journal of Virology, 2005. **79**(17): p. 11095-11104.

213. Hadlock, K.G., et al., *Human Monoclonal Antibodies That Inhibit Binding of Hepatitis C Virus E2 Protein to CD81 and Recognize Conserved Conformational Epitopes.* Journal of Virology, 2000. **74**(22): p. 10407-10416.

214. Law, M., et al., *Broadly neutralizing antibodies protect against hepatitis C virus quasispecies challenge.* Nature Medicine, 2008. **14**(1): p. 25-27.

215. Liang, Y., et al., *Visualizing Hepatitis C Virus Infections in Human Liver by Two-Photon Microscopy.* Gastroenterology, 2009. **137**(4): p. 1448-1458.

216. Schoggins, J.W., et al., *A diverse range of gene products are effectors of the type I interferon antiviral response.* Nature, 2011. **472**(7344): p. 481-485.

217. Theofilopoulos, A.N., et al., *Type I interferons (α/β) in immunity and autoimmunity.* Annu. Rev. Immunol., 2005. **23**(1): p. 307-335.

218. Sadler, A.J. and B.R.G. Williams, *Interferon-inducible antiviral effectors.* Nat Rev Immunol, 2008. **8**(7): p. 559-568.

219. Thompson, J.E., et al., *Photochemical preparation of a pyridone containing tetracycle: A jak protein kinase inhibitor.* Bioorganic & Medicinal Chemistry Letters, 2002. **12**(8): p. 1219-1223.

220. Ramachandran, A. and C.M. Horvath, *Paramyxovirus disruption of interferon signal transduction: STATus report.* Journal of Interferon & Cytokine Research, 2009. **29**(9): p. 531-537.

221. Childs, K., et al., *mda-5, but not RIG-I, is a common target for paramyxovirus V proteins.* Virology, 2007. **359**(1): p. 190-200.

222. Feldman, R.I., et al., *Novel small molecule inhibitors of 3-phosphoinositide-dependent kinase-1 (PDK1).* J. Biol. Chem., 2005: p. M501367200.

223. Clark, K., et al., *Use of the Pharmacological Inhibitor BX795 to Study the Regulation and Physiological Roles of TBK1 and IκB Kinase ϵ.* Journal of Biological Chemistry, 2009. **284**(21): p. 14136-14146.

224. Bain, J., et al., *The selectivity of protein kinase inhibitors: a further update.* Biochemical Journal, 2007. **408**: p. 297-315.

225. Johnson, D.C. and M.T. Huber, *Directed Egress of Animal Viruses Promotes Cell-to-Cell Spread.* J. Virol., 2002. **76**(1): p. 1-8.

226. Timpe, J.M., et al., *Hepatitis C virus cell-cell transmission in hepatoma cells in the presence of neutralizing antibodies.* Hepatology, 2008. **47**(1): p. 17-24.

227. Liang, Y.Q., et al., *Visualizing Hepatitis C Virus Infections in Human Liver by Two-Photon Microscopy.* Gastroenterology, 2009. **137**(4): p. 1448-1458.

228. Heim, M.H., D. Moradpour, and H.E. Blum, *Expression of Hepatitis C Virus Proteins Inhibits Signal Transduction through the Jak-STAT Pathway.* J. Virol., 1999. **73**(10): p. 8469-8475.

229. Lin, W., et al., *Hepatitis C Virus Core Protein Blocks Interferon Signaling by Interaction with the STAT1 SH2 Domain.* J. Virol., 2006. **80**(18): p. 9226-9235.

230. Chang, S., K. Kodys, and G. Szabo, *Impaired expression and function of toll-like receptor 7 in hepatitis C virus infection in human hepatoma cells.* Hepatology, 2010. **51**(1): p. 35-42.

231. Lang, K.S., et al., *Immunoprivileged status of the liver is controlled by Toll-like receptor 3 signaling.* The Journal of Clinical Investigation, 2006. **116**(9): p. 2456-2463.

232. Protzer, U., M.K. Maini, and P.A. Knolle, *Living in the liver: hepatic infections.* Nat Rev Immunol, 2012. **12**(3): p. 201-213.

233. Crispe, I.N., et al., *Cellular and molecular mechanisms of liver tolerance.* Immunological Reviews, 2006. **213**(1): p. 101-118.

234. Tiegs, G. and A.W. Lohse, *Immune tolerance: What is unique about the liver.* Journal of Autoimmunity, 2010. **34**(1): p. 1-6.

235. Calne, R.Y., et al., *Induction of Immunological Tolerance by Porcine Liver Allografts.* Nature, 1969. **223**(5205): p. 472-476.

236. Callery, M.P., T. Kamei, and M.W. Flye, *The effect of portacaval shunt on delayed-hypersensitivity responses following antigen feeding.* Journal of Surgical Research, 1989. **46**(4): p. 391-394.

237. Heinrich, P.C., et al., *Interleukin-6-type cytokine signalling through the gp130/Jak/STAT pathway.* Biochem J, 1998. **334**: p. 297-314.

238. Hussain, S.F., et al., *A Novel Small Molecule Inhibitor of Signal Transducers and Activators of Transcription 3 Reverses Immune Tolerance in Malignant Glioma Patients.* Cancer Research, 2007. **67**(20): p. 9630-9636.

239. Love, K.T., et al., *Lipid-like materials for low-dose, in vivo gene silencing.* Proceedings of the National Academy of Sciences, 2010. **107**(5): p. 1864-1869.

240. March, S., et al., *Establishment of liver stages of Plasmodium falciparum and vivax in a microscale human liver platform.* submitted.

241. Bilzer, M., F. Roggel, and A.L. Gerbes, *Role of Kupffer cells in host defense and liver disease.* Liver International, 2006. **26**(10): p. 1175-1186.

242. Jones, S.A., J. Scheller, and S. Rose-John, *Therapeutic strategies for the clinical blockade of IL-6/gp130 signaling.* The Journal of Clinical Investigation, 2011. **121**(9): p. 3375-3383.

243. Flint, M., et al., *Characterization of Hepatitis C Virus E2 Glycoprotein Interaction with a Putative Cellular Receptor, CD81.* Journal of Virology, 1999. **73**(8): p. 6235-6244.

244. Spudich, J.L. and D.E. Koshland, *Non-genetic individuality: chance in the single cell.* Nature, 1976. **262**(5568): p. 467-471.

245. Raj, A., et al., *Stochastic mRNA Synthesis in Mammalian Cells.* PLoS Biol, 2006. **4**(10): p. e309.

246. Snijder, B., et al., *Population context determines cell-to-cell variability in endocytosis and virus infection.* Nature, 2009. **461**(7263): p. 520-523.

247. Tilsner, J. and K.J. Oparka, *Tracking the green invaders: advances in imaging virus infection in plants.* Biochem. J., 2010. **430**(1): p. 21-37.

248. Sivaraman, D., et al., *Detecting RNA viruses in living mammalian cells by fluorescence microscopy.* Trends Biotechnol., 2011. **29**(7): p. 307-313.

249. Jouvenet, N., S.M. Simon, and P.D. Bieniasz, *Imaging the interaction of HIV-1 genomes and Gag during assembly of individual viral particles.* Proc Natl Acad Sci, 2009. **106**(45): p. 19114-19119.

250. Santangelo, P.J., et al., *Single molecule-sensitive probes for imaging RNA in live cells.* Nat Meth, 2009. **6**(5): p. 347-349.

251. Lindenbach, B.D., et al., *Complete Replication of Hepatitis C Virus in Cell Culture.* Science, 2005. **309**(5734): p. 623-626.

252. Vargas, D.Y., et al., *Mechanism of mRNA transport in the nucleus.* Proc Natl Acad Sci USA, 2005. **102**(47): p. 17008-17013.

253. Miller, S. and J. Krijnse-Locker, *Modification of intracellular membrane structures for virus replication.* Nat Rev Micro, 2008. **6**(5): p. 363-374.

254. Novoa, R.R., et al., *Virus factories: associations of cell organelles for viral replication and morphogenesis.* Biol Cell, 2005. **97**(2): p. 147-172.

255. Salonen, A., T. Ahola, and L. Kääriäinen, *Viral RNA Replication in Association with Cellular Membranes. Membrane Trafficking in Viral Replication*, M. Marsh, Editor. 2005, Springer Berlin Heidelberg. p. 139-173.

256. Schermelleh, L., et al., *Subdiffraction Multicolor Imaging of the Nuclear Periphery with 3D Structured Illumination Microscopy.* Science, 2008. **320**(5881): p. 1332-1336.

257. Gosert, R., et al., *Identification of the Hepatitis C Virus RNA Replication Complex in Huh-7 Cells Harboring Subgenomic Replicons.* J. Virol., 2003. **77**(9): p. 5487-5492.

258. Krawczynski, K., et al., *Hepatitis C virus antigen in hepatocytes: Immunomorphologic detection and identification.* Gastroenterology, 1992. **103**(2): p. 622-629.

259. Andrus, L., et al., *Expression of paramyxovirus V proteins promotes replication and spread of hepatitis C virus in cultures of primary human fetal liver cells.* Hepatology, 2011. **54**(6): p. 1901-1912.

260. Itzkovitz, S., et al., *Single-molecule transcript counting of stem-cell markers in the mouse intestine.* Nat Cell Biol, 2012. **14**(1): p. 106-114.

261. McGuinness, P.H., et al., *False detection of negative-strand hepatitis C virus RNA.* The Lancet, 1994. **343**(8896): p. 551-552.

262. Revie, D. and S. Salahuddin, *Human cell types important for Hepatitis C Virus replication in vivo and in vitro. Old assertions and current evidence.* Virology, 2011. **8**(1): p. 346.

263. Purcell, M.K., et al., *Strand-specific, real-time RT-PCR assays for quantification of genomic and positive-sense RNAs of the fish rhabdovirus, Infectious hematopoietic necrosis virus.* J. Virol. Methods, 2006. **132**(1–2): p. 18-24.

264. Laskus, T., et al., *Detection of Hepatitis G Virus Replication Sites by Using Highly Strand-Specific Tth-Based Reverse Transcriptase PCR.* J. Virol., 1998. **72**(4): p. 3072-3075.

265. Agnello, V., et al., *Detection of widespread hepatocyte infection in chronic hepatitis C.* Hepatology, 1998. **28**(2): p. 573-584.

266. Chang, M., et al., *Dynamics of Hepatitis C Virus Replication in Human Liver.* Am. J. Pathol., 2003. **163**(2): p. 433-444.

267. Komurian-Pradel, F., et al., *Strand specific quantitative real-time PCR to study replication of hepatitis C virus genome.* J. Virol. Methods, 2004. **116**(1): p. 103-106.

268. Lanford, R.E., et al., *Lack of detection of negative-strand hepatitis C virus RNA in peripheral blood mononuclear cells and other extrahepatic tissues by the highly strand-specific rTth reverse transcriptase PCR.* J. Virol., 1995. **69**(12): p. 8079-83.

269. Lohmann, V., et al., *Replication of Subgenomic Hepatitis C Virus RNAs in a Hepatoma Cell Line.* Science, 1999. **285**(5424): p. 110-113.

270. Pal, S., et al., *Intrahepatic Hepatitis C Virus Replication Correlates with Chronic Hepatitis C Disease Severity In Vivo.* J. Virol., 2006. **80**(5): p. 2280-2290.

271. Quinkert, D., R. Bartenschlager, and V. Lohmann, *Quantitative Analysis of the Hepatitis C Virus Replication Complex.* J. Virol., 2005. **79**(21): p. 13594-13605.

272. Yuki, N., et al., *Significance of liver negative-strand HCV RNA quantitation in chronic hepatitis C.* J. Hepatol., 2006. **44**(2): p. 302-309.

273. Ahlquist, P., et al., *Host Factors in Positive-Strand RNA Virus Genome Replication.* J. Virol., 2003. **77**(15): p. 8181-8186.

274. Buck, K.W., *Comparison of The Replication of Positive-Stranded Rna Viruses of Plants and Animals*, in *Adv. Virus Res.*, F.A.M. Karl Maramorosch and J.S. Aaron, Editors. 1996, Academic Press. p. 159-251.

275. Lohmann, V., et al., *Viral and Cellular Determinants of Hepatitis C Virus RNA Replication in Cell Culture.* J. Virol., 2003. **77**(5): p. 3007-3019.

276. Evans, M.J., C.M. Rice, and S.P. Goff, *Genetic Interactions between Hepatitis C Virus Replicons.* J. Virol., 2004. **78**(21): p. 12085-12089.

277. Dahari, H., et al., *Mathematical Modeling of Subgenomic Hepatitis C Virus Replication in Huh-7 Cells.* J. Virol., 2007. **81**(2): p. 750-760.

278. Srivastava, R., et al., *Stochastic vs. Deterministic Modeling of Intracellular Viral Kinetics.* J. Theor. Biol., 2002. **218**(3): p. 309-321.

279. Sardanyés, J., R.V. Solé, and S.F. Elena, *Replication Mode and Landscape Topology Differentially Affect RNA Virus Mutational Load and Robustness.* J. Virol., 2009. **83**(23): p. 12579-12589.

280. Neumann, A.U., et al., *Hepatitis C Viral Dynamics in Vivo and the Antiviral Efficacy of Interferon-α Therapy.* Science, 1998. **282**(5386): p. 103-107.

281. Dahari, H., et al., *Modeling Subgenomic Hepatitis C Virus RNA Kinetics during Treatment with Alpha Interferon.* J. Virol., 2009. **83**(13): p. 6383-6390.

282. Dahari, H., et al., *Mathematical modeling of primary hepatitis C infection: Noncytolytic clearance and early blockage of virion production.* Gastroenterology, 2005. **128**(4): p. 1056-1066.

283. Hensel, S., J. Rawlings, and J. Yin, *Stochastic Kinetic Modeling of Vesicular Stomatitis Virus Intracellular Growth.* Bull. Math. Biol., 2009. **71**(7): p. 1671-1692.

284. Weinberger, L.S., et al., *Stochastic Gene Expression in a Lentiviral Positive-Feedback Loop: HIV-1 Tat Fluctuations Drive Phenotypic Diversity.* Cell, 2005. **122**(2): p. 169-182.

285. Zhao, M., et al., *Stochastic Expression of the Interferon-β Gene.* PLoS Biol, 2012. **10**(1): p. e1001249.

286. François-Newton, V., et al., *USP18-Based Negative Feedback Control Is Induced by Type I and Type III Interferons and Specifically Inactivates Interferon α Response.* PLoS ONE, 2011. **6**(7): p. e22200.

287. Krebs, D.L. and D.J. Hilton, *SOCS Proteins: Negative Regulators of Cytokine Signaling.* Stem Cells, 2001. **19**(5): p. 378-387.

288. Wormald, S., et al., *The Comparative Roles of Suppressor of Cytokine Signaling-1 and -3 in the Inhibition and Desensitization of Cytokine Signaling.* J Biol Chem, 2006. **281**(16): p. 11135-11143.

289. Garaigorta, U. and F.V. Chisari, *Hepatitis C Virus Blocks Interferon Effector Function by Inducing Protein Kinase R Phosphorylation.* Cell Host Microbe, 2009. **6**(6): p. 513-522.

290. Pietschmann, T., et al., *Construction and characterization of infectious intragenotypic and intergenotypic hepatitis C virus chimeras.* Proc. Natl. Acad. Sci., 2006. **103**(19): p. 7408-7413.

291. Walters, K.-A., et al., *Genomic Analysis Reveals a Potential Role for Cell Cycle Perturbation in HCV-Mediated Apoptosis of Cultured Hepatocytes.* PLoS Pathog., 2009. **5**(1): p. e1000269.

292. Chen, A.A., et al., *Humanized mice with ectopic artificial liver tissues.* Proceedings of the National Academy of Sciences, 2011.

293. Le Rouzic, V., J. Corona, and H. Zhou, *Postnatal development of hepatic innate immune response.* Inflammation, 2011. **34**(6): p. 576-584.

294. Patel, S.J., et al., *DNA-triggered innate immune responses are propagated by gap junction communication.* Proceedings of the National Academy of Sciences, 2009. **106**(31): p. 12867-12872.

295. Raptis, L., et al., *Beyond structure, to survival: activation of Stat3 by cadherin engagement.* Biochemistry and Cell Biology, 2009. **87**(6): p. 835-843.